

**Report No. CDOT-DTD-R-2001-10
Final Report**

Forensic Investigation of Early Cracking on I-25 in Denver, Colorado

**Prepared for
Colorado Department of Transportation**

By

**Mike Anderson, P.E. (Asphalt Institute)
John D'Angelo, P.E. (Federal Highway Administration)
Gerry Huber, P.E. (Heritage Research Group)**

[This page left blank]

DISCLAIMER

The analyses, viewpoints, and recommendations are those of the authors and do not necessarily represent the views and opinions of the Colorado Department of Transportation, Asphalt Institute, Federal Highway Administration, or Heritage Research Group.

[This page left blank]

TABLE OF CONTENTS

DISCLAIMER.....	I
EXECUTIVE SUMMARY.....	1
BACKGROUND.....	3
INITIAL REVIEW (OCTOBER 16-18, 2000)	5
CONSTRUCTION.....	13
REVIEW OF CROSS SECTION SLAB	15
TRANSVERSE LOCATION OF DISTRESS	21
SAMPLING AND TESTING PLAN	23
PRE-TESTING.....	24
MIXTURE COMPONENT ANALYSES	24
MIXTURE STIFFNESS DETERMINATION.....	25
MATERIALS TESTING AND ANALYSES.....	27
VOLUMETRIC PROPERTIES	27
MIXTURE COMPOSITION – ASPHALT BINDER CONTENT AND GRADATION.....	28
SIEVE SIZE	29
ASPHALT CONTENT	29
RECOVERED ASPHALT BINDER P PROPERTIES	32
<i>Direct Tension Testing (DTT) and Determination of Critical Temperature.....</i>	<i>33</i>
<i>Comparison of Intermediate Temperature Stiffness With and Without PAV Aging</i>	<i>34</i>
<i>DSR Strain Sweep at Intermediate Temperature.....</i>	<i>35</i>
MIXTURE SHEAR STIFFNESS.....	36
<i>Shear Stiffness of the Lower Layer Mixtures</i>	<i>40</i>
INDIRECT TENSILE STRENGTH AND STRAIN AT FAILURE.....	43
ADDITIONAL COLORADO DOT RESULTS	47
MOISTURE DAMAGE.....	47
SEGREGATION.....	47
DISCUSSION OF RESULTS	51
VOLUMETRIC PROPERTIES	51
MIXTURE COMPOSITION.....	52
RECOVERED ASPHALT BINDER P PROPERTIES	53
MIXTURE MECHANICAL (STIFFNESS) PROPERTIES.....	54
TOP-DOWN FATIGUE CRACKING.....	55
SUMMARY AND CONCLUSIONS.....	57
LIMITED STUDY AREA	59
RECOMMENDATIONS	61
SURFACE MIXTURE TYPE	61
DENSITY MEASUREMENT.....	61

ASPHALT BINDER CONTENT.....	62
MECHANICAL PROPERTIES OF ASPHALT MIXTURES	63
TESTING FOR SEGREGATION.....	63
PAVEMENT REHABILITATION SUGGESTIONS	63
PROPERTIES OF THE ASPHALT BINDER.....	64
REFERENCES	65

LIST OF TABLES

Table 1 Distance of Each Core in Distress Section South of Milepost 224	8
Table 2 Distance of Each Core in Distress Section From Milepost 224	11
Table 3 Maximum Theoretical Specific Gravity – Surface Mixtures	27
Table 4 Bulk Specific Gravity and Percentage of Air Voids – Surface Mixtures	28
Table 5 Mixture Composition for I-25D and I-25N Surface Mixtures	29
Table 6 Mixture Composition for I-70 Surface Mixture	30
Table 7 Recovered Asphalt Binder Properties	32
Table 8 Critical Temperatures of Recovered Asphalt Binder	33
Table 9 Direct Tension Test Data and Critical Cracking Temperature Determination	33
Table 10 Recovered Asphalt Binder Properties (w/ and w/o PAV-aging)	35
Table 11 Shear Stiffness – Surface Mixtures	37
Table 12 Shear Stiffness – Intermediate Mixtures	42
Table 13 Shear Stiffness at 10 Hz – All Mixtures	43
Table 14 Indirect Resilient Modulus at 22°C	44
Table 15 Indirect Tensile Strength at 22°C	45
Table 16 Tensile Strength Ratio	47

LIST OF FIGURES

Figure 1 Layout of Cores at I-25 Distress Site.....	7
Figure 2 Shows the Coring in Progress.	8
Figure 3 Layout of Slab at I-25 Distress Site	9
Figure 4 Layout for Cutting Slab	10
Figure 5 Layout of Cores at I-25 Non-distress Site.....	11
Figure 6 Paving Construction Sequence	13
Figure 7 Location of the Cross Section Slab Prior to Removal.....	15
Figure 8 Close-up Cross Section at Crack Beside Right Wheelpath.....	16
Figure 9 Cross Sectional View of Outside Half of Lane Shortly After Sawing	17
Figure 10 Cross Sectional View of Inside Half of Lane Shortly After Sawing	18
Figure 11 Bottom of Core Showing Signs of Stripping in 1984 Overlay Mixture	19
Figure 12 Recovered Aggregate Gradations for I-25D and I-25N Surface Mixtures	30
Figure 13 Comparison of Gradations for I-70 and I-25 Surface Mixtures	31
Figure 14 DSR Strain Sweep – I-25N and I-70 Recovered Asphalt Binders.....	36
Figure 15 Shear Stiffness of the I-25D Surface Mixture	38
Figure 16 Shear Stiffness of the I-25N Surface Mixture	38
Figure 17 Shear Stiffness of the I-70 Surface Mixture	39
Figure 18 Average Shear Stiffness at 22°C – All Surface Mixtures	39
Figure 19 Average Shear Stiffness at 10 Hz – All Surface Mixtures	40
Figure 20 Horizontal Deformation from IDT Tests (22°C, 12.5 mm/min.)	45
Figure 21 Vertical Deformation from IDT Tests (22°C, 12.5 mm/min.).....	46
Figure 22 Layout of Cores Taken to Investigate Segregation.....	48
Figure 23 Gradations from Colorado DOT Cores	49
Figure 24 Plot of Asphalt Content Vs Percent Passing 2.36 mm Sieve for DOT Cores.....	50

Figure 25 Development of Fatigue Cracking In Asphalt Pavements	55
--	----

[This page left blank]

EXECUTIVE SUMMARY

The pavement distress on I-25 includes both transverse cracking and longitudinal cracking within the wheelpaths. The transverse cracking is very likely reflective cracking from the underlying layers. The longitudinal cracking is surface-initiated (top-down). Regardless of the cracking mechanism, the appearance of the longitudinal cracks was earlier in the pavement life than would be expected.

A sampling plan was developed to obtain cores from two sections, one with distress and the other without distress. A slab was taken from a trench across the lane. Three longitudinal cracks were present in the lane. There was also a comparison to a rehabilitation project on I-70. I-70 is an HMA overlay of a PCC pavement and the pavement structure will not respond exactly the same; however, it is one year older and has similar traffic to I-25.

At each of the longitudinal cracks on I-25 there was segregation present within the mat. The segregation was particularly severe at one of the cracks.

There are no signs of moisture damage in the 1997 overlay. Some stripping was observed in the remaining portion of the 1984 mixture and there is some indication of stripping in the older mixture in the lower layers. Stripping does not appear to be severe.

The difference in cracking performance between the I-25 and I-70 pavements is likely caused by a number of contributing factors which include:

- percentage of air voids in the pavement;
- volume of effective asphalt binder; and
- physical properties of the asphalt binder.

Test results indicated that the physical properties of the recovered asphalt binder from the I-25 and I-70 cores were the same. Thus, asphalt binder properties were not the principal reason for the cracking.

Asphalt mixture composition for the I-25 cores indicated that the asphalt binder content was 4.1%, 0.5% lower than design value of 4.6% and consistently lower than any of the quality control/quality assurance data. This is a very low asphalt binder content for a surface (wearing course) mixture. By contrast, the recovered asphalt binder content of the I-70 cores was 4.8 percent. A difference of 0.7% between the two pavements is significant for this type of mixture.

Asphalt mixture volumetric properties of the I-25 cores indicated that the percentage of air voids was relatively high. This result did not match expectations for a pavement subjected to three years of traffic.

In two of the three factors (percentage of air voids and volume of asphalt binder) the I-70 mixture had superior properties compared to the I-25 mixture. The similarities in recovered asphalt binder physical properties suggest that the asphalt binder was not the main contributing factor. By contrast, the I-70 mixture had a higher asphalt binder volume and lower percentage of air voids. The resulting mixture was more resistant to the stresses and strains induced by traffic.

Based on the data analysis, it is our opinion that the early cracking of I-25 could not necessarily have been predicted or prevented by the Colorado Department of Transportation or the Contractor using the current specifications and tests.

In summary the premature cracking on I-25 is caused by several factors which were combined on this project which include:

- a. Higher in-place air voids than expected.
- b. Low effective asphalt content and
- c. Segregation within the mat.

Recommendations to minimize occurrence of similar behavior in the future include:

- a. Evaluate alternate surface mixtures
- b. Evaluate method of measuring in-place density
- c. Evaluate method of measuring asphalt content
- d. Evaluate methods of measuring mechanical properties of mixtures.

BACKGROUND

In July 1997, Western Mobile, Inc. completed an overlay of the north and southbound lanes of I-25 between Colorado State Highway 7 (SH-7) and 120th Street in Denver, Colorado. Construction included milling the existing pavement up to three inches depth (tapered from the outside lane to the inside lane) and replacing with a 19-mm Superpave asphalt mixture as the wearing (surface) course. The 19-mm mixture was designed using the Superpave gyratory compactor (109 design gyrations) with a PG 76-28 asphalt binder (including elastic recovery specifications). The design mixture also passed torture tests in the Colorado Department of Transportation's (CDOT) Euro-Lab.

A total of 62,000 tons of the mixture was placed. The project received bonuses for material quality and smoothness.

In early 1998, CDOT investigated early longitudinal cracking appearing on the I-25 surface. According to the CDOT report [\[Aschenbrener, 1998\]](#) the cracking severity was, in some instances, high. Initial evaluation of cores removed from areas with existing longitudinal cracks indicated that the surface cracks were reflective cracks from the underlying pavement, caused by moisture damage and traffic.

Two years later, in May 2000, CDOT – Region 6 requested a forensic evaluation of the I-25 project, as the pavement appeared to be rapidly deteriorating. CDOT – Region 6 suggested that a team of asphalt materials and construction experts perform a forensic evaluation of the project and provide recommendations describing: (a) what was the cause of the early pavement distress, and (b) how to avoid future occurrences.

[This page left blank]

INITIAL REVIEW (OCTOBER 16-18, 2000)

The forensic team visited Colorado from October 16 to 18, 2000. On the afternoon of October 16, 2000 the team met with representatives of the Colorado DOT Central Office and Regional Office. Tim Aschenbrener opened the meeting by providing a project overview and stating the objective of the team.

The I-25 project, constructed by Western Mobile Paving, won a National Asphalt Pavement Association award. It was a Superpave mixture (fine-graded) containing PG 76-28 asphalt binder from Koch Materials. The following year some longitudinal cracking was observed.

An internal investigation by Tim Aschenbrener was done in May 1998. Cores indicated the presence of moisture damage. Two of the three cores taken showed the cracking to be a reflection of cracking that existed before the overlay. The report provided recommendations for project selection and a rehabilitation strategy workshop.

Over the next two years cracking continued to develop and in the summer of 2000 Reza Akhavan, the new Regional Materials Engineer, proposed a forensic investigation.

October 16th

At the meeting on October 16, 2000 the objective of the group was declared as follows:

1. Determine what happened to cause the longitudinal cracking on this section of I-25
2. Provide recommendations for future rehabilitation work to prevent a re-occurrence of this cracking.

Following familiarization at the regional office and a review of project documents an on-site reconnaissance visit was held.

October 17th

On the second day the forensic team met with members of the CDOT project team including the project engineer, and technicians. Details of the construction were reviewed. Condition video tapes from the pavement management system were viewed.

1996 Condition (prior to rehabilitation, van in center lane)

Northbound:

- center lane has most distress
- generally lots of transverse cracking
- poor construction joints, particularly between the outside and center lanes
- some patched areas

Southbound:

- condition about same as northbound
- patches in center lane

- some longitudinal cracking

2000 Condition (van in outside driving lane)

Northbound and southbound

- nearly continuous longitudinal cracking, particularly in left wheelpath
- many areas of double cracking, one on either side of wheelpath

A study plan was developed. Two representative areas would be selected from the I-25 project, one where distress was occurring and another that had no distress. The focus of the testing would be to evaluate differences between the two. As a secondary point, limited testing would be done on a section of I-70 which had been rehabilitated one year earlier using a similar rehabilitation technique.

A sampling plan was developed as follows:

I-25 Distressed area in the outside driving lane

- 6 cores from the left wheelpath
- 2 cores between the wheelpath
- trench cut from shoulder line to lane line

I-25 Non-distressed area in the outside driving lane

- 6 cores from the left wheelpath
- 2 cores between the wheelpath

I-70 Non-distressed area in the outside driving lane

- 6 cores from the left wheelpath

A study plan was developed as follows:

I-25 Top layer

- thickness
- in-place density
- percent asphalt
- gradation
- binder recovery
- binder temperature grading
- mixture shear stiffness

I-25 Second layer

- mixture shear stiffness

I-70 Top layer

- thickness
- in-place density
- percent asphalt
- gradation
- binder recovery

- binder temperature grading
- mixture shear stiffness

On the afternoon of October 17th locations were selected.

I-25 Distressed location

- northbound, outside lane
- near milepost 224
- slab to be taken at milepost 224.06

I-25 Non-distressed location

- northbound, outside lane
- near milepost 224.3

I-70 Non-distressed location

- eastbound, outside lane

October 18th

On October 18th, cores and slabs were taken from I-25. Notes are as follows:

Distress Area

Rut depth measured

- 2 mm in LWP
- less than 1 mm in RWP

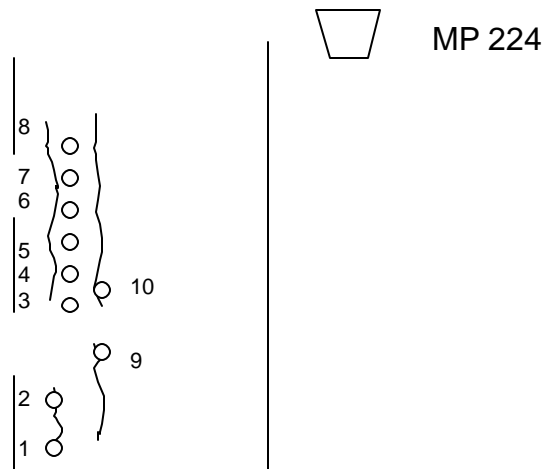


Figure 1 Layout of Cores at I-25 Distress Site

Cores were taken as follows:

- cores 1, 2, 9 and 10 were taken on the edge of the wheelpath

- cores 3, 4, 5, 6, 7 and 8 were taken in the center of the wheelpath where no cracking was occurring
- distance to south from Milepost 224 is in Table 1 for each core

Table 1 Distance of Each Core in Distress Section South of Milepost 224

<u>Core</u>	<u>Distance</u>	<u>Core</u>	<u>Distance</u>	<u>Core</u>	<u>Distance</u>
1	71 ft	5	45 ft	9	57 ft
2	67 ft	6	43 ft	10	50 ft
3	50 ft	7	41 ft		
4	47 ft	8	39 ft		

Figure 2 shows the coring in progress.



Figure 2 Coring in the Wheelpath of the Site with Distress

In addition to the cores a slab was taken across the outside driving lane as shown in Figure 3. The location of the slab was 327 feet north of the Milepost 224 marker. The slab was 10.75 feet long and started at the shoulder line.

Three cuts were made across the width of the pavement and five cuts were made across the slab to produce four pieces. The larger width pieces were removed by drilling a hole in the top and anchoring a lag bolt into it. The slabs were lifted out with a front end loader. The remaining pieces, about 7 inches wide, were tilted on their sides and lifted into the back of a pickup truck.

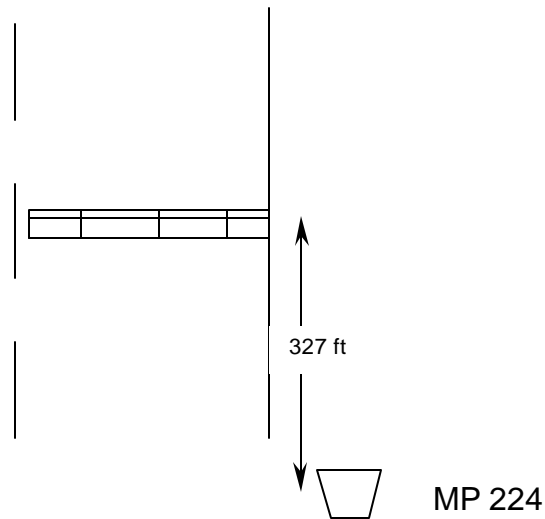


Figure 3 Layout of Slab at I-25 Distress Site

Figure 4 shows the pavement as marked for cutting.

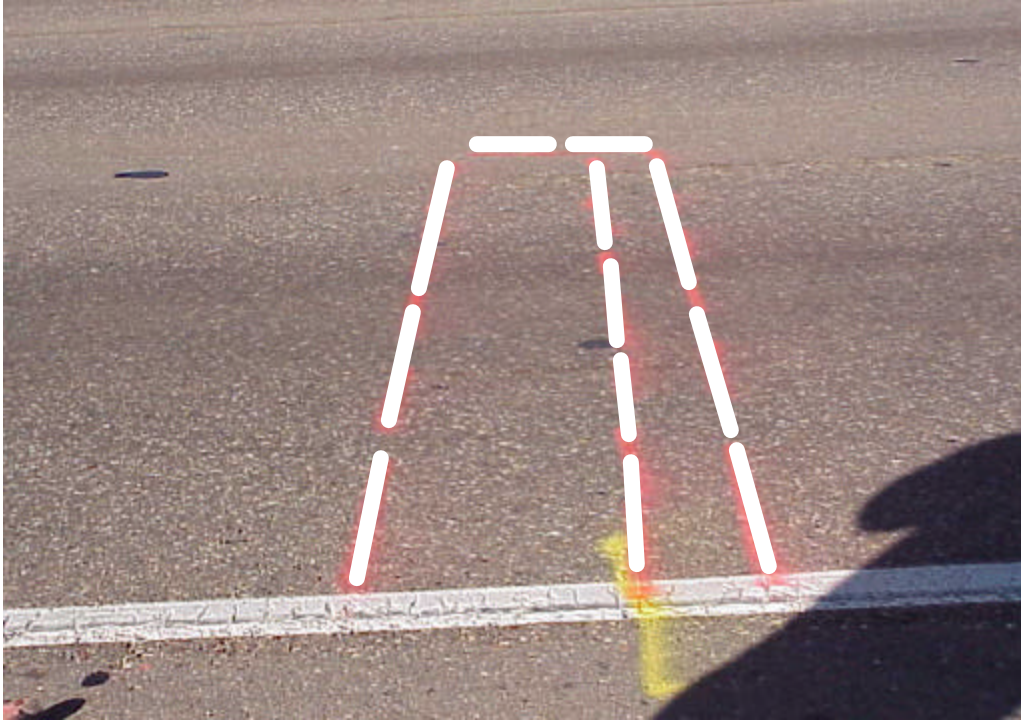


Figure 4 Layout for Cutting Slab

Non-Distress Area

- 2 mm in LWP
- 1 mm in RWP
- cores 11, 12, 13, 14, 15, and 16 were taken in the center of the wheelpath
- cores 17 and 18 were taken on the edge of the wheelpath
- distance to south from Milepost 224 is as follows for each core

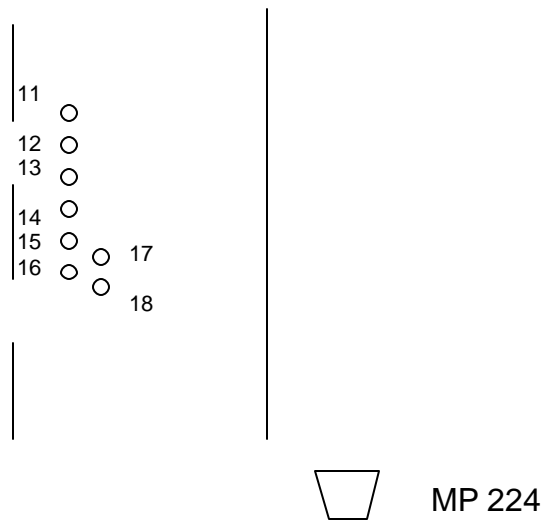


Figure 5 Layout of Cores at I-25 Non-distress Site

Table 2 Distance of Each Core in Distress Section From Milepost 224

<u>Core</u>	<u>Distance</u>	<u>Core</u>	<u>Distance</u>	<u>Core</u>	<u>Distance</u>
11	1904 ft	14	1895 ft	17	? ft
22	1901 ft	15	1893 ft	18	? ft
33	1898 ft	16	1891 ft		

[This page left blank]

CONSTRUCTION

A brief summary of the pavement construction history is listed below:

- The pavement was originally built of hot mix asphalt in 1956.
- The roadway was widened to 6 lanes with hot mix asphalt in 1975.
- The roadway was overlaid with 3 inches of hot mix asphalt in 1984. A paving fabric was placed before the overlay.
- In 1997 the road was milled and overlaid with 3 inches of hot bituminous pavement.



Figure 6 Paving Construction Sequence

In the 1997 construction, a milling machine was used to establish a new cross-slope. Hence, the thickness remaining of the 1984 overlay varies from $\frac{1}{2}$ inch to about 2 inches. The paving sequence is as follows:

- The inner driving lane and inside shoulder were paved on the first pass using a Blaw Knox 220 paver and Barber Greene 655 windrow elevator.
- The center driving lane and outside driving lane were paved in echelon. The center lane was paved 11 feet wide using a Blaw Knox 3200 paver with a Caterpillar 851WB windrow elevator. The outside driving lane was paved 13 feet wide using the 220 paver and 655 elevator combination.
- The outside shoulder was paved using a different mix design using the 3200 paver and 851WB combination.

Review of Cross Section Slab

Figure 7 shows the location of the slab removal before sawing. There are two cracks adjacent to the left wheel path and one on the inside of the right wheel path.

Three saw cuts were made across the lane. The width of the lane was broken into four pieces as marked by the short dashes. The larger pieces were discarded. The narrower sections were retained.

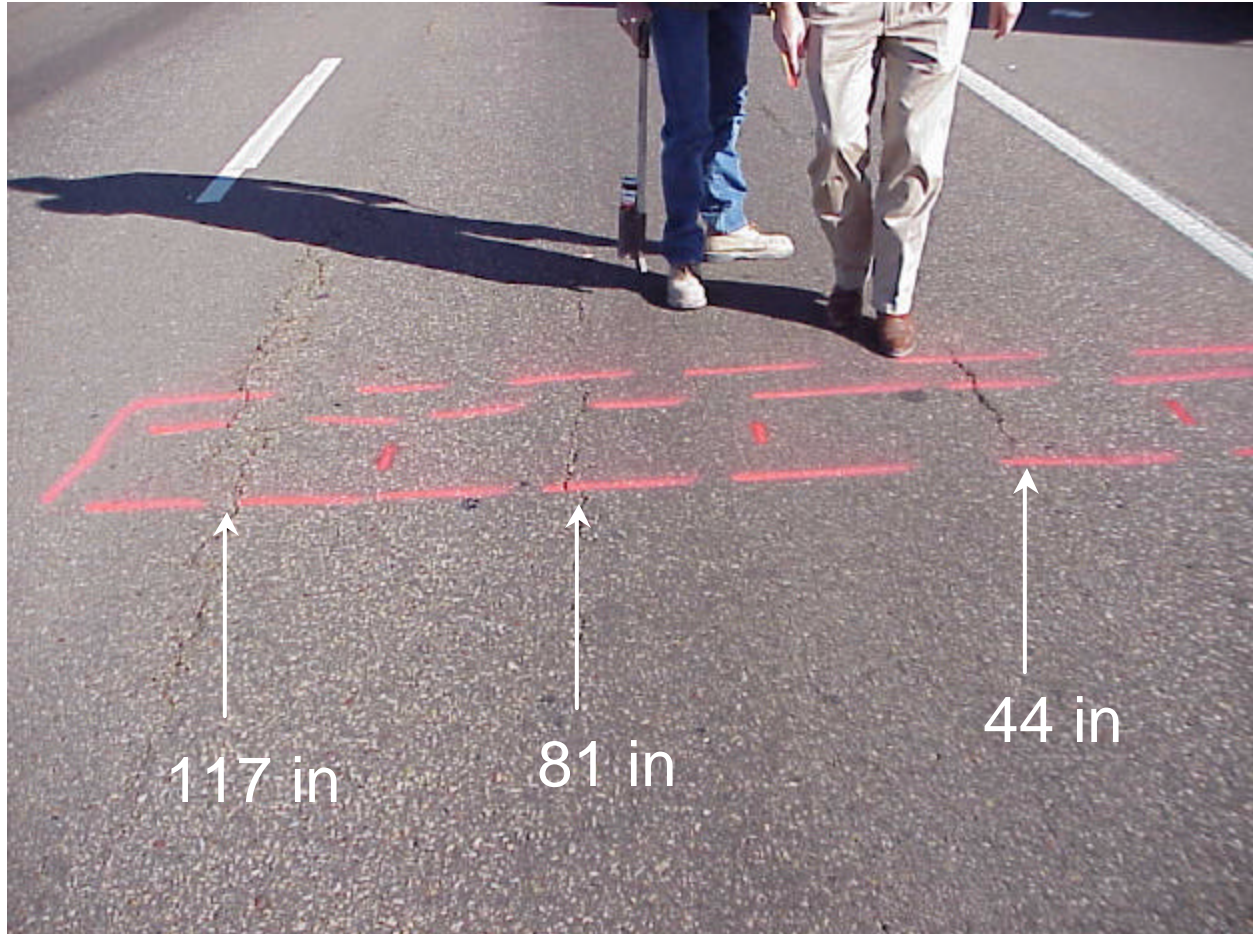


Figure 7 Location of the Cross Section Slab Prior to Removal

Close-up photos of the slabs are located in Appendix B. The tape measure in the Appendix B photos is shown as a reference system. The beginning of the tape indicates the outside shoulder line. The cracks are located at 44, 81, and 117 inches.

The photo showing the crack at 44 inches is shown in Figure 8. Note that the photo is from the point of view of the observers in Figure 7. The photo clearly shows there is a pocket of segregation at the bottom of the lift. Interestingly, there is not a concentration

of rocks near the surface so no segregation is visible from the surface. Close inspection of Figure 7 before sawing also confirms that no segregation is visible at the surface.

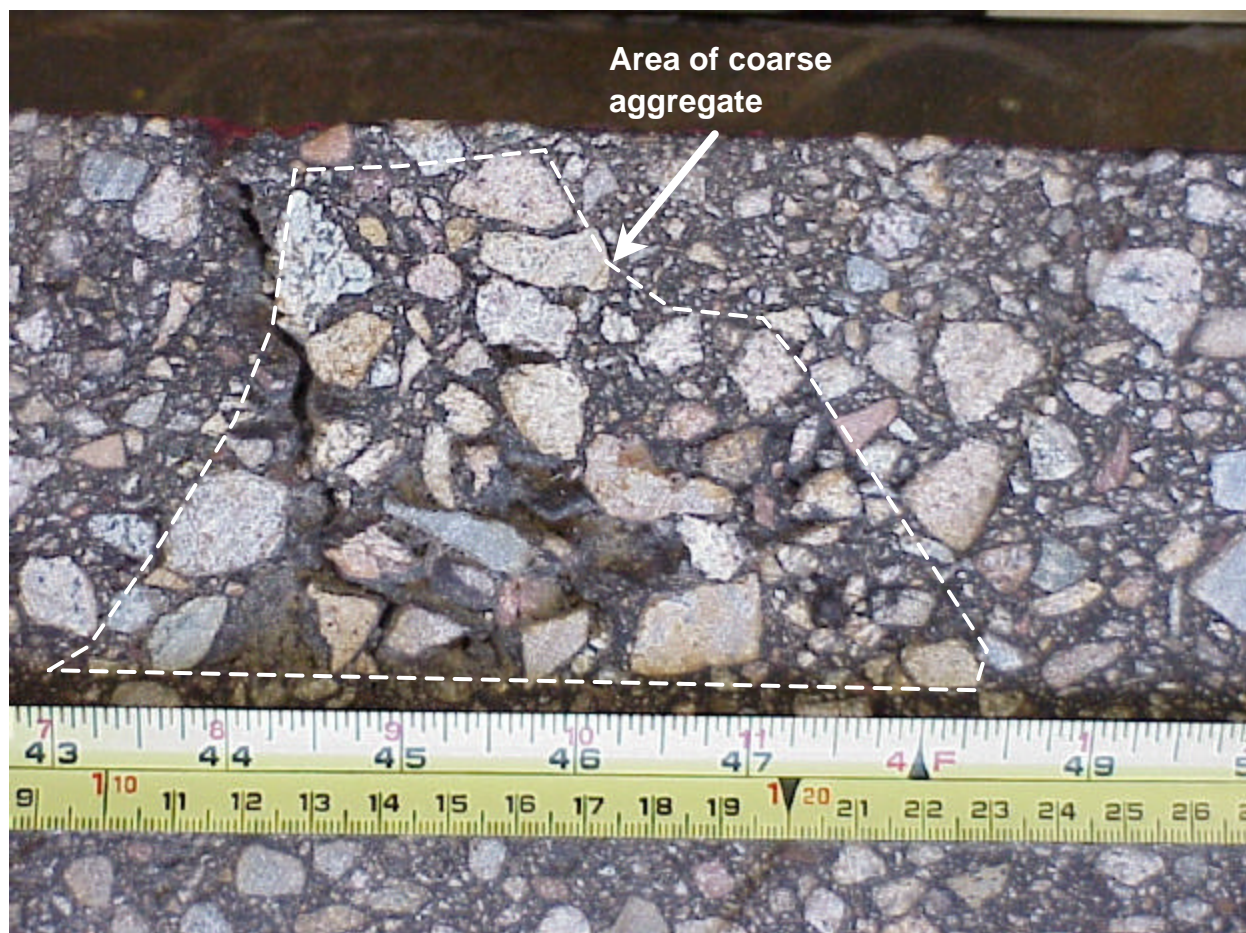


Figure 8 Close-up Cross Section at Crack Beside Right Wheelpath

The area of segregation has lower density and higher air voids. Water can permeate and saturate this area. The presence of water was clearly visible after the slabs were removed and the face had begun to dry. Areas with water soaked into the mixture remained damp. Figure 9 shows the outside half of the cross section. There is a wet spot in the vicinity of the crack at 44 inches. Figure 10 shows the other half of the lane. The wet spots are more localized. They are concentrated at the crack at 81 inches and 117 inches.

It is interesting to note that most of the 1997 overlay has a wet area along the bottom of the lift suggesting the density is low.

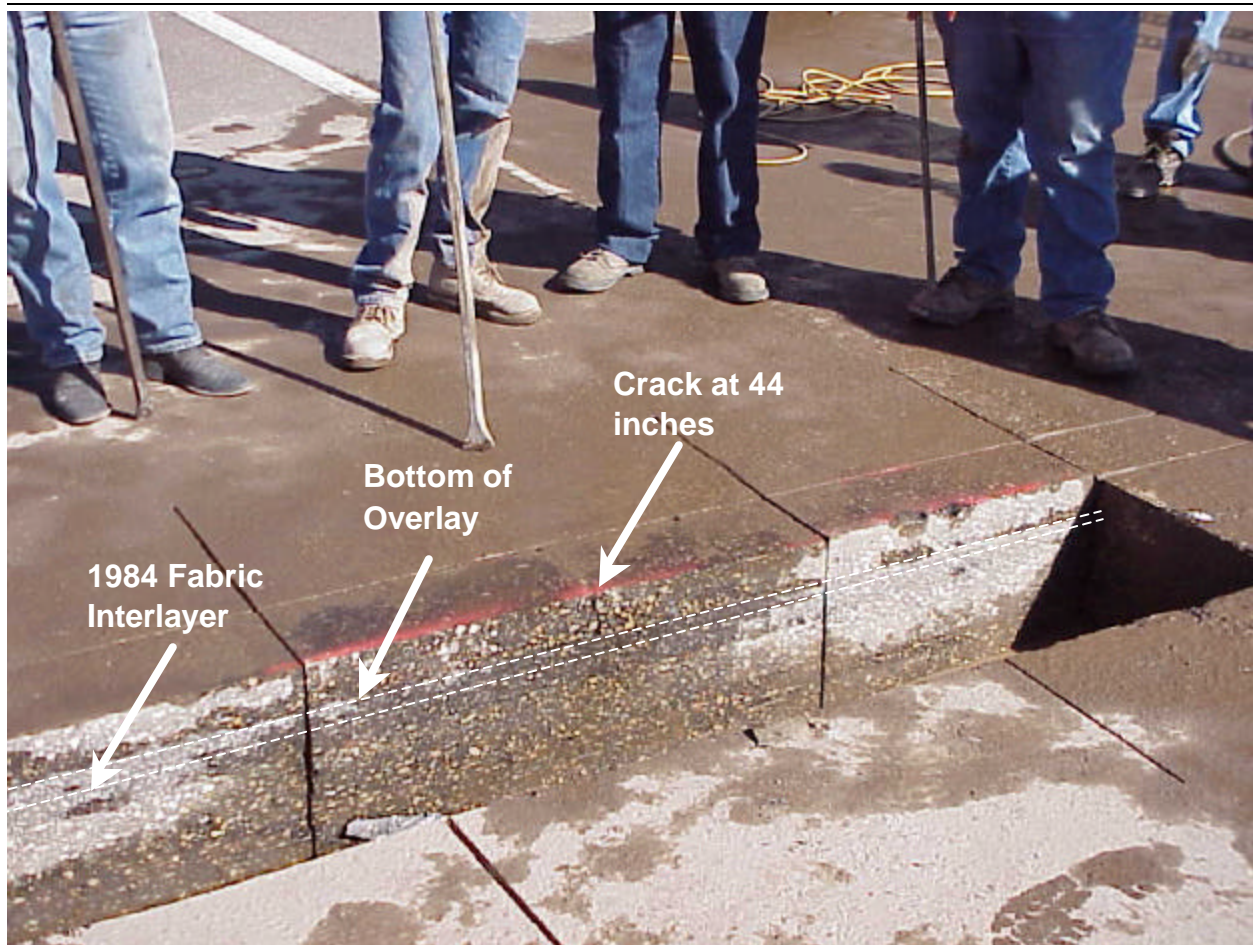


Figure 9 Cross Sectional View of Outside Half of Lane Shortly After Sawing

The 1984 and older hot mix is showing signs of holding water in the areas directly underneath the wheelpaths. The slowness to dry indicates the presence of water in the mixture and possibly the beginning of stripping. The location of these areas directly under the wheelpaths correlates with documented histories of stripping in which the pulsating wheel loads combine with moisture in the mixture to cause stripping. Once again, there were no signs of severe stripping or mixture disintegration.

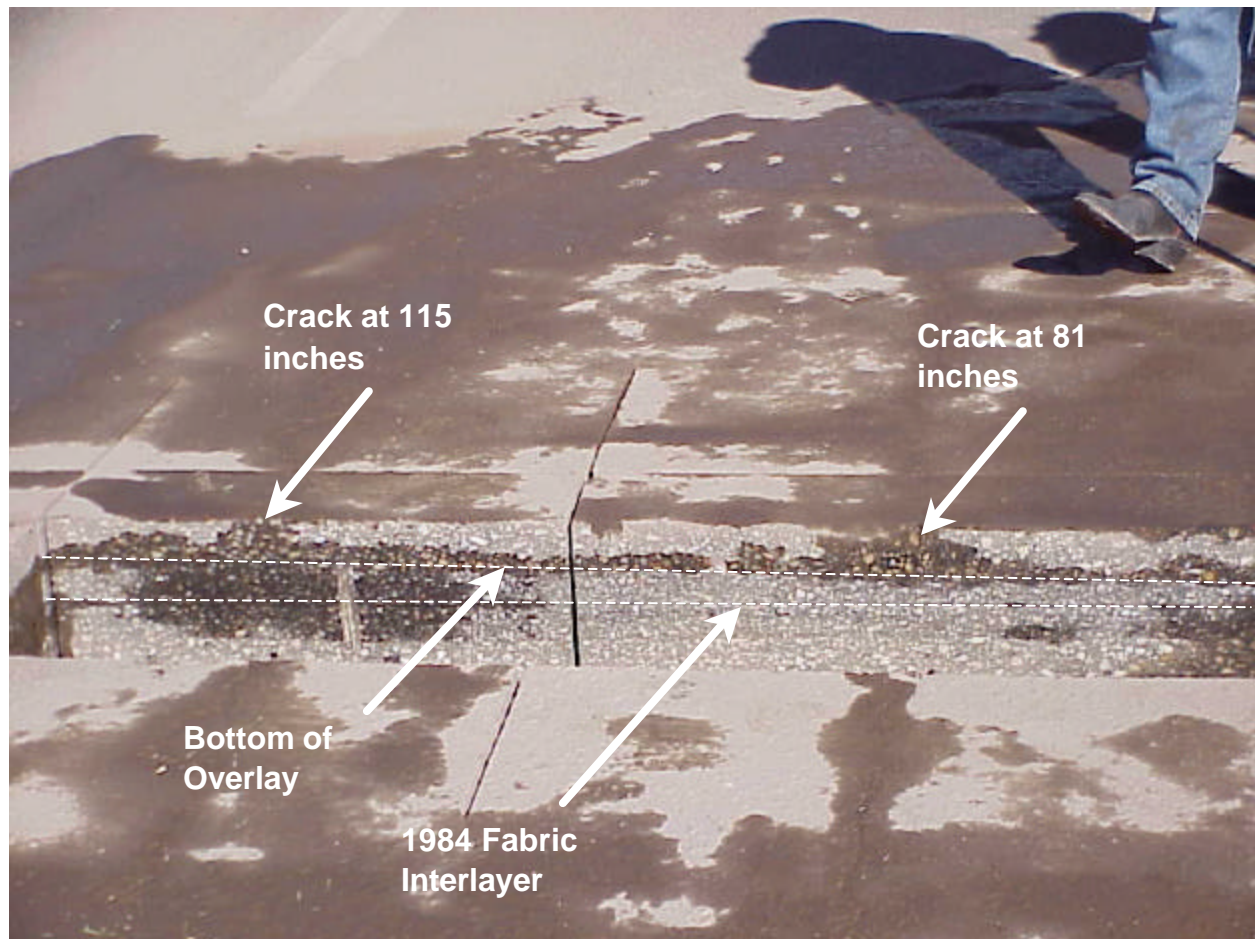


Figure 10 Cross Sectional View of Inside Half of Lane Shortly After Sawing

There were some signs of moisture damage in the old hot mix asphalt under the overlay. Figure 11 shows the bottom of a core which broke off at the fabric interlayer. The 1984 mixture below the overlay shows some stripping. The stripping has not advanced to the point of total mixture disintegration.



Figure 11 Bottom of Core Showing Signs of Stripping in 1984 Overlay Mixture

[This page left blank]

Transverse Location of Distress

Video tapes of pavement conditions are collected annually for the Colorado pavement management system. These tapes include a windshield view and a view straight down onto the pavement surface.

The following tapes were available:

- April 1997 (prior to construction in the fall of 1997).
Shot from the center of the three driving lanes. All three lanes are visible. The detailed down-facing camera shows only the center driving lane.
- April 1998
Shot from the center of the three driving lanes. All three lanes are visible. The detailed down-facing cameras show only the center driving lane.
- March 1999
Produced by a different van than the 1997 and 1998 tapes. Shot from the outside lane of the three driving lanes. All three lanes are visible. Four detail cameras are used. Two are down-facing cameras showing only the surface of the outside driving lane.
- April 2000
Produced by a different van than the 1997, 1998 or 1999 tapes. Shot from the outside lane of the three driving lanes. All three lanes are visible. Detail cameras are down-facing camera and show the surface of the outside driving lane.

The longitudinal cracking is readily visible in the down-facing camera shots. The exact location where the cores and cross section slab were taken has been identified on the 2000 video. There is no longitudinal cracking in this section in the 1997 tape.

The 2000 video was reviewed in detail for both the northbound and southbound lanes. The following observations were made:

Northbound

- The longitudinal cracks are in approximately the same transverse location throughout the length.
- The most predominant crack occurs inside the left wheel path. This crack is very consistent in its location, rarely wandering from side to side.
- Almost as common is the crack on the outside of the left wheel path. This crack tends to wander a bit from side to side.
- There is quite a bit of cracking on the inside of the right wheel path though not nearly as much as there is on the left wheel path. It tends to be fairly consistent in its location.
- Cracking on the outside of the right wheel path is very intermittent and not very long.

Southbound

- The cracking is very similar to the northbound lane.
- The crack inside the left wheelpath is quite consistent.
- The crack outside the left wheelpath wanders a bit from side to side.
- The crack on the inside of the right wheelpath is quite consistent in its location and is about as common as on the northbound lanes.
- There is a crack on the outside of the right wheelpath that is very straight and consistent in its location. It is nearly continuous. It looks like a longitudinal joint that has opened up.

SAMPLING AND TESTING PLAN

During the on-site review, the initial concern was that there was something different about the PG 76-28 asphalt binder that was used on this project. The same grade of asphalt binder was used on a project on I-70 constructed the year prior to construction of the I-25 project. Despite similar traffic, the I-70 mixture performed well, while the I-25 mixture exhibited substantial early cracking.

Based on this information, a sampling and testing plan was developed that included core samples from both the I-25 and I-70 pavements. Recovered component analysis of the cores would determine if the asphalt binder properties were substantially different between the two pavements. In addition, mechanical property testing of the mixtures would determine if there was a difference in the stiffness of the mixtures used on the two pavements.

Two sites were identified on I-25 Northbound for coring. The **Distressed** site, identified as **I-25D** in the following sections, was selected in an area where substantial cracking was observed. The sampling plan required that six cores were taken in the left wheel path (LWP) of the outside lane, and two cores between the wheel path (BWP) in the outside lane. All cores were taken longitudinally within a short distance (less than 10 meters). The **Non-Distressed** site, identified as **I-25N** in the following sections, was selected in an area where no (or minimal) cracking was observed. The same coring pattern (6 cores LWP, 2 cores BWP in the outside lane) was followed.

In addition, a full depth trench was cut across the outside lane in the **Distressed** area. This pavement slab was then removed and transported to the Colorado Department of Transportation (CDOT) Materials Laboratory.

One site was selected for the I-70 sampling. The same core sampling pattern was followed for this pavement section as the I-25 sections. All cores were shipped to the Asphalt Institute for testing.

The testing plan was developed around five hypotheses:

1. The PG 76-28 asphalt binder in the **I-25D** cores has the same physical properties as the PG 76-28 asphalt binder in the **I-25N** cores and significantly different physical properties than the PG 76-28 asphalt binder in the **I-70** cores.
2. The stiffness of the **I-25D** surface mixture is the same as the stiffness of the **I-25N** surface mixture and significantly different than the stiffness of the **I-70** surface mixture.
3. The dust content (percentage passing the #200 or 0.075-mm sieve) of the **I-25D** and **I-25N** mixtures is higher than indicated by the quality control/acceptance data.

4. The stiffness of the lower layer (mixture) of the **I-25D** section is different than the stiffness of the lower layer of the **I-25N** section.
5. There is a high percentage of air voids in the **I-25D** and **I-25N** surface mixture that, when combined with the milling of the outside lane, contributed to possible moisture damage in the I-25 lower layer.

The materials testing plan was developed to test each of these hypotheses as follows:

Pre-Testing

Cores were to be digitally photographed before cutting. Layers were identified within the core, labeled, and marked for cutting. Cores were then cut at the layer interfaces and allowed to dry to constant mass. Once the cut cores dried sufficiently, the bulk specific gravity of the core, G_{mb} , was determined using the standard SSD procedure (ASTM D2726) and using the CoreLok™ method.

Mixture Component Analyses

Testing for mixture component analyses was intended to evaluate three of the five hypotheses (asphalt binder properties, dust content, and percentage of air voids).

Two cores were designated from each section (**I-25D**, **I-25N**, and **I-70**) for material component analyses. These cut cores (surface layers only) were heated in a forced-draft oven at 110°C until the core was soft enough to break down.

After the core was separated into a loose mixture, the sample was split into two equal portions (approximately 1,500 grams each) and the maximum theoretical specific gravity, G_{mm} , of the mixture was determined using ASTM D2041. The average of the two tests is reported as the G_{mm} for the core.

Determination of the G_{mm} allowed for a comparison with the design and production values reported for the mixture. It also permitted calculation of the percentage of air voids within the core specimens.

After the G_{mm} was determined, the two portions from the loose mixture obtained by the destruction of the core were recombined and dried to a constant mass. The recombined loose mixture sample was then subjected to centrifuge extraction (ASTM D2172) with trichloroethylene followed immediately by recovery of the asphalt binder from solution using the Rotavapor procedure (ASTM D5404).

Following the asphalt binder extraction and recovery procedures, the asphalt binder content of the sample was determined. The gradation of the recovered aggregate was also determined.

The recovered asphalt binder from each sample was split into separate containers. The first container, which required very little material (about 10 grams) was retained for testing using the dynamic shear rheometer, or DSR, (AASHTO TP5) at high temperatures (64°C and higher) and intermediate temperatures (16°C to 25°C). This recovered asphalt binder was treated as if it were aged using the rolling thin film oven (RTFO) for purposes of classification in the performance graded asphalt binder specification (AASHTO MP-1). This assumption was made since the asphalt binder had been subjected to construction and three years of actual service.

The asphalt binder remaining in the second container was subjected to long-term aging using the pressure aging vessel, or PAV (AASHTO PP1). The sample was subjected to PAV-aging at 100°C and 2.07 MPa for 20 hours. Following this aging, the asphalt binder was tested at intermediate temperatures (16°C to 25°C) using the DSR and at low temperatures (-12°C to -24°C) using the bending beam rheometer, or BBR (AASHTO TP1). This testing, in conjunction with the high temperature testing, allowed the determination of the performance grade of the recovered asphalt binder from each sample.

In addition, the direct tension test (AASHTO TP3) and associated determination of the critical cracking temperature [1] was performed on the PAV-aged asphalt binder from each sample.

Mixture Stiffness Determination

Testing to determine the mixture stiffness is intended to evaluate two of the five hypotheses (stiffness of the surface mixture, and stiffness of the lower layers).

Three cores were designated from each section (**I-25D**, **I-25N**, and **I-70**) for determination of mixture stiffness. The surface layers of the cores was further cut to a height of 38 millimeters (**I-70**) or 50-mm (**I-25D** and **I-25N**) dependent on the overall layer thickness. The lower layers of the cores were also cut to a height of 38 millimeters (**I-25D** and **I-25N**) or 50-mm (**I-70**) dependent on the overall layer thickness.

The bulk specific gravity (G_{mb}) and corresponding percentage of air voids of the cut specimens were determined before testing.

Mixture stiffness testing was conducted using the Superpave shear tester (SST) and the shear frequency sweep test at constant height (FSCH). This test procedure (AASHTO TP7) is conducted by applying a small sinusoidal shear strain (0.01%) to a test specimen and recording the resulting shear stress required to achieve that strain at ten different loading frequencies. The loading frequencies extend from fast loading (10 Hz – representing highway speeds) to very slow loading (0.01 Hz). The complex shear modulus (G^*), or shear stiffness, is calculated for each loading frequency as the ratio of measured shear stress (τ) to applied shear strain (γ). Since the FSCH test is conducted

at a small strain level, the test is usually assumed to occur within the linear viscoelastic region. As a result, the test is considered non-destructive; meaning that one specimen can be tested at multiple temperatures. Usually, the FSCH test is conducted at two or more temperatures.

In this investigation, specimens were tested at three temperatures – the effective temperature for fatigue cracking, or $T_{\text{eff}}(\text{FC})$, $T_{\text{eff}}(\text{FC}) - 6^{\circ}\text{C}$, and $T_{\text{eff}}(\text{FC}) + 6^{\circ}\text{C}$. The effective temperature for fatigue cracking is determined using the mean annual air temperature at the pavement location and the equations provided in the SHRP A-407 report [2]. For Denver, the $T_{\text{eff}}(\text{FC})$ is calculated to be 22°C (using a 50% reliability). Thus, the three testing temperatures are 16, 22, and 28°C .

While the data was examined at all loading frequencies, the shear stiffness at 10 Hz loading frequency ($G^*_{10\text{Hz}}$) is considered to be most similar to the stiffness of the mixture at normal highway speeds.

MATERIALS TESTING AND ANALYSES

Volumetric Properties

The percentage of air voids in the cores was calculated using two different means of measuring the mixture's bulk specific gravity (G_{mb}) and the maximum theoretical specific gravity (G_{mm}). The G_{mb} was determined using the standard SSD method (ASTM D2726) and the newer CoreLok™ procedure. The G_{mm} data is shown in Table 3.

Table 3 Maximum Theoretical Specific Gravity – Surface Mixtures

Mixture	Replicate 1	Replicate 2	Average	Design
I-25D	2.476	2.473	2.475	2.466
I-25N	2.476	2.474	2.475	2.466
I-70	2.551	2.549	2.550	na

The data in Table 3 indicates that the average maximum theoretical specific gravity for the **I-25D** and **I-25N** surface mixtures are identical. The G_{mm} values are also slightly higher (2.475) than the design G_{mm} value (2.466).

The G_{mb} data for the surface mixture, with calculations on the percentage of air voids, is shown in Table 4. The G_{mb} of the core specimens (and associated percentage of air voids) are very similar regardless of the test method selected. The percentage of air voids in the **I-25D** surface mixture is high (8.3%) for a mixture that has been under traffic for a period of three years and was constructed with acceptable in-place density according to the production QC data. The slightly higher measured G_{mm} value will cause the percentage of air voids to be 0.4% higher than if the design G_{mm} value was used.

The percentage of air voids in the **I-25N** surface mixture is slightly lower (7.2%) than the I-25D surface mixture specimens, but still would be considered high for a mixture that has undergone three years of traffic.

The percentage of air voids in the **I-70** surface mixture is slightly lower on the average (6.4%) than the **I-25D** and **I-25N** mixtures. However, the uncut specimens (I-70-1e and I-70-2e) have percentages of air voids very similar to the **I-25N** specimens.

Table 4 Bulk Specific Gravity and Percentage of Air Voids – Surface Mixtures

Specimen	G _{mb}		G _{mm}	Air Voids	
	SSD	CoreLok™		SSD	CoreLok™
I-25D-3	2.277	2.278	2.475	8.0%	8.0%
I-25D-4	2.266	2.267	2.475	8.4%	8.4%
I-25D-5 cut	2.279	2.280	2.475	7.9%	7.9%
I-25D-6 cut	2.259	2.264	2.475	8.7%	8.5%
I-25D-7 cut	2.263	2.266	2.475	8.6%	8.4%
Average I-25D	2.269	2.271	2.475	8.3%	8.2%
I-25N-11	2.294	2.295	2.475	7.3%	7.3%
I-25N-12	2.288	2.288	2.475	7.6%	7.6%
I-25N-13 cut	2.295	2.301	2.475	7.3%	7.0%
I-25N-15 cut	2.298	2.305	2.475	7.2%	6.9%
I-25N-16 cut	2.298	2.305	2.475	7.2%	6.9%
Average I-25N	2.295	2.299	2.475	7.2%	7.1%
I-70-1e	2.364	2.366	2.550	7.3%	7.2%
I-70-2e	2.350	2.358	2.550	7.8%	7.5%
I-70-3e cut	2.412	2.400	2.550	5.4%	5.9%
I-70-4e cut	2.397	2.391	2.550	6.0%	6.2%
I-70-5e cut	2.405	2.406	2.550	5.7%	5.6%
Average I-70	2.386	2.384	2.550	6.4%	6.5%

Mixture Composition – Asphalt Binder Content and Gradation

The recovered aggregate gradation and calculated asphalt binder content for the **I-25D** and **I-25N** surface mixtures are indicated in Table 5. The **I-25D** and **I-25N** recovered gradations are also illustrated in Figure 12 compared with the reported production gradations. The gradation and asphalt binder content for the **I-70** surface mixture are indicated in Table 6. The gradation for the **I-70** surface mixture is illustrated in Figure 13 along with the reported production gradation from the I-25 project.

Table 5 Mixture Composition for I-25D and I-25N Surface Mixtures

Sieve Size		Percent Passing						
Standard	mm	I-25D-4	I-25D-8	Average	I-25N-11	I-25N-12	Average	Production
1"	25	100	100	100	100		100	100
¾"	19	98.7	100	99.4	100		100	100
½"	12.5	88.6	87.2	87.9	89.5		89.5	89.9
3/8"	9.5	79.3	76.4	77.8	77.3		77.3	80.8
#4	4.75	58.2	55.6	56.9	53.6		53.6	59.0
#8	2.36	44.4	43.1	43.7	40.6		40.6	44.3
#16	1.18	30.6	30.7	30.6	27.8		27.8	
#30	0.600	20.3	21.2	20.8	18.5		18.5	22.9
#50	0.300	11.1	12.2	11.6	10.1		10.1	
#100	0.150	4.9	5.5	5.2	4.3		4.3	
#200	0.075	2.2	2.4	2.3	1.8		1.8	5.6
Asphalt Content		4.3%	4.0%	4.15%	4.0%	4.2%	4.10%	4.6

The I-25N-12 recovered aggregate was inadvertently discarded before performing gradation testing.

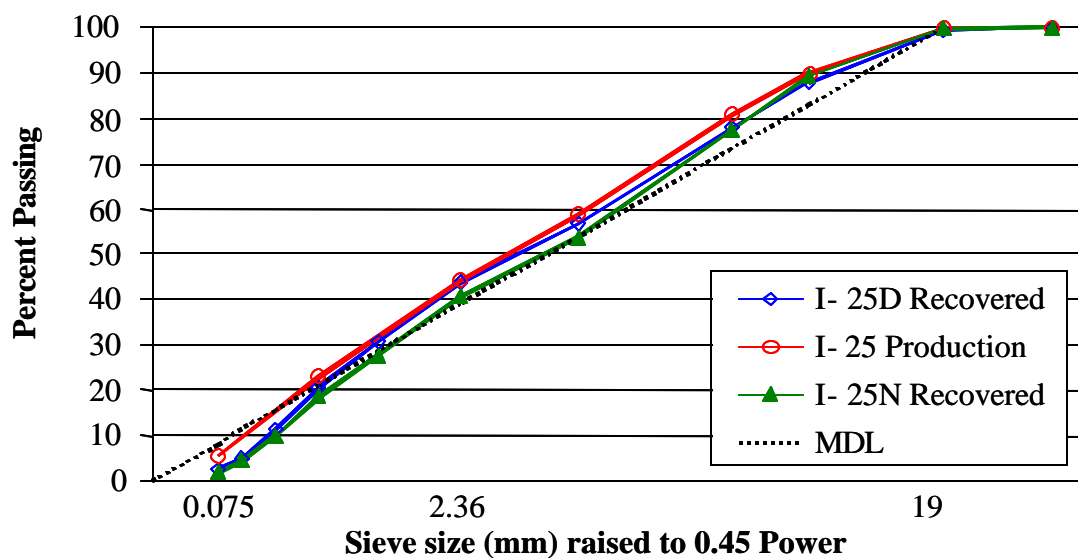


Figure 12 Recovered Aggregate Gradations for I-25D and I-25N Surface Mixtures

Table 6 Mixture Composition for I-70 Surface Mixture

Sieve Size		Percent Passing			
Standard	mm	I-70-1e	I-70-2e	Average	I-25 Production
1"	25	100	100	100	100
¾"	19	100	100	100	100
½"	12.5	87.7	86.8	87.2	89.9
3/8"	9.5	75.1	72.1	73.6	80.8
#4	4.75	57.3	54.8	56.0	59.0
#8	2.36	40.6	38.8	39.7	44.3
#16	1.18	27.1	26.4	26.7	
#30	0.600	17.4	16.9	17.2	22.9
#50	0.300	8.6	8.5	8.6	
#100	0.150	3.9	4.2	4.0	
#200	0.075	2.1	2.4	2.2	5.6
Asphalt Content		4.9%	4.7%	4.80%	4.6

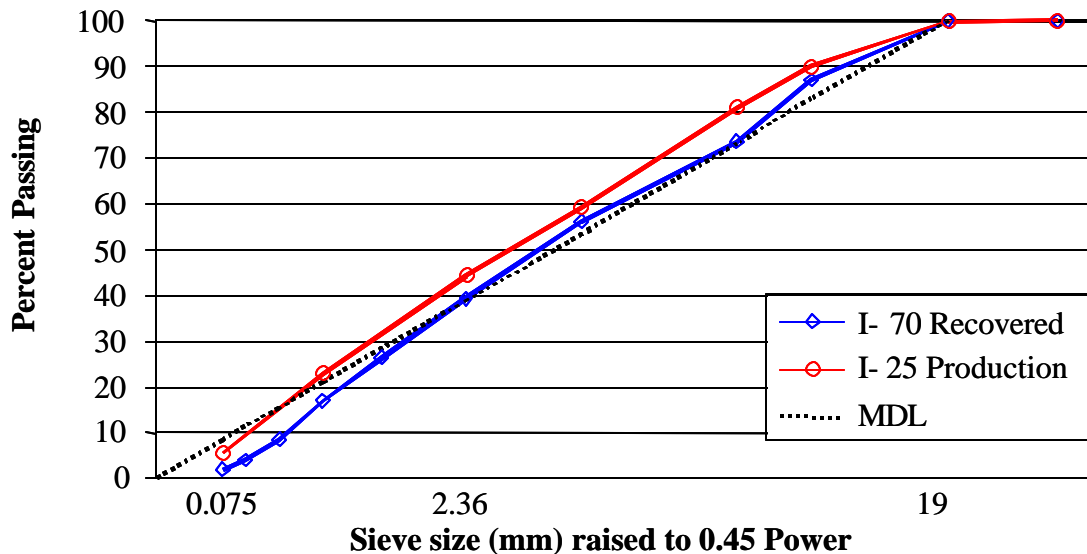


Figure 13 Comparison of Gradations for I-70 and I-25 Surface Mixtures

The data in Table 5 indicates that the recovered aggregate gradations of the **I-25D** and **I-25N** surface mixtures are very similar. In general, the recovered aggregate gradation is close to the average production values, but is slightly coarser.

The data in Table 5 also indicates two unexpected bits of information. The first is that the recovered dust content (percent passing the #200 or 0.075-mm sieve) is significantly lower than the average production value (5.6%). The production gradation is from cold feed samples. Gradation of the **I-25D** and **I-25N** surface mixtures is from produced hot-mix asphalt. Generally the dust content increases after going through the plant and the expected result from the cores should have been higher than the average production value.

The other piece of interesting information in Table 5 is that the measured asphalt binder content is significantly lower (approximately 4.1%) compared to the average production value (4.6%).

The data in Table 6 indicates that the recovered aggregate gradation of the **I-70** surface mixture is slightly more coarse than the I-25 average production values, but is similar to the recovered aggregate gradation from the **I-25D** and **I-25N** surface mixtures. As with the data in Table 5, the percent passing the #200 (0.075-mm) sieve is relatively low (2.2%). It should also be noted that the measured asphalt binder content is significantly higher (4.8%) than for the **I-25D** and **I-25N** surface mixtures (4.1%).

Figures 12 and 13 indicate average gradations that are very similar. All the mixtures have gradations that closely follow the Superpave maximum density line.

Recovered Asphalt Binder Properties

The recovered asphalt binder was tested in accordance with AASHTO MP-1. Since the asphalt binder had been in-service for three years, it was considered RTFO-aged after the recovery was complete. Some of the recovered asphalt binder was further PAV-aged for additional (low temperature) testing. Individual test results are indicated in Table 7. Each section has two replicates except for the **I-25D** mixture. The second replicate of the **I-25D** mixture was lost to equipment breakdown. The calculated critical temperatures are indicated in Table 8.

The data in Tables 7 and 8 provide two interesting observations. None of the five recovered asphalt binders would grade as a PG 76-28 asphalt binder. This is even true for three of the five samples if the recovered asphalt binder were compared to the original, or unaged, criterion (1.00 kPa) as opposed to the RTFO-aged criterion (2.20 kPa). Second, all five samples have substantially the same physical properties when tested in accordance with the AASHTO MP-1 procedures.

Table 7 Recovered Asphalt Binder Properties

	Temp, C	Sample				
		I-25D-4	I-25N-11	I-25N-12	I-70-1e	I-70-2e
RTFO ¹	64	3.44	2.99	---	3.15	---
G*/sin δ , kPa	70	1.62	1.44	2.56	1.50	2.41
	76	---	---	1.24	---	1.19
PAV	25	---	---	---	1599	2251
G*sin δ , kPa	22	2592	2293	3849	2400	3224
	19	3805	3346	5254	3538	4586
	16	5423	4815	---	5423	6415
	13	---	6805	---	---	---
PAV	-12	---	---	110	---	104
BBR S, MPa	-18	174	172	223	173	215
	-24	360	356	461	362	428
PAV	-12	---	---	0.349	---	0.356
BBR m-value	-18	0.326	0.330	0.300	0.326	0.306
	-24	0.274	0.276	0.250	0.271	0.256

¹ Assumed based on pavement age.

“---” indicates that data was not acquired at the listed temperature.

Table 8 Critical Temperatures of Recovered Asphalt Binder

Sample	Critical Temperature		
	High	Intermediate	Low
I-25D-4	67.7	16.7	-31.0
I-25D-8	---	---	---
I-25D Ave.	67.7	16.7	-31.0
I-25N-11	66.6	15.6	-31.2
I-25N-12	71.2	19.5	-28.0
I-25N Ave.	68.9	17.6	-29.6
I-70-1e	66.9	16.2	-30.8
I-70-2e	70.8	18.2	-28.7
I-70 Ave.	68.8	17.2	-29.8

Direct Tension Testing (DTT) and Determination of Critical Temperature

In addition to the AASHTO MP-1 tests, the direct tension test (AASHTO TP3) was performed on the PAV-aged samples of the recovered asphalt binders. After this information was collected, the critical cracking temperature was determined using AASHTO PP-xx and the TSARplus™ (Thermal Stress Analysis) software. The average failure stress, average failure strain, and critical temperature are indicated in Table 9.

Table 9 Direct Tension Test Data and Critical Cracking Temperature Determination

	Temp, C	Sample				
		I-25D-4	I-25N-11	I-25N-12	I-70-1e	I-70-2e
DTT	-18	4.02	4.03	3.84	4.22	4.32
Stress, MPa	-24	4.53	4.79	4.64	4.74	3.55
DTT	-18	1.98	1.99	1.18	2.06	1.68
Strain, %	-24	0.91	0.93	0.77	0.95	0.58
Critical Temp., C		-30.5	-31.2	-27 ^a	-31.0	-28.9

a Value estimated from graph. Insufficient material to complete T_c determination.

The data in Table 9 indicates that all five recovered asphalt binder samples have substantially the same low temperature physical properties and similar critical temperatures. The critical cracking temperatures are also very similar to the critical temperatures in Table 8 which were determined using AASHTO MP-1. The average critical temperature of the three recovered I-25 asphalt binders was -29.6°C . The average critical temperature of the two recovered I-70 asphalt binders was -30.0°C .

Comparison of Intermediate Temperature Stiffness With and Without PAV Aging

As developed during SHRP, the Pressure Aging Vessel (PAV) procedure was intended to subject the asphalt binder to a combination of elevated temperature and air pressure to provide a laboratory simulation of the actual aging expected in-service after an extended period of time (such as 5 – 15 years). Asphalt binders recovered from pavements that had been in-service for a long time (i.e., 10 years) would not have any further aging required before testing. It would be assumed that the in-service life would substitute for the PAV-aging. Since the I-25 and I-70 mixtures had been in place less than 5 years, the recovered asphalt binder was subjected to PAV-aging before conducting intermediate temperature DSR tests, and low temperature BBR and DTT tests.

In addition, some of the recovered asphalt binder from the I-25 and I-70 mixtures was tested at intermediate temperatures without PAV-aging. A comparison of the test results from the two conditions allows an estimate of the actual aging imposed on the asphalt binders. Table 10 provides information on the intermediate temperature stiffness and critical temperature for the two aging conditions of the recovered asphalt binders.

The recovered asphalt binder from all five samples indicates very similar intermediate temperatures regardless of additional aging. The critical temperature of the unaged (recovered) asphalt binder was lower than the PAV-aged recovered asphalt binder by $1.1 - 1.7^{\circ}\text{C}$. At 19°C , the $G^*\sin \delta$ value only increased by a factor of 1.14 to 1.33 times after additional PAV-aging. It is usually expected to see a much greater increase in PAV-aged values – 4 or more times the unaged values. This is an indication that the asphalt binder in both pavements had already aged significantly in three to four years of service.

Table 10 Recovered Asphalt Binder Properties (w/ and w/o PAV-aging)

	Temp, C	Sample				
		I-25D-4	I-25N-11	I-25N-12	I-70-1e	I-70-2e
PAV	25	---	---	---	1599	2251
G* $\sin \delta$, kPa	22	2592	2293	3849	2400	3224
	19	3805	3346	5254	3538	4586
	16	5423	4815	---	5423	6415
	13	---	6805	---	---	---
Crit. Temp, C		16.7	15.6	19.5	16.2	18.2
Unaged	25	---	---	---	1124	1576
G* $\sin \delta$, kPa	22	1837	---	---	1793	2412
	19	2933	2514	4625	2809	3662
	16	4393	3889	6639	4233	5383
	13	6421	5763	---	6139	---
Crit. Temp, C		15.0	14.1	18.4	14.7	16.6

¹ Assumed based on pavement age.

“---” indicates that data was not acquired at the listed temperature.

DSR Strain Sweep at Intermediate Temperature

An additional test being developed by the FHWA to check for the presence of modification in an asphalt binder is a strain sweep performed using the dynamic shear rheometer (DSR) at an intermediate grade temperature. In this test, the asphalt binder is tested at an intermediate temperature using strain levels from approximately 0.5% to 20%. The resulting response of the phase angle is believed to be related to the presence and type of modification.

Figure 14 illustrates DSR strain sweep for the **I-25N** and **I-70** recovered asphalt binders in addition to several other modified and unmodified binders. The phase angle response to shear strain is identical for the **I-25N** and **I-70** asphalt binders. The phase angle is an indicator of the molecular structure of the binder. The I-25N and I-70 binders have the same molecular structure. The initial phase angle (approximately 41°) for the Colorado binders indicates that they are similar to other modified binders such as the 74-28 EVA and the 75-28 SBS shown in Figure 3. The 70-28 and the 58-28 are unmodified binders and have higher phase angles than the modified systems. The slope of the Colorado binders is different than the other binders; however, that is because a different base asphalt binder was used.

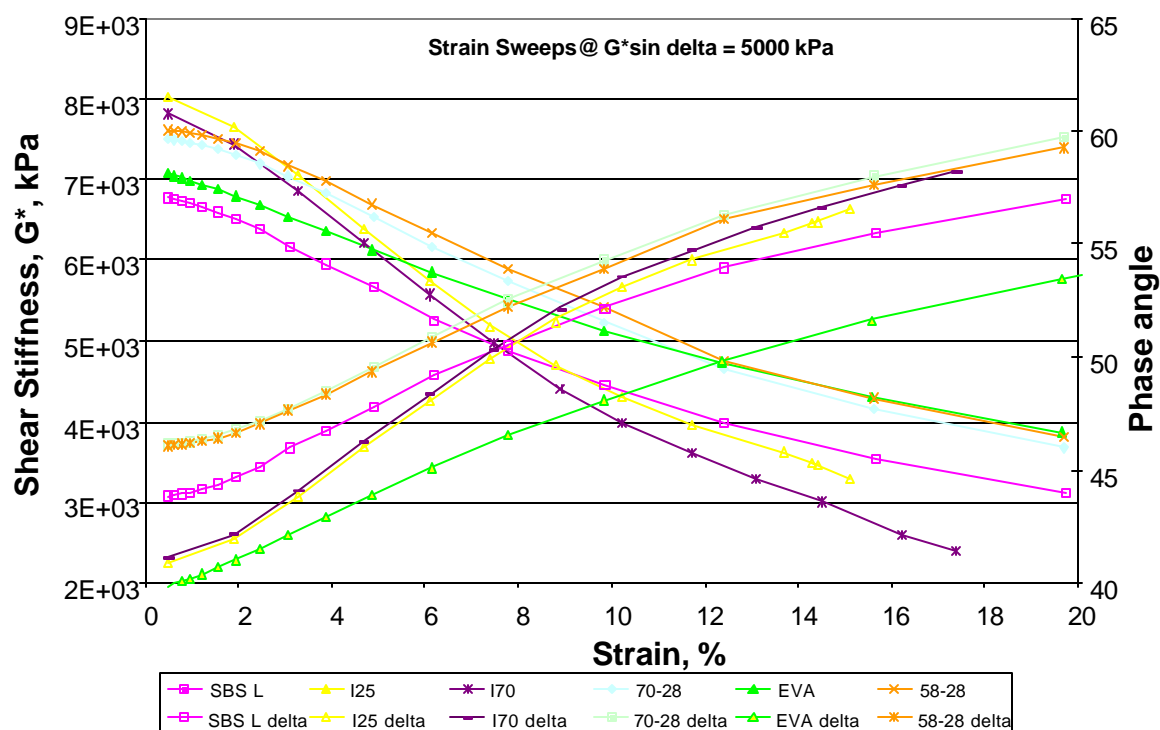


Figure 14 DSR Strain Sweep – I-25N and I-70 Recovered Asphalt Binders

Mixture Shear Stiffness

Core specimens designated for mechanical property tests were first cut at the layer interface and then trimmed to the appropriate height for testing in the Superpave shear tester (SST). Usually, the final specimen height is 50 millimeters. In the case of the **I-70** surface mixture, there was insufficient layer thickness to produce a 50-mm specimen. Instead the specimens were cut to a height of 38 millimeters for testing.

All mixture specimens were tested using the shear frequency sweep test at constant height procedure (AASHTO TP7). Testing was conducted at three test temperatures (16, 22, and 28°C) and ten loading frequencies (10 Hz to 0.01 Hz). Table 11 provides average test results for each mixture at the three different temperatures. Individual test data is included in Appendix C.

Table 11 Shear Stiffness – Surface Mixtures

	Complex Shear Modulus, MPa		
	I-25D	I-25N	I-70
Frequency, Hz	Temperature 16°C		
10	1801	2041	2567
5	1637	1872	2325
2	1427	1645	2040
1	1258	1460	1796
0.5	1102	1292	1567
0.2	920	1084	1300
0.1	795	939	1115
0.05	679	806	956
0.02	548	662	771
0.01	466	570	667
Frequency, Hz	Temperature 22°C		
10	1425	1641	2320
5	1255	1457	2082
2	1045	1228	1772
1	888	1052	1540
0.5	752	893	1328
0.2	595	713	1075
0.1	501	599	919
0.05	421	504	784
0.02	332	398	632
0.01	284	335	532
Frequency, Hz	Temperature 28°C		
10	1016	1204	1410
5	861	1029	1187
2	683	814	921
1	559	668	739
0.5	457	544	595
0.2	348	413	446
0.1	285	338	360
0.05	233	276	292
0.02	182	214	227
0.01	152	179	190

Figures 15, 16 and 17 illustrate the average response of the shear modulus to frequency for each of the three mixtures. Figure 18 compares the average response of the three mixtures at 22°C. Figure 19 indicates the average response of the three mixtures at a loading frequency of 10 Hz.

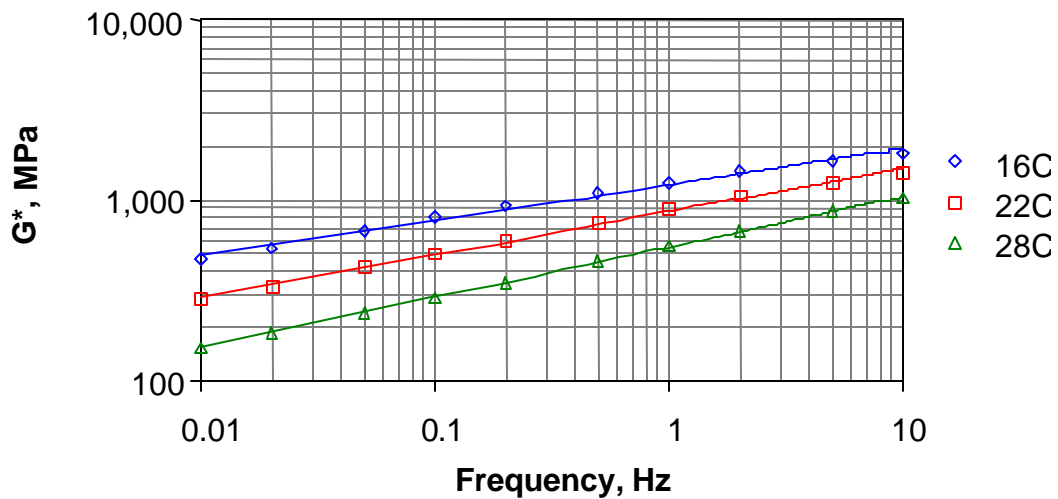


Figure 15 Shear Stiffness of the I-25D Surface Mixture

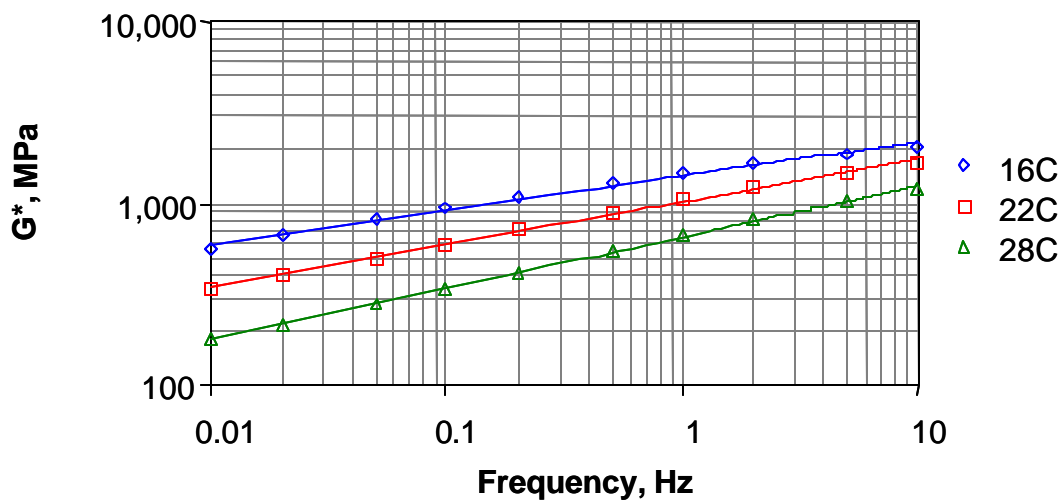


Figure 16 Shear Stiffness of the I-25N Surface Mixture

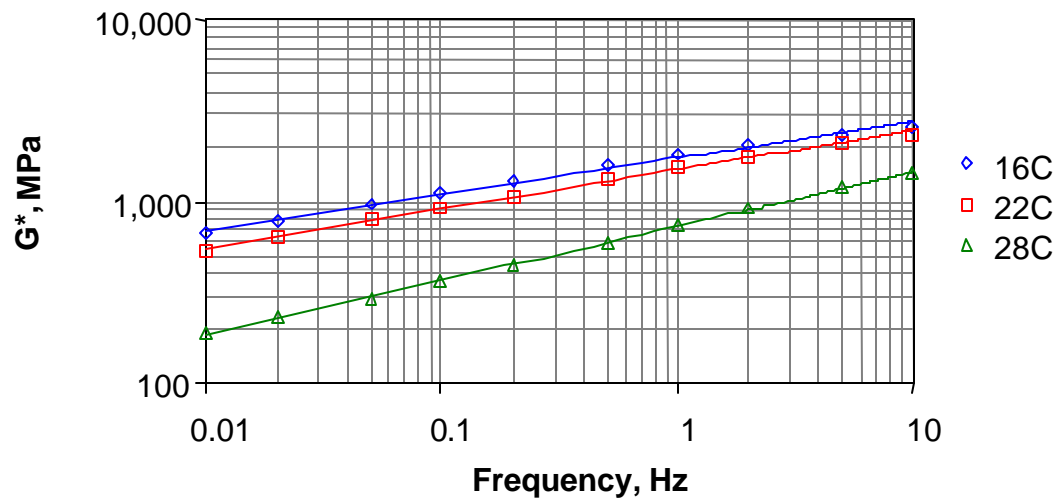


Figure 17 Shear Stiffness of the I-70 Surface Mixture

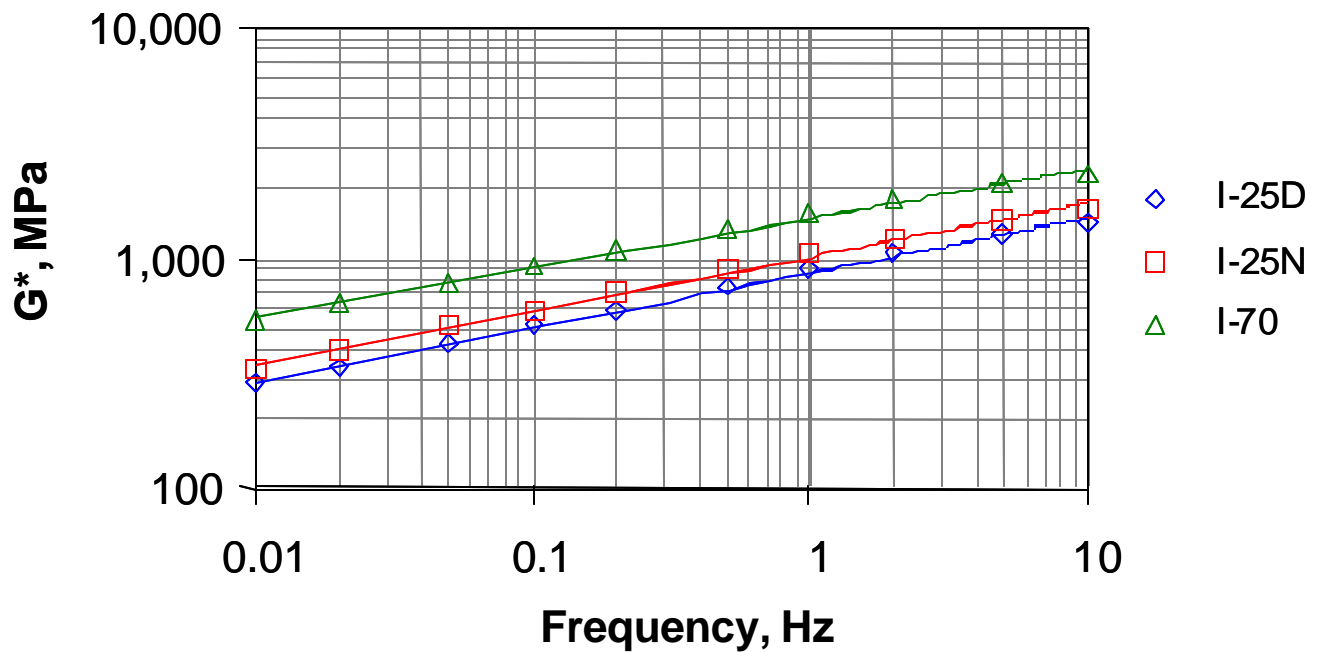


Figure 18 Average Shear Stiffness at 22°C – All Surface Mixtures

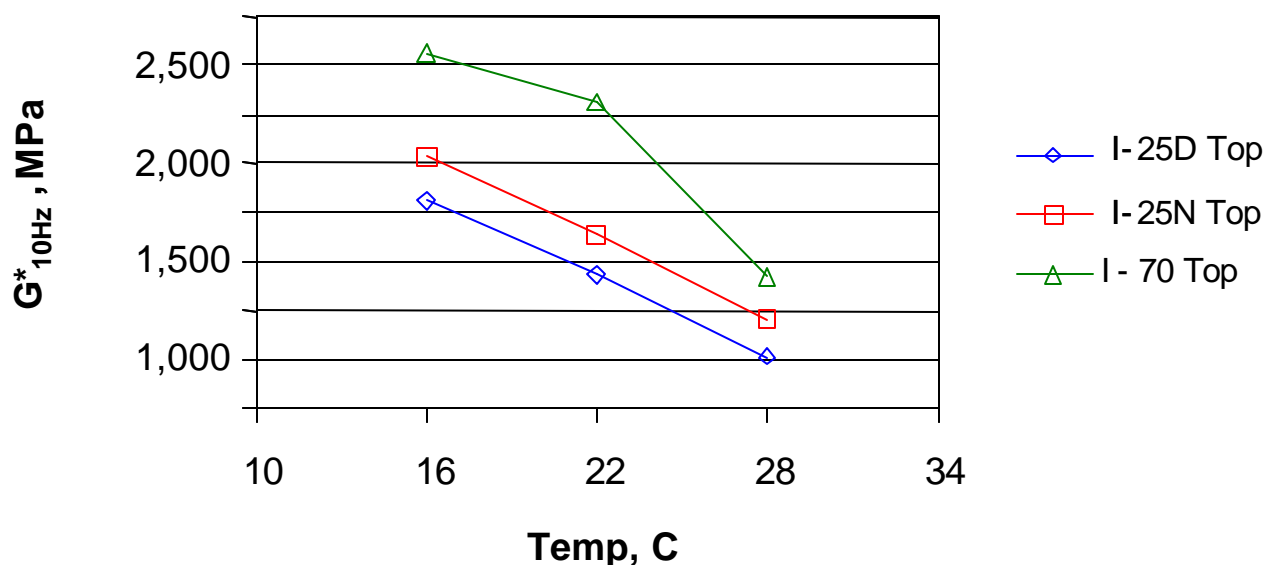


Figure 19 Average Shear Stiffness at 10 Hz – All Surface Mixtures

The data in Figure 18 indicates that the **I-70** surface mixture has a higher shear stiffness than the **I-25N** and **I-25D** mixtures at 22°C for all loading frequencies. At a loading frequency of 10 Hz (selected to simulate highway traffic speed), the **I-70** mixture has higher shear stiffness at all three temperatures (Figure 19) than the **I-25N** and **I-25D** mixtures. A statistical analysis performed on the shear stiffness values at 10 Hz ($G^*_{10\text{Hz}}$) indicates that the **I-70** surface mixture is significantly stiffer ($\alpha = 0.05$) than the **I-25N** and **I-25D** surface mixtures at 16°C and 22°C. At 28°C, the **I-70** mixture is significantly stiffer than the **I-25D** mixture, but statistically equal to the **I-25N** mixture. The **I-25D** and **I-25N** mixtures are statistically equal at all three temperatures.

Shear Stiffness of the Lower Layer Mixtures

The lower (intermediate) layer mixtures were also tested to determine shear stiffness. Table 12 provides average test results for each intermediate mixture at the three different temperatures. Individual test data is included in Appendix C. Table 13 provides a summary of the shear stiffness at 10 Hz for the top (surface) and lower (intermediate) layer mixtures.

As indicated in Table 12, the shear stiffness of the **I-70** intermediate layer mixture is much lower than the **I-25D** and **I-25N** intermediate mixtures. As with the surface mixtures, the **I-25N** intermediate mixture is slightly stiffer than the **I-25D** mixture.

The data in Table 13 indicates that the intermediate mixtures from the **I-25D** and **I-25N** sections are approximately 1.17 to 1.25 times stiffer than the surface mixtures. The **I-70** intermediate mixture, however, is 0.42 times as stiff as the **I-70** surface mixture.

Table 12 Shear Stiffness – Intermediate Mixtures

	Complex Shear Modulus, MPa		
	I-25D	I-25N	I-70
Frequency, Hz	Temperature 16°C		
10	2368	2421	1298
5	2126	2236	1134
2	1812	1987	928
1	1577	1800	786
0.5	1348	1611	662
0.2	1090	1382	527
0.1	907	1219	440
0.05	755	1069	370
0.02	578	881	290
0.01	480	759	248
Frequency, Hz	Temperature 22°C		
10	1730	1898	853
5	1480	1700	711
2	1192	1450	558
1	980	1256	456
0.5	792	1074	371
0.2	592	867	285
0.1	471	730	235
0.05	376	614	192
0.02	277	485	151
0.01	227	405	130
Frequency, Hz	Temperature 28°C		
10	1228	1393	563
5	997	1203	456
2	746	970	342
1	587	806	273
0.5	454	661	218
0.2	322	506	165
0.1	249	412	135
0.05	193	334	113
0.02	141	253	89
0.01	116	204	76

Table 13 Shear Stiffness at 10 Hz – All Mixtures

Mixture	Shear Stiffness $G^*_{10\text{Hz}}$ (MPa)		
	16° C	22° C	28° C
I-25D Surface	1801	1425	1016
Intermediate	2368	1730	1228
I-25N Surface	2041	1641	1204
Intermediate	2421	1898	1393
I-70 Surface	2567	2320	1410
Intermediate	1298	853	563

Indirect Tensile Strength and Strain at Failure

Additional cores were obtained from I-25 for resilient modulus and indirect tensile strength testing. Two cores remained from the original set of I-70 cores. The surface layer of the I-25 cores was separated from the remainder of the core and sawed to a thickness of 50 millimeters. The surface layer of the I-70 cores was sawed at the layer interface to provide a specimen with 38 millimeters thickness. Specimen dimensions (thickness, diameter) were measured as well as the bulk specific gravity of the cut cores. The percentage of air voids in the test specimens was determined using the previously measured maximum theoretical specific gravity values for the I-25 and I-70 mixtures. The average percentage of air voids was 7.0% and 5.0% for the I-25 and I-70 specimens, respectively.

The indirect resilient modulus of the test specimens was determined in accordance with ASTM D4123. Specimens were tested at 22°C. In accordance with the test procedure, the resilient modulus was determined at six different loading conditions – three loading/rest periods at two rotations. Each test used a 0.1-second pulse load followed by a rest period. The three rest periods were 0.9, 1.9, and 2.9 seconds. The specimens were also tested at two rotations with a 90-degree separation. If the specimen is uniform and the mixture is homogeneous, the results of the two rotations should be equal. However, if the specimen is non-uniform and/or the mixture is non-homogeneous, the resilient modulus test results for the two rotations will be different.

The axial load used in the resilient modulus tests was determined by performing the indirect tensile strength test on the I-25-1 test specimen at 22°C using a displacement rate of 12.5 mm/min. The peak load at failure for this specimen was 2,252 pounds.

Thus, the target load used in the resilient modulus tests was 25% of this load – 563 pounds.

After the resilient modulus testing was completed, the indirect tensile strength of the test specimens was determined by loading the specimen at a displacement rate of 12.5 mm/min until failure at 22°C. The load and deformations (horizontal and vertical) were measured throughout the test to determine the ultimate load at failure and strain at failure (maximum load).

Indirect resilient modulus results are indicated in Table 14.

Table 14 Indirect Resilient Modulus at 22°C

Rest Period (sec)	Rotation	Resilient Modulus, MPa			
		I-25-7	I-25-8	I-70-6e	I-70-7e
0.9	0	4,626	4,656	4,355	3,933
	90	4,517	4,449	4,362	5,179
1.9	0	4,585	4,599	4,407	3,979
	90	4,505	4,464	4,348	5,304
2.9	0	4,747	4,665	4,393	3,978
	90	4,432	4,417	4,423	5,253

Specimen I-25-6 was not tested because of high variance in the deformations on each face. This is usually an indication that the specimen (core) is not right angle cylindrical.

The data in Table 14 indicates that only Specimen I-70-7e had a significant difference in resilient modulus based on rotation. This is an indication that the specimen may have been slightly non-uniform in dimensions. Rest periods had no measurable effect on the resilient modulus values.

The average indirect resilient modulus for the I-25 specimens was 4,555 MPa at 22°C. The average indirect resilient modulus for the I-70 specimens was 4,492 MPa at 22°C. A t-test (at $\alpha = 0.05$) indicated that these values are statistically equal.

Test results from the indirect tensile strength tests are indicated in Table 15.

Although the I-25 specimens have average values of tensile strength, horizontal strain, and vertical strain at failure that are higher than the I-70 specimens, the average values are not considered statistically different ($\alpha = 0.05$).

Table 15 Indirect Tensile Strength at 22°C

Mixture	St, kPa	Horizontal Strain (10^{-6})	Vertical Strain (10^{-6})
I-25-6	896	6,266	8,552
I-25-7	998	7,412	8,041
I-25-8	950	6,413	6,859
I-25 Average	948	6,697	7,817
I-70-6e	871	6,166	7,419
I-70-7e	906	4,955	7,145
I-70 Average	888	5,560	7,282

As a further illustration, the horizontal and vertical deformations for the test specimens are shown in Figures 20 and 21.

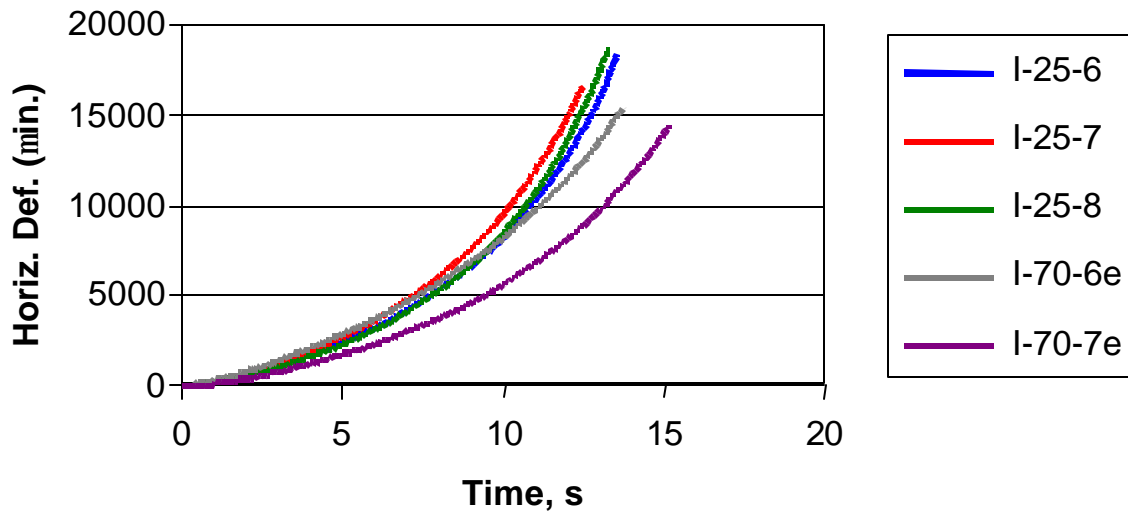


Figure 20 Horizontal Deformation from IDT Tests (22°C, 12.5 mm/min.)

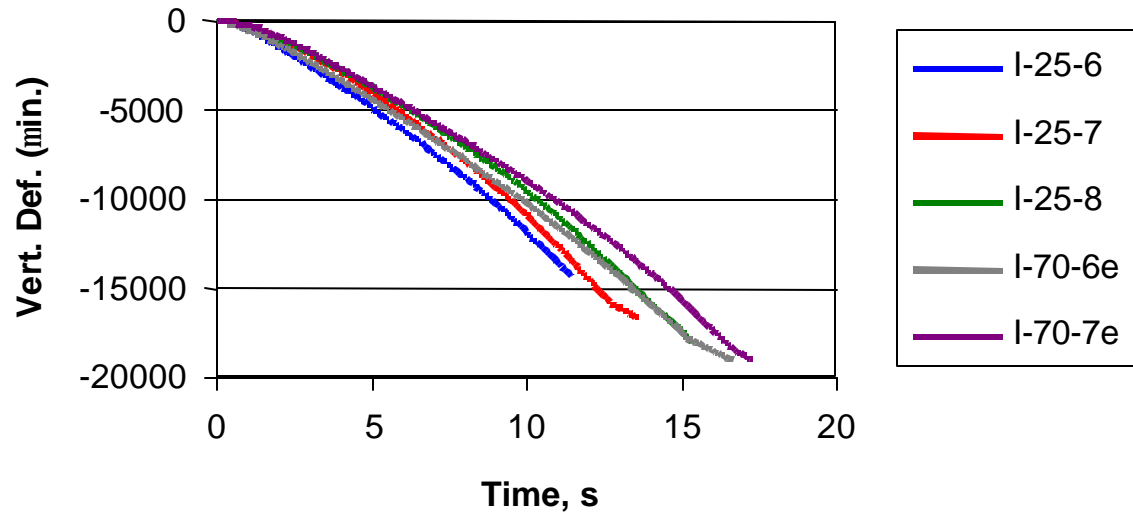


Figure 21 Vertical Deformation from IDT Tests (22°C, 12.5 mm/min.)

ADDITIONAL COLORADO DOT RESULTS

Colorado DOT initiated some additional testing that is included here for completeness. Test data is located in Appendix D.

Two ideas were tested:

- Is there any indication of moisture damage potential in the overlay?
- Is the segregation identified in the slab removed from the road present at other places where the crack occurs?

Moisture Damage

Two sets of cores were taken from the I-25 northbound outside lane. The first set was taken in an area 487 feet north of the Milepost 224 marker that had longitudinal cracking. The second was taken 600 feet north of the MP 224 marker, a non-distressed area.

Tensile strength ratio (Lottman) testing was done on the sets of cores. At each of the distressed and non-distressed locations three cores were moisture conditioned and three were not. Table 16 lists the unconditioned and conditioned loads and the tensile strength ratio for each.

Both the distressed and non-distressed sites have nearly the same TSR. Also both sites have nearly the same unconditioned strengths.

Table 16 Tensile Strength Ratio

	Distress Location	Non-Distress Location
Conditioned Load (lb.)	1519	1472
Unconditioned Load (lb.)	1867	1919
TSR	81%	77%

Segregation

Three sets of cores were taken starting from 316 feet north of MP 224 and continuing to 487 feet north of MP 224. Cores were taken on top of the crack which occurred about 44 inches from the shoulder line and from the wheelpath. Figure 22 shows the layout of the cores.

Figure 23 shows the gradation obtained from the cores. Gradation of the cores from atop the crack is labeled as 44 inches from the shoulder. The gradation of cores from between the crack and the shoulder is labeled as 20 inches from the shoulder. Also shown is the gradation of cores taken in the forensic study. They were taken approximately 100 inches from the shoulder.

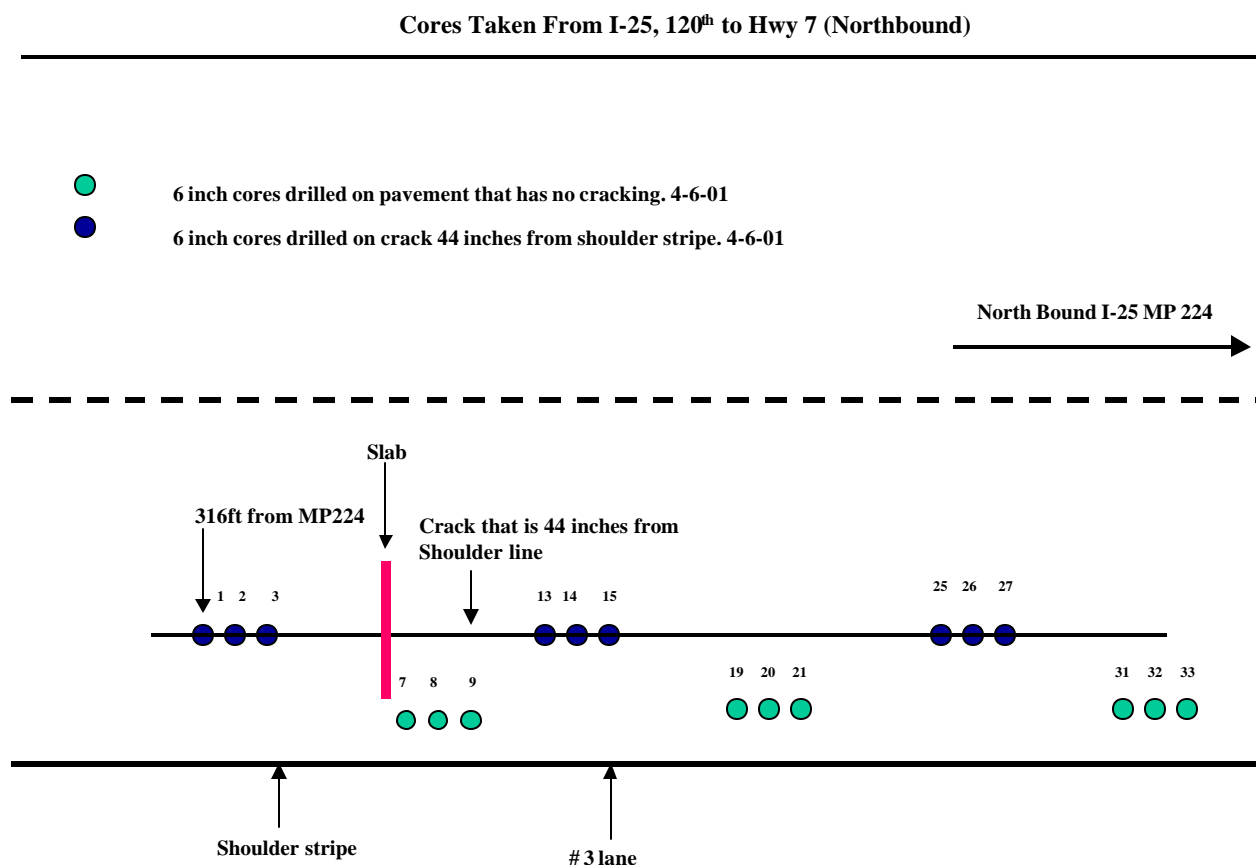


Figure 22 Layout of Cores Taken to Investigate Segregation

As shown previously in Figure 12, the gradation at 100 inches from the shoulder closely matched the average quality control gradation. As shown in Figure 23 the cores at 44 inches are considerably coarser and cores at 20 inches are considerably finer than the quality control gradation. On the 4.75 mm sieve the gradation at 20 inches is 7 percent finer (65 Vs 58%) and the gradation at 44 inches is 9 percent coarser (49 Vs 58%).

The asphalt content was considerably different for the 44 inch and 20 inch cores, 4.2% compared to 5.2%. Figure 24 shows a plot of asphalt content for the individual cores

taken at 44 and 20 inches and the percent passing the 2.36 mm sieve. There is clearly a relationship between the measured asphalt content and the gradation, indicating the mixture was segregated after it left the hot mix plant.

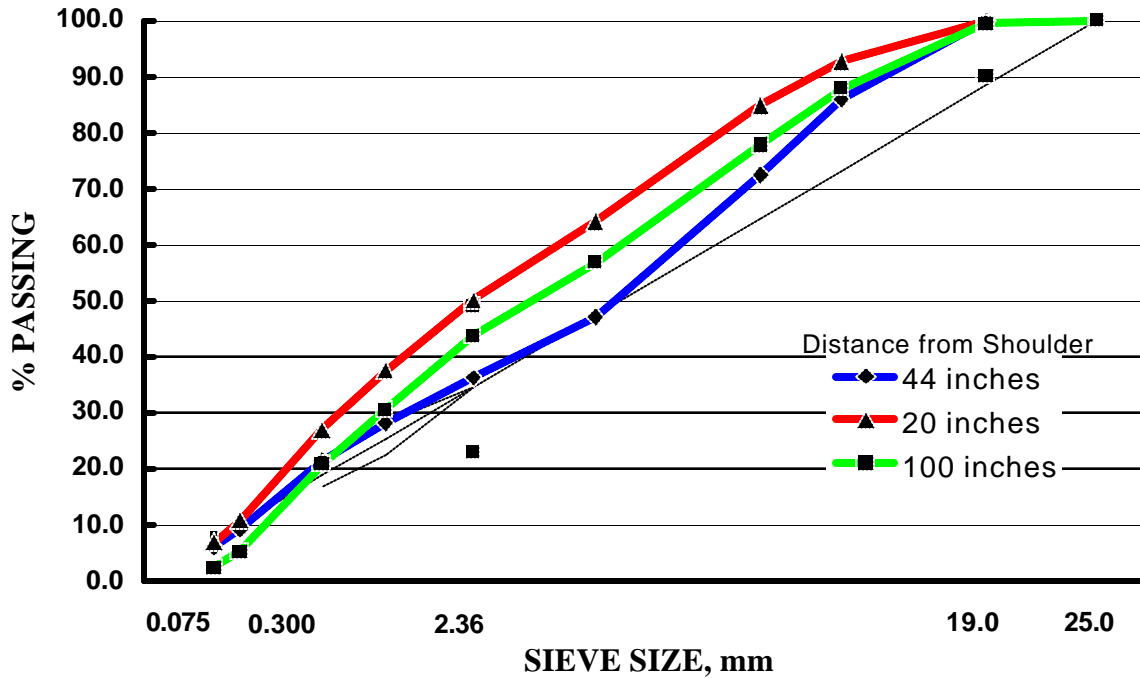


Figure 23 Gradations from Colorado DOT Cores

Figure 24 Plot of Asphalt Content Vs Percent Passing 2.36 mm Sieve for CDOT Cores

DISCUSSION OF RESULTS

The testing plan was developed around five hypotheses:

1. The PG 76-28 asphalt binder in the **I-25D** cores has the same physical properties as the PG 76-28 asphalt binder in the **I-25N** cores and significantly different physical properties than the PG 76-28 asphalt binder in the **I-70** cores.
2. The stiffness of the **I-25D** surface mixture is the same as the stiffness of the **I-25N** surface mixture and significantly different than the stiffness of the **I-70** surface mixture.
3. The dust content (percentage passing the #200 or 0.075-mm sieve) of the **I-25D** and **I-25N** mixtures is higher than indicated by the quality control/acceptance data.
4. The stiffness of the lower layer (mixture) of the **I-25D** section is different than the stiffness of the lower layer of the **I-25N** section.
5. There is a high percentage of air voids in the **I-25D** and **I-25N** surface mixture that, when combined with the milling of the outside lane, contributed to possible moisture damage in the I-25 lower layer.

Following initial testing, additional cores were taken to test a sixth hypothesis:

6. The indirect tensile strength and strain at failure of the **I-25D** and **I-25N** cores are significantly different (lower) than the indirect tensile strength and strain at failure of the **I-70** cores.

Volumetric Properties

Volumetric property testing and analysis indicated that the maximum theoretical specific gravity (G_{mm}) values of the **I-25D** and **I-25N** cores were the same. These G_{mm} values were slightly higher (2.475) than indicated by the design data (2.466). This difference should cause an increase in the percentage of air voids in test specimens by 0.4% and a decrease in the actual density measured in the field by the same amount. Assuming that the effective specific gravity of the aggregate (G_{se}) did not change during production, the slightly higher G_{mm} values should correlate with a decrease in the asphalt binder content to 4.36% from the design of 4.6%.

The measured percentages of air voids in the **I-25D** and **I-25N** cores were 8.3% and 7.2%, respectively. Quality assurance data indicated that the average density achieved on the project during construction was 93.6% of maximum theoretical density (using $G_{mm} = 2.466$). This corresponds to an average percentage of air voids of 6.4%. The highest and lowest reported density values out of 124 tests were 96.3% (3.7% air voids)

and 91.8% (8.2% air voids), respectively. The percentage of air voids obtained from the quality assurance data does not agree with the percentage of air voids measured within the pavement cores.

The relatively high percentage of air voids in the I-25 cores is also unusual for a pavement that has been subjected to three years of traffic. Past experience by asphalt technologists indicate that:

- The majority of traffic densification will occur within the first three years - generally as a function of the logarithm of the number of traffic applications [3,4]; and
- Superpave mixtures compacted using 86 to 128 gyrations exhibited appropriate densification with the percentage of air voids between 3.5% and 6.0% [5].

Considering that the I-25 cores had been subjected to three years of traffic at the time of coring, two possibilities exist for the relatively high percentage of air voids. Either the mixture did not densify under traffic, or the initial percentage of air voids was higher than indicated by the quality assurance data.

The I-70 cores also indicated a higher than anticipated percentage of air voids (6.4%) for a mixture that had been subjected to approximately three years of traffic.

The first part of Hypothesis 5 was confirmed by the relatively high percentage of air voids in the I-25 cores. However, moisture damage was not indicated in the lower layers of I-25. Consequently, this hypothesis was considered unlikely.

Mixture Composition

The recovered asphalt binder content (4.1%) from the I-25 cores was approximately 0.5% lower than indicated by the design (4.6%). The average asphalt binder content determined using 62 tests from the quality assurance data was 4.67%. The highest and lowest reported asphalt binder contents were 4.91% and 4.41%, respectively. The highest recovered asphalt binder content from the I-25 cores (4 samples) was 4.3%. As noted earlier, the slightly higher G_{mm} value measured from the cores should correlate with an asphalt binder content of 4.36%.

The calculated absorption of the asphalt binder was approximately 0.44% (assuming the bulk specific gravity of the aggregate is 2.617 and the effective specific gravity of the aggregate is 2.647). As a result, the effective asphalt binder content for the design was 4.16%. The effective asphalt binder content recovered from the I-25 cores was 3.70%.

The measured asphalt binder content of the I-25 cores (4.1%) and the corresponding effective asphalt binder content (3.7%) are low for a mixture that is a 19-mm nominal

mixture – particularly when the mixture could be considered very nearly a 12.5-mm nominal mixture. By contrast, the I-70 cores indicated a similar, but slightly coarser aggregate gradation and a significantly higher recovered asphalt binder content (4.8%).

The average recovered aggregate gradation for the I-25 cores was substantially close to the design and production values except for dust content. The measured percentage of aggregate passing the 0.075-mm (#200) sieve was 2.1%. This is substantially less than the average production value of 5.6%. The recovered dust content is consistent for all the samples, but is unexpectedly low. The research team does not have an explanation for the low percentage passing the 0.075-mm (#200) sieve.

The low percentage passing the 0.075-mm (#200) sieve definitely disproves Hypothesis 3.

Recovered Asphalt Binder Properties

The critical temperatures and physical properties of the recovered asphalt binders from the **I-25D**, **I-25N**, and **I-70** cores were determined to be equal. There appears to be no significant difference between the asphalt binders from the I-25 and I-70 cores. Based on these findings, Hypothesis 1 was rejected.

The recovered asphalt binder from the I-25 and I-70 cores was determined to meet the criteria for a PG 64-28 asphalt binder. The theoretical grade of the asphalt binder was PG 68-29. This is significantly different than the PG 76-28 asphalt binder specified in both project mixtures. In addition to the actual grading, the recovered asphalt binder did not behave as a typical modified asphalt binder (not elastic, high phase angle) at high test temperatures.

Although the high temperature grade of the asphalt binder did not meet expectations, the intermediate and low temperature properties were considered acceptable for the climate. Strain sweeps conducted on the DSR at an intermediate temperature indicated....

Low temperature analysis conducted using the new procedure for determining critical cracking temperature (using the direct tension test) indicated that the critical cracking temperature was substantially the same as the low temperature grade determined using just the bending beam rheometer data.

All of this information suggests that the recovered asphalt binder from the I-25 and I-70 cores was not behaving as a elastomer-modified asphalt binder (as expected from a PG 76-28 asphalt binder with the elastic recovery test required). The loss in expected high temperature grade suggests that one (or more) of the following occurred:

- The original asphalt binder was modified by some means other than, or in addition to, elastomer modification. This additional modification either was

unstable and the high temperature effects transient, or the additional modification was not capable of being recovered using the selected extraction/recovery procedure.

- The original asphalt binder was only modified with the elastomer modification, but the product was unstable and the high temperature effects were transient.
- The original asphalt binder was only modified with the elastomer modification, but the selected extraction/recovery procedure was unable to recover the modifier, thus leaving the base asphalt binder properties to be tested.

Of the three possibilities, the last was tested by recovering an asphalt mixture made in AI's lab with a PG 76-22 asphalt binder (SBS-modified). The recovered grade of the asphalt binder was a PG 82-22. This indicated that an elastomer-modified asphalt binder could be successfully recovered.

Finally, a comparison of the recovered asphalt binder properties with and without additional PAV-aging indicated that the intermediate temperature DSR values (and critical temperatures) were very similar. This is an indication that the asphalt binder had apparently aged significantly in only three years.

Mixture Mechanical (Stiffness) Properties

The **I-70** cores have significantly higher shear stiffness values (G^*) at highway loading frequency than the **I-25D** cores at a range of temperatures surrounding T_{eff} (FC) – the intermediate temperature for fatigue cracking (22°C). The **I-25N** cores have slightly higher shear stiffness values at 22°C than the **I-25D** cores, but the difference is not considered statistically significant. The difference in shear stiffness between the **I-25N** and **I-25D** cores is likely due to the difference in the percentage of air voids. Higher percentages of air voids result in lower shear stiffness values. The lack of a statistical difference suggests that cracking should be expected in the **I-25N** section, also.

Based on these findings, Hypothesis 2 was accepted as correct.

The shear stiffness (at 22°C) of the lower layers of the **I-25D** and **I-25N** cores were approximately the same. These stiffness values were 1.2 times the stiffness of the surface layers. The shear stiffness of the lower layer of the **I-70** cores was much lower than the **I-25** cores and much lower than the shear stiffness of the **I-70** surface layer. Based on these findings, Hypothesis 4 was rejected.

The indirect tensile strength and strain at failure of the I-25 and I-70 cores were also considered statistically equal. This is an indication that the tensile strength of the mixtures was likely not the main factor affecting the surface-initiated longitudinal cracking.

Top-Down Fatigue Cracking

Fatigue cracking is classically thought to be a crack that begins at the bottom of a structural layer and progresses upward. Top-down fatigue cracking is a phenomena where pavement cracking begins at the pavement surface and progresses downward. Bottom-up and top-down cracking is shown in Figure 25.

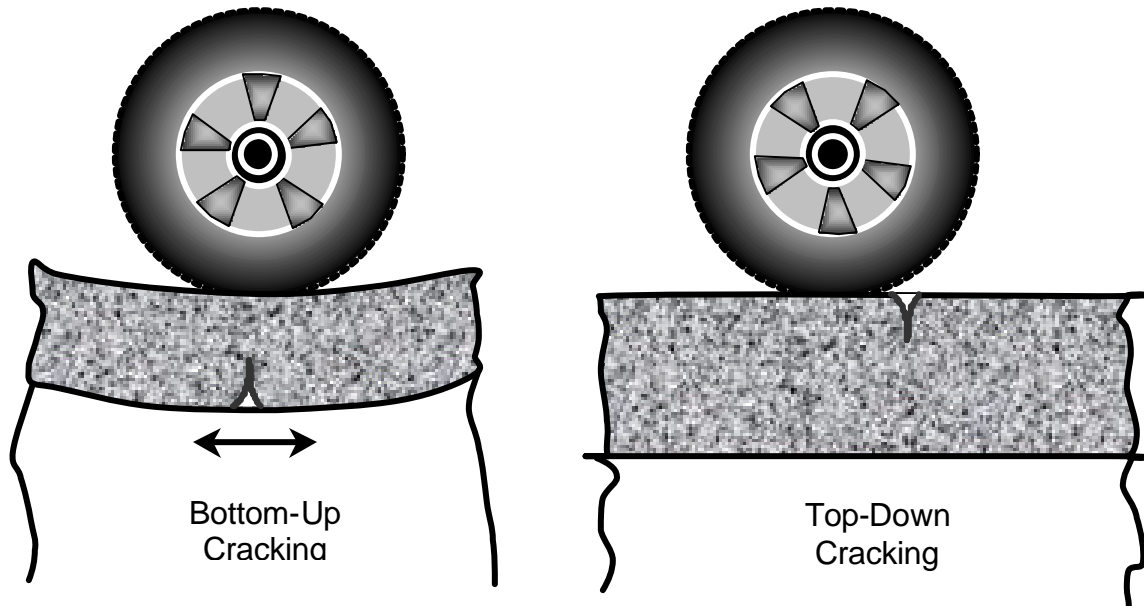


Figure 25 Development of Fatigue Cracking In Asphalt Pavements

Bottom-up fatigue cracking occurs when the asphalt allows enough flexing such that critical tensile strains are generated at the bottom of the asphalt layer. If the pavement is sufficiently thick, strains at the bottom of the asphalt layer are sufficiently small that bottom-up fatigue cracking is delayed nearly indefinitely. Slight bending and deflection at the surface of the pavement will cause cracks to begin developing at the road surface and begin to move downward. Surface-initiated cracks can be either transverse across the wheelpath or longitudinal along the edge of the wheelpath.

Commonly, surface-initiated cracking does not occur until later in the life of the pavement. Surface strains are usually small enough and the pavement is resilient enough that surface cracking does not initiate. If surface cracking does begin, it will not propagate through the entire pavement layer. Instead it will progress downward and stop partway through the layer. Figure 26 shows a core taken on top of a longitudinal crack on I-25. It is clear that the crack has started at the pavement surface and has propagated downwards.



Figure 26 Core taken on top of a longitudinal crack on I-25. The cracking is clearly contained only within the top layer of the pavement.

Top-down cracking would be expected in the later life of a pavement because earlier in the pavement life the surface layer would be sufficiently resilient to accommodate the strains imposed on it. If the surface layer is unable to accommodate the strains, the layer could begin to crack early in the pavement life. Low asphalt content or unusually aged asphalt binder could make the surface layer intolerant of strain. Segregation can also make the pavement layer intolerant of strain because asphalt content is low in areas of coarse aggregate concentration.

SUMMARY AND CONCLUSIONS

The pavement distress on I-25 includes both transverse cracking and longitudinal cracking within the wheelpaths. The transverse cracking is very likely reflective cracking from the underlying layers. The longitudinal cracking is surface-initiated (top-down). Regardless of the cracking mechanism, the appearance of the longitudinal cracks was earlier in the pavement life than would be expected.

A sampling plan was developed to obtain cores from two sections, one with distress and the other without distress. A slab was taken from a trench across the lane. Three cracks were present across the lane, at 44, 81 and 117 inches.

There was segregation present within the mat at each of the cracks. The segregation was particularly severe at the 44-inch-crack.

There are signs of low density at the bottom of the 1997 overlay. The distress is believed to be related to the low density.

There are no signs of stripping in the 1997 overlay. Some stripping was observed in the remaining portion of the 1984 mixture and there is some indication of stripping in the older mixture in the lower layers. Stripping does not appear to be severe.

A testing plan was developed to determine the physical characteristics of the asphalt surface mixture on I-25 and compare it to a mixture that had not cracked with similar age, asphalt binder, and traffic (I-70).

Test results indicated that the physical properties of the recovered asphalt binder from the I-25 and I-70 cores were the same. Thus, asphalt binder properties were not the principal reason for the cracking. However, the recovered asphalt binder from both pavements failed to meet the high temperature grade expected on the project. Instead of achieving a PG 76-28 grade, the recovered asphalt binders were PG 64-28 grade. While the intermediate and low temperature properties of the recovered asphalt binders were acceptable, the lack of apparent elastomeric-modification could have been a contributing, but not sole, factor in the cracking of the I-25 pavement.

Asphalt mixture composition for the I-25 cores indicated that the asphalt binder content was 4.1% – 0.5% lower than design value (4.6%) and consistently lower than any of the quality control – quality assurance data. By contrast, the recovered asphalt binder content of the I-70 cores was 4.8%. When the absorption of the asphalt binder into the aggregate is considered, the effective asphalt binder content (recovered) for the I-25 cores was 3.7%. This is a very low asphalt binder content for a surface (wearing course) mixture.

Asphalt mixture volumetric properties of the I-25 cores indicated that the percentage of air voids (7.2 – 8.3%) was relatively high for a pavement that had been subjected to three years of traffic. This result did not match expectations, as the quality control –

quality assurance data indicated that the initial percentage of air voids after construction was 6.4%.

Finally, the shear stiffness of the asphalt mixtures at 22°C indicated that the I-70 surface mixture was significantly stiffer than the I-25 surface mixture (both I-25D and I-25N sections).

Excluding segregation that was identified on I-25, the difference in cracking performance between the I-25 and I-70 pavements is likely caused by a number of contributing factors. These factors create a principal difference. The shear stiffness of the I-70 mixture is higher than the I-25 mixture, indicating better resistance to shear stresses (lower shear strains) at intermediate temperatures. The contributing factors include:

- percentage of air voids in the pavement;
- volume of effective asphalt binder; and
- physical properties of the asphalt binder.

In two of the three factors (percentage of air voids and volume of asphalt binder) the I-70 mixture had superior properties compared to the I-25 mixture. The lower percentage of air voids in the I-70 mixture contributes to higher shear stiffness. The higher asphalt binder volume contributes to improved cracking resistance. The similarities in recovered asphalt binder physical properties suggest that the asphalt binder was not the main contributing factor.

The I-25 mixture had lower than anticipated asphalt binder volume and higher than anticipated percentage of air voids in-place. As a result, the thinner asphalt binder films were subjected to early aging and higher shear strains for the same traffic loading. When combined with an asphalt binder that apparently did not have the expected elasticity, the overall effect was a mixture that was not sufficiently resistant to the shear strain induced by traffic.

By contrast, the I-70 mixture had a higher asphalt binder volume and lower percentage of air voids. Combined with the fact that the I-70 mixture was slightly coarser than the I-25 mixture, the resulting film thickness of the asphalt binder was greater for the I-70 mixture. The resulting mixture was more resistant to the shear strain induced by traffic, even with an asphalt binder that did not indicate the expected elastic behavior.

Based on the data analysis, it is our opinion that the early cracking of I-25 could not necessarily have been predicted or prevented by the Colorado Department of Transportation or the Contractor using the current specifications and tests. Initial materials testing, mix design, and construction testing all indicated a mixture within acceptable tolerance limits. A combination of factors (percentage of air voids, volume of asphalt binder, asphalt binder properties) resulted in a mixture that exhibited early aging and poor resistance to the shear strain induced by traffic.

In summary the premature cracking is caused by several factors which were combined on this project. These factors include:

- a. Higher in-place air voids than expected.
- b. Low effective asphalt content and
- c. Segregation within the mat.

Limited Study Area

The findings and conclusions of this investigation are based on surface observations of the entire project and sampling, by cores and cross sectional slab, of representative areas. The sampling is by necessity constrained to a small percentage of the roadway area. Observation of segregation within the mixture is limited to the one cross sectional slab that was removed and a series of cores used to confirm the segregation in a larger area. The areas for testing were selected as being representative of the remainder of the project and it is believed that the findings are appropriate for the remainder of the project.

[This page left blank]

Recommendations

Surface Mixture Type

Since surface-initiated longitudinal cracking is not affected by pavement structure as much as material properties [6,7], the surface material should be selected to achieve higher cracking resistance. Selecting mixtures with high design asphalt content will increase resistance to cracking.

The 19-mm nominal surface course mixture used on this project had a relatively low design volume of asphalt binder. The design asphalt content was acceptable for a 19-mm mixture. The asphalt content measured in the forensic study was unacceptably low for a 19-mm mixture. Consideration should be given to using a rut-resistant surface mixture with a greater asphalt binder volume on high-traffic pavements. This can be accomplished through the use of a mixture with a smaller nominal maximum aggregate size, such as a 12.5-mm mixture. A 12.5 mm mixture requires one percent more VMA than a 19.0 mm mixture, which increases the minimum allowable design asphalt binder content about 0.4%.

Many agencies are implementing stone mastic asphalt (SMA) mixtures for wearing course on high volume pavements. SMA has a higher design asphalt content which makes the mixture much more resistant to cracking and to embrittlement with aging. High dust content in the mixtures make it very stiff and highly resistant to rutting. SMA's have exhibited excellent rutting and cracking resistance.

Density Measurement

The I-25 pavement would likely have performed better (although not necessarily great) if the percentage of air voids on the road was lower (the in-place density was higher). Since the construction data indicated acceptable density (by nuclear gauge), CDOT should consider refinements to the density testing method.

When calibrating nuclear gages to cores the method used is to determine an offset between the cores and the gauge. That is, the average density as measured by cores is compared to the average density measured by the gauge. An alternative method is to plot the paired measurements for each location. On a plot of density as measured by core against density as measured by the gauge a best fit line is plotted. The equation of the line can be used to convert nuclear density readings into core density. Usually, there is not a constant offset between the two. It depends on the nuclear reading. Also, it is possible to see the goodness of fit of the correlation which gives an indication of the amount of scatter.

As an alternative to using a correlation between nuclear density gauge readings and core density, CDOT may want to consider measuring cores directly for density acceptance. The Department could evaluate selected projects using both cores and

nuclear gauges. The Department may want to consider using the CoreLOK device for measuring bulk specific gravity as part of the evaluation.

Asphalt Binder Content

There are three sets of data for the binder content for this project, the QC data, QA data, and the forensic data. The QC and QA binder content data was determined using the nuclear asphalt content gauge on samples taken from the windrow. The forensic binder content was determined by solvent extraction from cores. There was an average difference of 0.5% between the QC/QA data and the forensic data. Sampling location can affect results causing differences and should be investigated.

The QC/QA samples were taken from the windrow, just in front of the paver. If there was any segregation in the windrow this segregation would also be present in the QC/QA samples. Field sampling, many times, is the cause of variability in test results. Field sampling can be very difficult to perform and should be reviewed on a continuing basis to assure that bias is not introduced into the samples. In the case of the I-25 project, if the samples were segregated by the loss of coarse aggregate the binder content would appear higher than actual. For the fine graded Superpave mix produced on this project the loss of coarse aggregate through segregation and the resulting higher binder content would make the void properties seem to be on target.

The forensic samples were cores taken from the roadway. The coring may cause some bias in test results due to cutting of aggregate during the coring, but should not affect the binder content.

To analyze if there has been some change from segregation or bias from sampling several different checks can be done. The first is to review the gradation of the actual sample being tested. This review could be done with the ignition oven to check the binder content and gradation of the same sample used for void properties. An alternate method to check on composition of the mix is to use the effective specific gravity (Gse) of the compacted mix. The Gse is affected by the binder content and the gradation, but calculated from the bulk specific gravity of the mix and the binder content. If the Gse is off from the target either the binder content is off or the gradation has changed. This makes the Gse a quick and easy check of the mix components.

It is recommended that the Colorado DOT perform a study of asphalt content by different methods and determine if there are any issues of interest to the Department. The I-25 pavement would have performed better if the volume of asphalt binder was closer to the design value, or if the design asphalt binder content was higher. The use of an asphalt ignition oven for acceptance testing should be evaluated as part of the study.

Mechanical Properties of Asphalt Mixtures

An asphalt mixture can be tested to determine its resistance to strain and fracture (tensile and/or shear). Several methods currently exist, such as the dynamic complex modulus, flexural beam fatigue, Superpave shear, and indirect tensile tests, that permit determinations of mixture stiffness and strain resistance. Unfortunately, criteria values (i.e., what constitutes a good mixture?) are not universally available. The Colorado Department of Transportation (CDOT) may want to undertake further research to identify the selected test method and criterion to minimize the possibility of mixtures with poor cracking resistance.

Asphalt mixture tests to measure rutting resistance also exist. These include dynamic complex modulus, Superpave shear, and rut testers. National research is currently in progress for each of these methods. Some guidance for criteria exists for each of the methods but CDOT should evaluate any method for reasonableness before implementing it.

To evaluate changes in mixture types, i.e., changing surface mixture from 19.0 mm to 12.5 mm, CDOT can use any of the identified methods to compare the rut resistance of a proposed mixture against the rut resistance of the 19.0 mm mixture that was placed on I-25.

Testing for Segregation

Segregation was identified as one of the causes of the longitudinal cracks. It would be helpful to have a test to identify segregation, particularly segregation that is not visible from the surface. Such a test is not currently available. Development of such a test was outside the scope and resources of this study. Areas of segregation will have higher air voids. It may be possible to relate differences in density to potential longitudinal segregation, although other causes, such as roller overlap, may also cause density differentials across the mat.

Paving personnel should be conscious of sources of longitudinal segregation. Longitudinal segregation could be caused by windrow segregation or paver set up. Personnel should closely observe the paving operation to determine if there is a potential for hidden longitudinal segregation.

Pavement Rehabilitation Suggestions

The requirement for pavement rehabilitation is dependant on the serviceability of the pavement, the amount of rehabilitation funds available and the ability of maintenance forces to maintain the section. Currently, there is no problem with rutting and the pavement has a smooth ride except for a couple of areas of severe segregation where

raveling has required some patching. From a user's point of view the pavement is serviceable.

From an engineering point of view there is a concern that the longitudinal cracks will continue to worsen, leading to ejection of material from the cracks and development of potholes. If construction funds are not readily available, and maintenance is able to handle the amount of work, the longitudinal cracks can be filled to resist further deterioration. Timely and diligent crack filling should significantly reduce the rate of deterioration of the cracks. Visually, this will not create an aesthetically pleasing surface, but it is probably the most cost-effective treatment. Such treatment could forestall rehabilitation for 5 to 7 years.

Another option would be to diligently fill all existing cracks and place a micro-surfacing on top. This option would provide a more pleasing visual appeal. The life of the micro-surfacing is not likely to be long. Most likely, the longitudinal cracks will continue to degrade and crack filling will most likely be required beginning a year, maybe two, after placement of the micro-surfacing. Generally, micro-surfacing would be better suited to prevent degradation of a pavement suffering durability problems. The asphalt content of this mixture is low for a typical interstate highway, but currently, there is no indication that raveling is a problem. The problem is more localized, i.e., the longitudinal cracks, and a better maintenance solution is more likely crack filling.

If funds are available, the best long-term solution is to remove and replace the deteriorating mixture. If this approach is used it may not be necessary to completely replace the overlay. The outside driving lane and portions of the middle driving lane may need to be completely removed; however, portions of the middle lane and all of the inside lane could be left intact. Alternately, the middle and inside lanes could be partially removed only to a partial depth. If a fine-graded half inch nominal maximum mixture was used, the partial removal could be 1½ inches with a 1½ inch overlay.

Properties of the Asphalt Binder

The properties of the asphalt binder used on this project were studied and although it is believed that the binder properties did not contribute to the pavement distress there were unexplained issues identified with the recovered binder properties. It is important that CDOT remain current on binder testing issues by participating in User-Producer Group and Binder Expert Task Group activities.

REFERENCES

1. Bouldin, M.G., R. Dongré, G.M. Rowe, M.J. Sharrock, and D.A. Anderson. "Predicting Thermal Cracking of Pavements from Binder Properties: Theoretical Basis and Field Validation", Asphalt Paving Technology, Journal of the Association of Asphalt Paving Technologists, Volume 69, 2000.
2. Cominsky, R.J., G.A. Huber, T.W. Kennedy, and R.M. Anderson. The Superpave Mix Design Manual for New Construction and Overlays, SHRP Report A-407, Strategic Highway Research Program, National Research Council, Washington, DC, 1994.
3. Foster, C.R. Selecting Proper Marshall Procedures for Optimum Asphalt Content of Dense-Graded Paving Mixtures, National Asphalt Pavement Association Information Series IS-85, Lanham, MD, 1992.
4. Stroup-Gardiner, M., D.E. Newcomb, R. Olson, and J. Teig. "Traffic Densification of Asphalt Concrete Pavements", Transportation Research Record No. 1575, Transportation Research Board, National Research Council, Washington, DC, 1997.
5. Anderson, R.M., G.A. Huber, R.B. McGennis, R. Bonaquist, R.W. May, and T.W. Kennedy. Evaluation and Update of Design Gyration for the Superpave Gyratory Compactor (N_{design} II Experiment, Phase 2), Federal Highway Administration Technical Report, National Asphalt Training Center II, Asphalt Institute, 1999.
6. Myers, L.A., R. Roque, and B.E. Ruth. "Mechanisms of Surface-Initiated Longitudinal Wheel Path Cracks in High-Type Bituminous Pavements", Asphalt Paving Technology, Journal of the Association of Asphalt Paving Technologists, Volume 67, 1998.
7. Komoriya, K., T. Yoshida, and H. Nitta. "'WA-DA-CHI-WA-RE' Surface Longitudinal Cracks on Asphalt Concrete Pavement", paper submitted for consideration at the 2001 Annual Meeting of the Transportation Research Board, unpublished.

[This page left blank]

Appendix A

Selected Photographs During I-25 Forensic Evaluation

[This page left blank]



The Forensic Team discusses location of the sites to be sampled
L-R John D'Angelo, Gerry Huber and Mike Anderson



A current sample of coarse crushed aggregate from the same
gravel source used in the I-25 construction.



A current sample of coarse crushed aggregate from the same gravel source used in the I-25 construction.



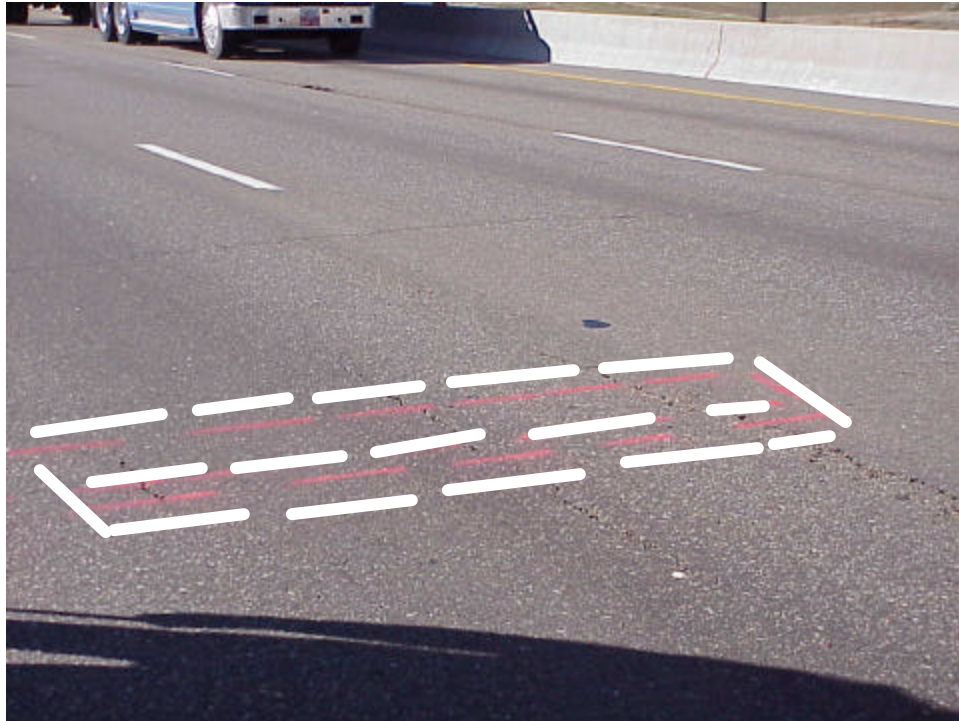
Condition of I-25 in the vicinity where the cores were taken in the distressed site.



Freshly cut, wet core showing aggregate skeleton. This is Core # 2 shown in the core location figure. It was taken at the end of a short longitudinal crack.



Location of the cross section slab before sawing.
From this angle the longitudinal cracks are not readily visible.



Location of the cross-section slab before sawing.
From this angle the longitudinal cracks are clearly visible.



View looking south of the distressed sampling site. Location of the cross section is where the three people are standing on the lane. Coring site is about 400 feet further south where the white half ton is parked diagonally across the lane.



View of the outside lane and center lane just north of where the cross section slab was taken. The vehicle in the corner of the photo is carrying the saw and is parked beside the cross section site.



Sawing of the cross section slab. Three saw cuts were made across the lane width. Cross cuts were made to break the slab into four pieces.



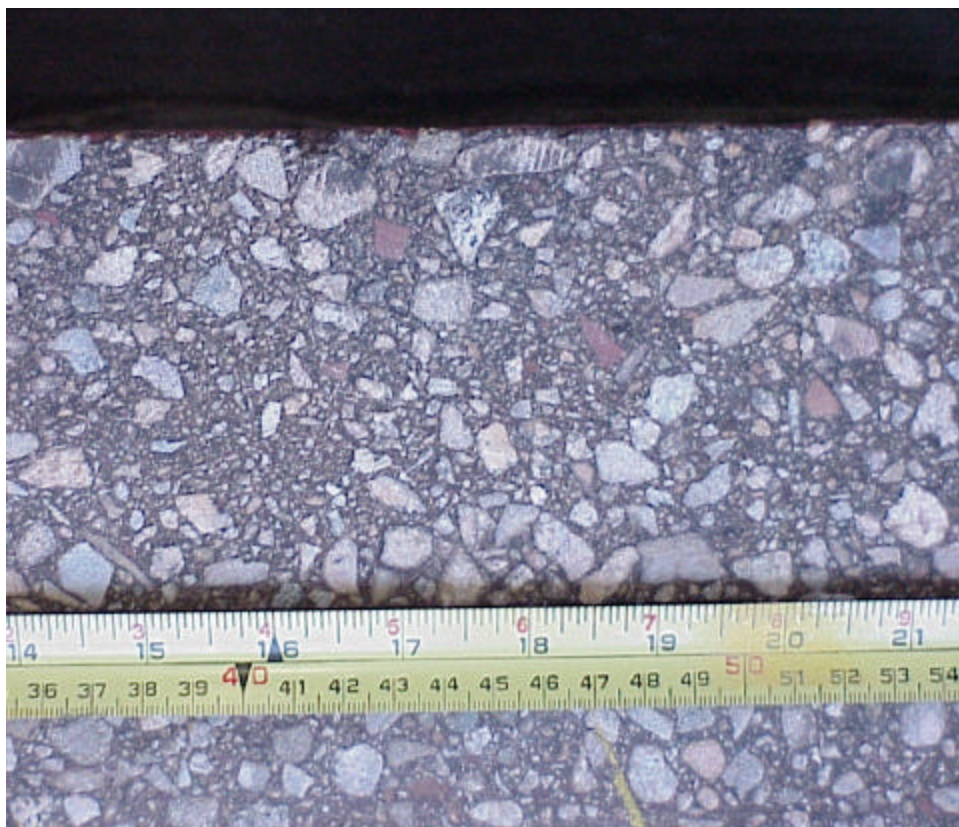
View looking south of distresses occurring on I-25. This location is about 0.3 miles north of where the cross section slab was cut. Just north of here is the no-distress site where cores were taken. Surface conditions could change very rapidly along the road. It was difficult to find sections that were not showing distress.

Appendix B

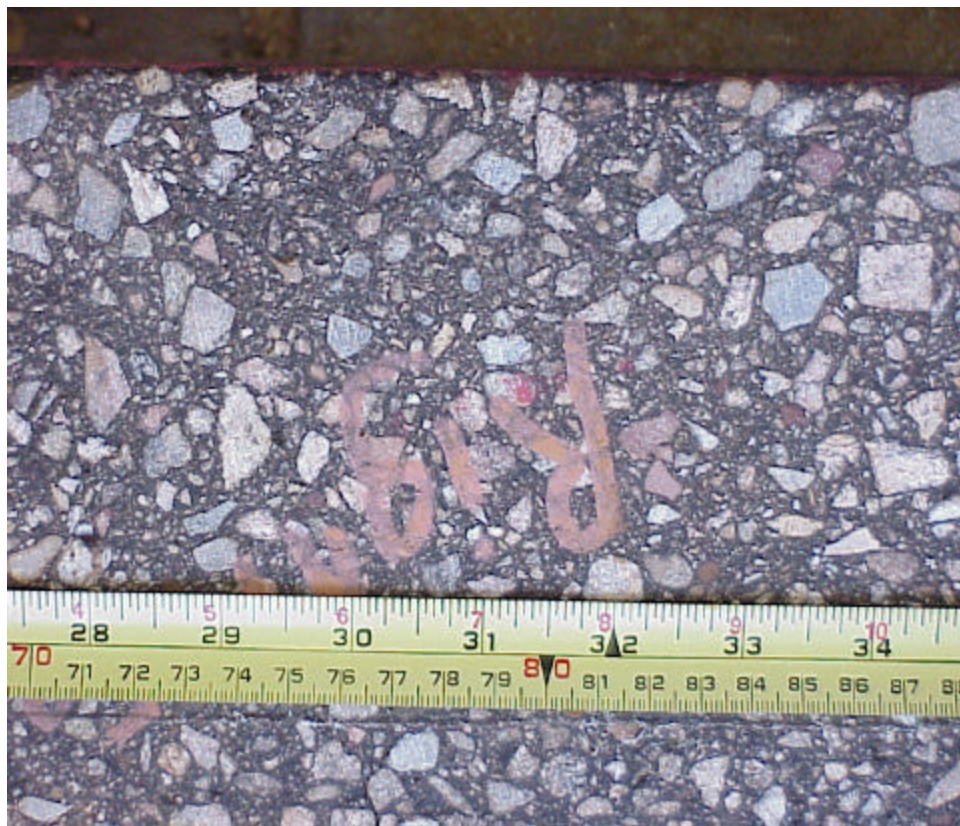
Photographs of Pavement Cross Section Slab

[This page left blank]



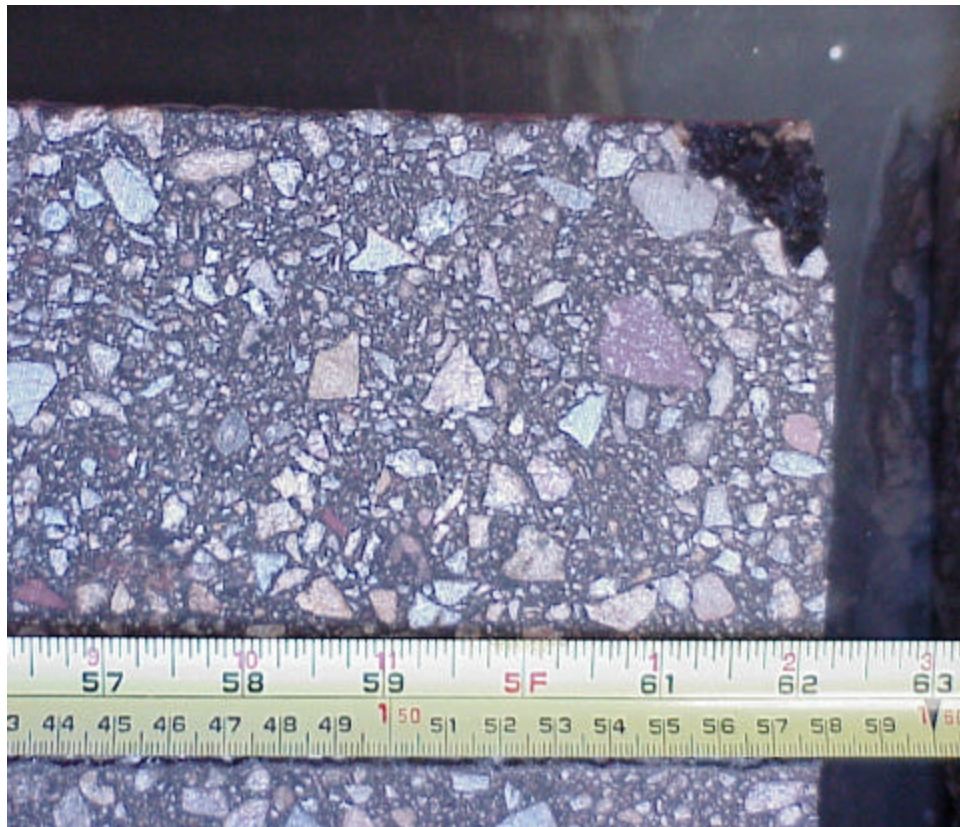


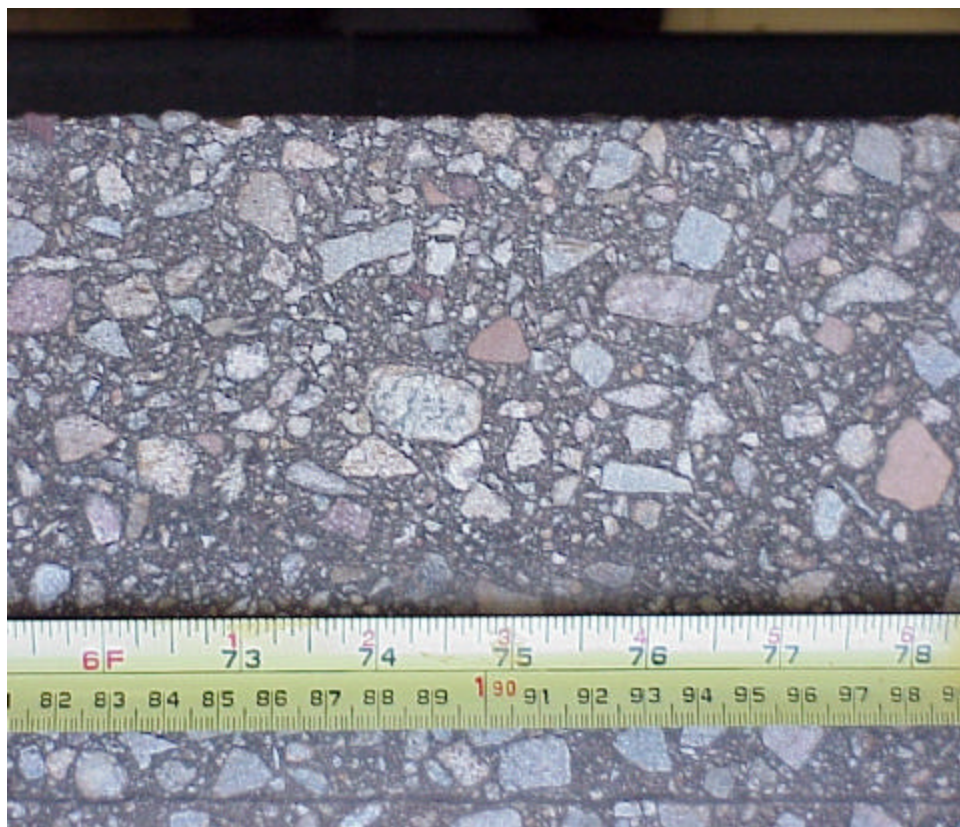
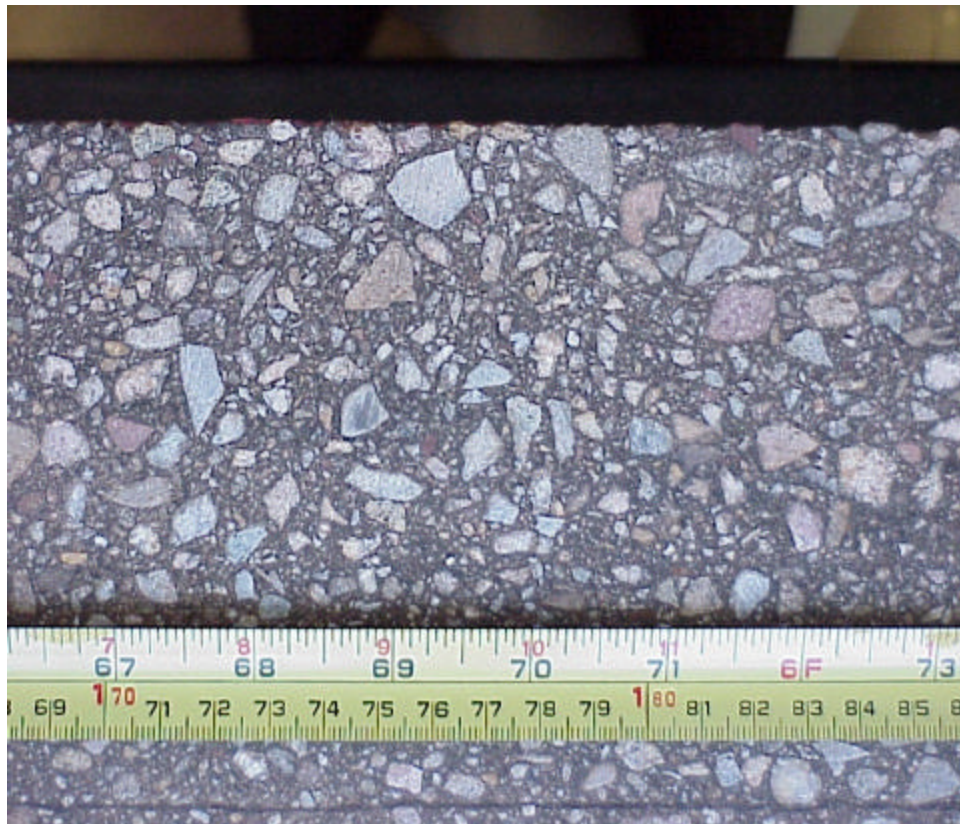


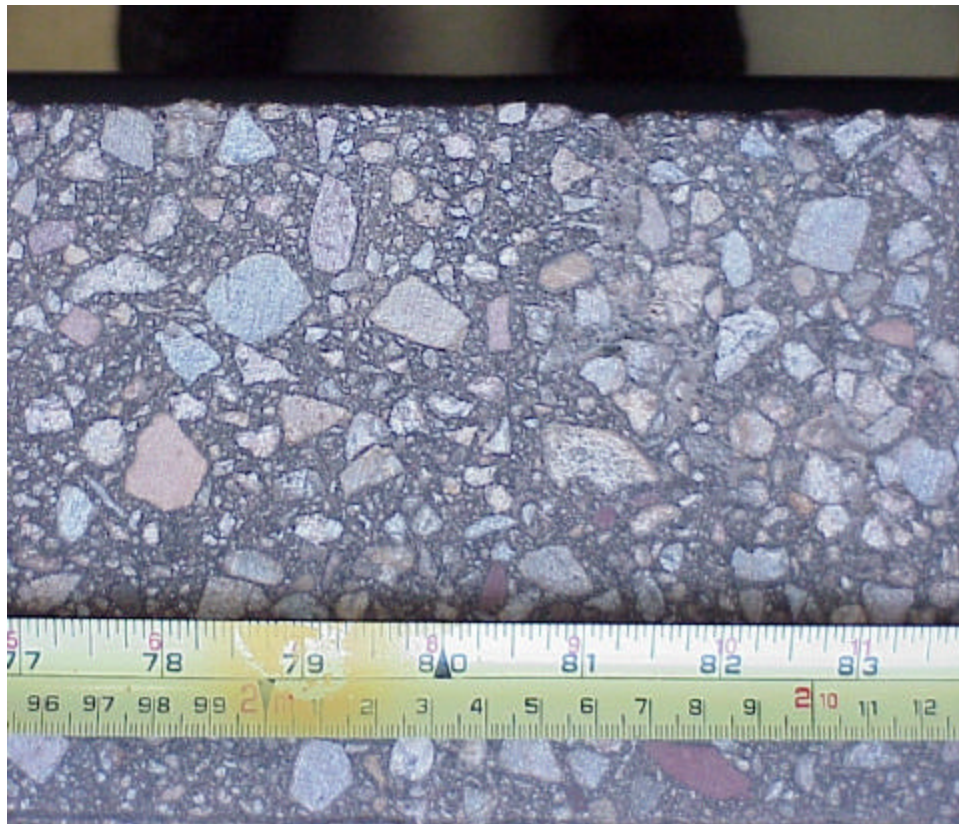






















Appendix C

**Asphalt Institute
Test Data**

[This page left blank]



I-70-1e Recovered Binder

ORIGINAL				
Test, Method			Test Results	Specification
DSR (Dynamic Shear Rheometer), AASHTO TP 5				
Test Temperature, °C	G*, kPa	Phase Angle, δ, degrees	G*/sinδ, kPa	1.00 kPa min
Recovered Asphalt Binder				
Mass Loss, AASHTO T 240			n/a	1.00% max
DSR (Dynamic Shear Rheometer), AASHTO TP 5				
Test Temperature, °C	G*, kPa	Phase Angle, δ, degrees	G*/sinδ, kPa	2.20 kPa min
64	3.108	80.5	3.150	
70	1.494	82.9	1.505	
DSR (Dynamic Shear Rheometer), AASHTO TP 5				
Test Temperature, °C	G*, kPa	Phase Angle, δ, degrees	G* sinδ, kPa	5000 kPa max
25	1356	55.9	1124	
22	2246	53.0	1793	
19	3688	49.6	2809	
16	5843	46.4	4233	
13	8951	43.3	6139	
PAV (PRESSURE AGING VESSEL), 100 °C				
DSR (Dynamic Shear Rheometer), AASHTO TP 5				
Test Temperature, °C	G*, kPa	Phase Angle, δ, degrees	G* sinδ, kPa	5000 kPa max
25	2095	49.7	1599	
22	3295	46.7	2400	
19	5112	43.8	3538	
16	7807	40.8	5100	
BBR (Bending Beam Rheometer), AASHTO TP1				
Test Temperature, °C				300MPa max 0.300 min
-18	Stiffness, MPa		173	
	m-value		0.326	
-24	Stiffness, MPa		362	
	m-value		0.271	

- DSR Original: T_{max}
Temperature at which $G^*/\sin\delta = 1.00$ kPa
- DSR RTFO: T_{max}
Temperature at which $G^*/\sin\delta = 2.20$ kPa
- DSR PAV: T_{min}
Temperature at which $G^*\sin\delta = 5000$ kPa
- BBR PAV: T_{min}
Temperature at which $S(t) = 300$ Mpa
Temperature at which $m = 0.300$

Limiting Temperature for T_{max}	
#NUM!	66.9
Limiting Temperature for T_{max}	
66.9	16.2
Limiting Temperature for T_{min}	
16.2	-20.3
(Limiting Performance Grade -)	
-22.0	66.9-30.8
-20.8	



I-70-2e Recovered Binder

ORIGINAL				
Test, Method		Test Results		Specification
DSR (Dynamic Shear Rheometer), AASHTO TP 5				
Test Temperature, °C	G*, kPa	Phase Angle, δ, degrees	G*/sinδ, kPa	1.00 kPa min
Recovered Asphalt Binder				
Mass Loss, AASHTO T 240		n/a		1.00% max
DSR (Dynamic Shear Rheometer), AASHTO TP 5				
Test Temperature, °C	G*, kPa	Phase Angle, δ, degrees	G*/sinδ, kPa	2.20 kPa min
70	2.381	81.1	2.411	
76	1.181	83.3	1.189	
DSR (Dynamic Shear Rheometer), AASHTO TP 5				
Test Temperature, °C	G*, kPa	Phase Angle, δ, degrees	G* sinδ, kPa	5000 kPa max
28	1231	55.3	1012	
25	1990	52.4	1576	
22	3178	49.4	2412	
19	5074	46.2	3662	
16	7873	43.1	5383	
PAV (PRESSURE AGING VESSEL), 100 °C				
DSR (Dynamic Shear Rheometer), AASHTO TP 5				
Test Temperature, °C	G*, kPa	Phase Angle, δ, degrees	G* sinδ, kPa	5000 kPa max
28	2067	48.2	1541	
25	3154	45.5	2251	
22	4733	43.0	3224	
19	7106	40.2	4586	
16	10560	37.4	6415	
BBR (Bending Beam Rheometer), AASHTO TP1				
Test Temperature, °C				300MPa max 0.300 min
-18	Stiffness, MPa	216		
	m-value	0.306		
-24	Stiffness, MPa	428		
	m-value	0.256		

1. DSR Original: T_{max} Temperature at which $G^*/\sin\delta = 1.00$ kPa

#NUM!

Limiting Temperature for T_{max}

70.8

2. DSR RTFO: T_{min} Temperature at which $G^*/\sin\delta = 2.20$ kPa

70.8

Limiting Temperature for T_{min}

18.3

3. DSR PAV: T_{min} Temperature at which $G^*\sin\delta = 5000$ kPa

18.3

Limiting Temperature for T_{min}

-18.7

4. BBR PAV: T_{min} Temperature at which $S(0) = 300$ Mpa

-20.4

(Limiting Performance Grade -)

70.8-28.7

Temperature at which $m = 0.300$

-18.7



I-25N-11 Recovered Binder

ORIGINAL				
Test, Method		Test Results		Specification
DSR (Dynamic Shear Rheometer), AASHTO TP 5				
Test Temperature, °C	G*, kPa	Phase Angle, δ, degrees	G*/sinδ, kPa	1.00 kPa min
Recovered Asphalt Binder				
Mass Loss, AASHTO T 240		n/a		1.00% max
DSR (Dynamic Shear Rheometer), AASHTO TP 5				
Test Temperature, °C	G*, kPa	Phase Angle, δ, degrees	G*/sinδ, kPa	2.20 kPa min
64	2.951	80.7	2.990	
70	1.430	83.0	1.440	
DSR (Dynamic Shear Rheometer), AASHTO TP 5				
Test Temperature, °C	G*, kPa	Phase Angle, δ, degrees	G*/sinδ, kPa	5000 kPa max
25				
22				
19	3277	50.1	2514	
16	5347	46.7	3889	
13	8387	43.4	5763	
PAV (PRESSURE AGING VESSEL), 100 °C				
DSR (Dynamic Shear Rheometer), AASHTO TP 5				
Test Temperature, °C	G*, kPa	Phase Angle, δ, degrees	G*/sinδ, kPa	5000 kPa max
22	3129	47.1	2293	
19	4804	44.2	3346	
16	7310	41.2	4815	
13	11000	38.2	6805	
BBR (Bending Beam Rheometer), AASHTO TP1				
Test Temperature, °C				300MPa max 0.300 min
-18	Stiffness, MPa	172		
	m-value	0.330		
-24	Stiffness, MPa	356		
	m-value	0.276		

1. DSR Original: T _{max} Temperature at which G*/sinδ = 1.00 kPa	#NUM!	Limiting Temperature for T _{max}	66.5
2. DSR RTFO: T _{max} Temperature at which G*/sinδ = 2.20 kPa	66.5	Limiting Temperature for T _{int}	15.7
3. DSR PAV: T _{eq} Temperature at which G*/sinδ = 5000 kPa	15.7	Limiting Temperature for T _{min}	-21.3
4. BBR PAV: T _{eq} Temperature at which S(t) = 300 Mpa	-22.2	(Limiting Performance Grade -)	
Temperature at which m = 0.300	-21.3		



I-25N-12 Recovered Binder

ORIGINAL				
Test, Method		Test Results		Specification
DSR (Dynamic Shear Rheometer), AASHTO TP 5				
Test Temperature, °C	G*, kPa	Phase Angle, δ, degrees	G*/sinδ, kPa	1.00 kPa min
Recovered Asphalt Binder				
Mass Loss, AASHTO T 240		n/a		1.00% max
DSR (Dynamic Shear Rheometer), AASHTO TP 5				
Test Temperature, °C	G*, kPa	Phase Angle, δ, degrees	G*/sinδ, kPa	2.20 kPa min
70	2.531	81.2	2.561	
76	1.237	83.4	1.245	
DSR (Dynamic Shear Rheometer), AASHTO TP 5				
Test Temperature, °C	G*, kPa	Phase Angle, δ, degrees	G*/sinδ, kPa	5000 kPa max
25				
22				
19	6620	44.3	4625	
16	10090	41.1	6639	
13				
PAV (PRESSURE AGING VESSEL), 100 °C				
DSR (Dynamic Shear Rheometer), AASHTO TP 5				
Test Temperature, °C	G*, kPa	Phase Angle, δ, degrees	G*/sinδ, kPa	5000 kPa max
25				
22	5724	42.3	3849	
19	8231	39.7	5254	
16				
BBR (Bending Beam Rheometer), AASHTO TP1				
Test Temperature, °C				300MPa max 0.300 min
-18	Stiffness, MPa		223	
	m-value		0.300	
-24	Stiffness, MPa		461	
	m-value		0.250	

1. DSR Original: T _{max} Temperature at which G*/sinδ = 1.00 kPa	#NUM!	Limiting Temperature for T _{max} 71.3
2. DSR RTFO: T _{max} Temperature at which G*/sinδ = 2.20 kPa	71.3	Limiting Temperature for T _{int} 19.5
3. DSR PAV: T _{min} Temperature at which G*/sinδ = 5000 kPa	19.5	Limiting Temperature for T _{min} -18.0
4. BBR PAV: T _{max} Temperature at which S(t) = 300 MPa	-19.9	(Limiting Performance Grade: -) 71.3-28.0
Temperature at which m = 0.300	-18.0	



I-25D-4 Recovered Binder

ORIGINAL				
Test, Method		Test Results		Specification
DSR (Dynamic Shear Rheometer), AASHTO TP 5				
Test Temperature, °C	G*, kPa	Phase Angle, δ, degrees	G*/sinδ, kPa	1.00 kPa min
Recovered Asphalt Binder				
Mass Loss, AASHTO T 240		n/a		1.00% max
DSR (Dynamic Shear Rheometer), AASHTO TP 5				
Test Temperature, °C	G*, kPa	Phase Angle, δ, degrees	G*/sinδ, kPa	2.20 kPa min
64	3.397	80.7	3.443	
70	1.606	83.0	1.619	
DSR (Dynamic Shear Rheometer), AASHTO TP 5				
Test Temperature, °C	G*, kPa	Phase Angle, δ, degrees	G* sinδ, kPa	5000 kPa max
25				
22	2265	54.2	1837	
19	3795	50.6	2933	
16	5995	47.1	4393	
13	9322	43.5	6421	
PAV (PRESSURE AGING VESSEL), 100 °C				
DSR (Dynamic Shear Rheometer), AASHTO TP 5				
Test Temperature, °C	G*, kPa	Phase Angle, δ, degrees	G* sinδ, kPa	5000 kPa max
25				
22	3480	48.1	2592	
19	5371	45.1	3805	
16	8096	42.1	5423	
BBR (Bending Beam Rheometer), AASHTO TP1				
Test Temperature, °C				300MPa max 0.300 min
-18	Stiffness, MPa		174	
	m-value		0.325	
-24	Stiffness, MPa		360	
	m-value		0.274	

1. DSR Original: T_{max}	Limiting Temperature for T_{max}
Temperature at which $G^*/\sin\delta = 1.00$ kPa	67.6
2. DSR RTFO: T_{max}	Limiting Temperature for T_{max}
Temperature at which $G^*/\sin\delta = 2.20$ kPa	67.6
3. DSR PAV: T_{min}	Limiting Temperature for T_{min}
Temperature at which $G^*\sin\delta = 5000$ kPa	16.7
4. BBR PAV: T_{min}	(Limiting Performance Grade -)
Temperature at which $S(t) = 300$ Mpa	-22.1
Temperature at which $m = 0.300$	-20.9

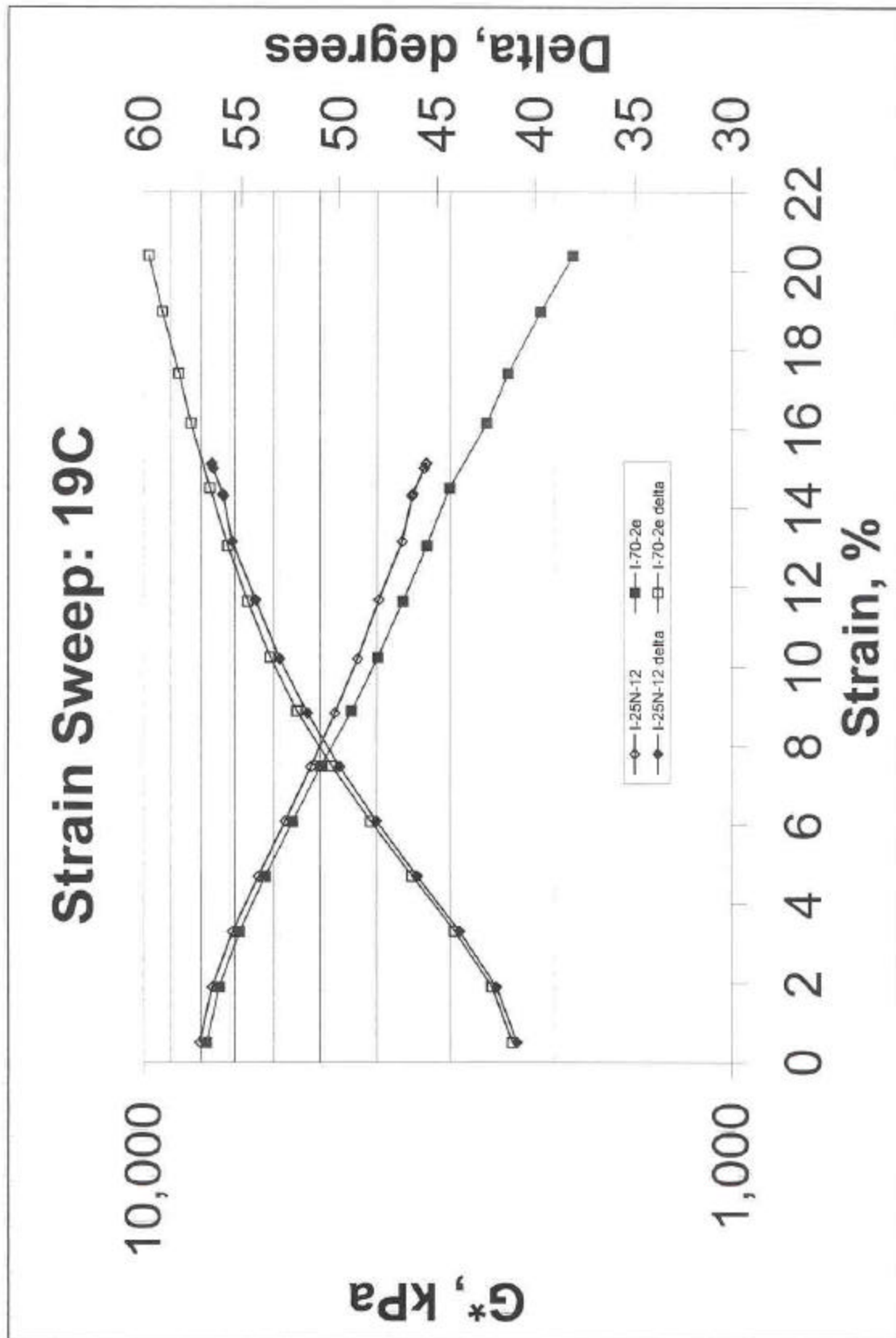
Strain Sweep

I-25N-12

ω rad/s	Time sec	Temp C	Stress Pa	Strain %	G* kPa	δ degrees	G*sin δ kPa
9.987	41.2	18.9	40180	0.50146	8025	40.9	5254
9.987	68.4	19.0	145400	1.9071	7638	41.95	5106
9.987	95.6	19.0	233600	3.3194	7049	43.84	4882
9.987	122.7	19.1	299500	4.7114	6368	46	4580
9.987	150.0	19.0	349200	6.1003	5735	48.08	4268
9.987	177.2	19.1	386400	7.4721	5181	49.96	3966
9.987	204.3	19.1	416000	8.836	4717	51.6	3697
9.987	231.6	19.1	439200	10.204	4313	53.02	3446
9.987	258.8	19.1	462700	11.69	3967	54.26	3220
9.987	294.0	19.1	475600	13.162	3622	55.47	2983
9.987	313.3	19.1	497300	14.364	3471	55.96	2876
9.987	324.5	19.1	497300	14.315	3483	55.91	2884
9.987	343.7	19.1	497300	15.124	3297	56.53	2750
9.987	354.8	19.1	497300	15.023	3319	56.45	2766
9.987	366.1	19.1	497300	15.147	3292	56.52	2746

I-70-2e

ω rad/s	Time sec	Temp C	Stress Pa	Strain %	G* kPa	δ degrees	G*sin δ kPa
9.987	41.1	19.1	39020	0.50041	7809	41.12	5135
9.987	68.4	19.1	141600	1.9082	7435	42.17	4991
9.987	95.6	19.1	227600	3.3239	6858	44.08	4771
9.987	122.8	19.1	291800	4.7148	6200	46.25	4479
9.987	149.9	19.1	338600	6.0962	5565	48.37	4160
9.987	177.1	19.1	372600	7.49	4984	50.36	3838
9.987	204.2	19.1	391200	8.8859	4412	52.14	3483
9.987	231.4	19.1	407300	10.252	3982	53.51	3202
9.987	258.7	19.1	419700	11.66	3608	54.67	2944
9.987	285.9	19.1	428300	13.061	3287	55.7	2716
9.987	313.0	19.0	435500	14.529	3006	56.61	2510
9.987	356.2	19.0	418000	16.163	2594	57.58	2190
9.987	383.5	19.0	414800	17.416	2390	58.19	2031
9.987	426.7	19.1	397900	18.978	2104	59.03	1804
9.987	469.8	19.0	378400	20.4	1862	59.73	1608

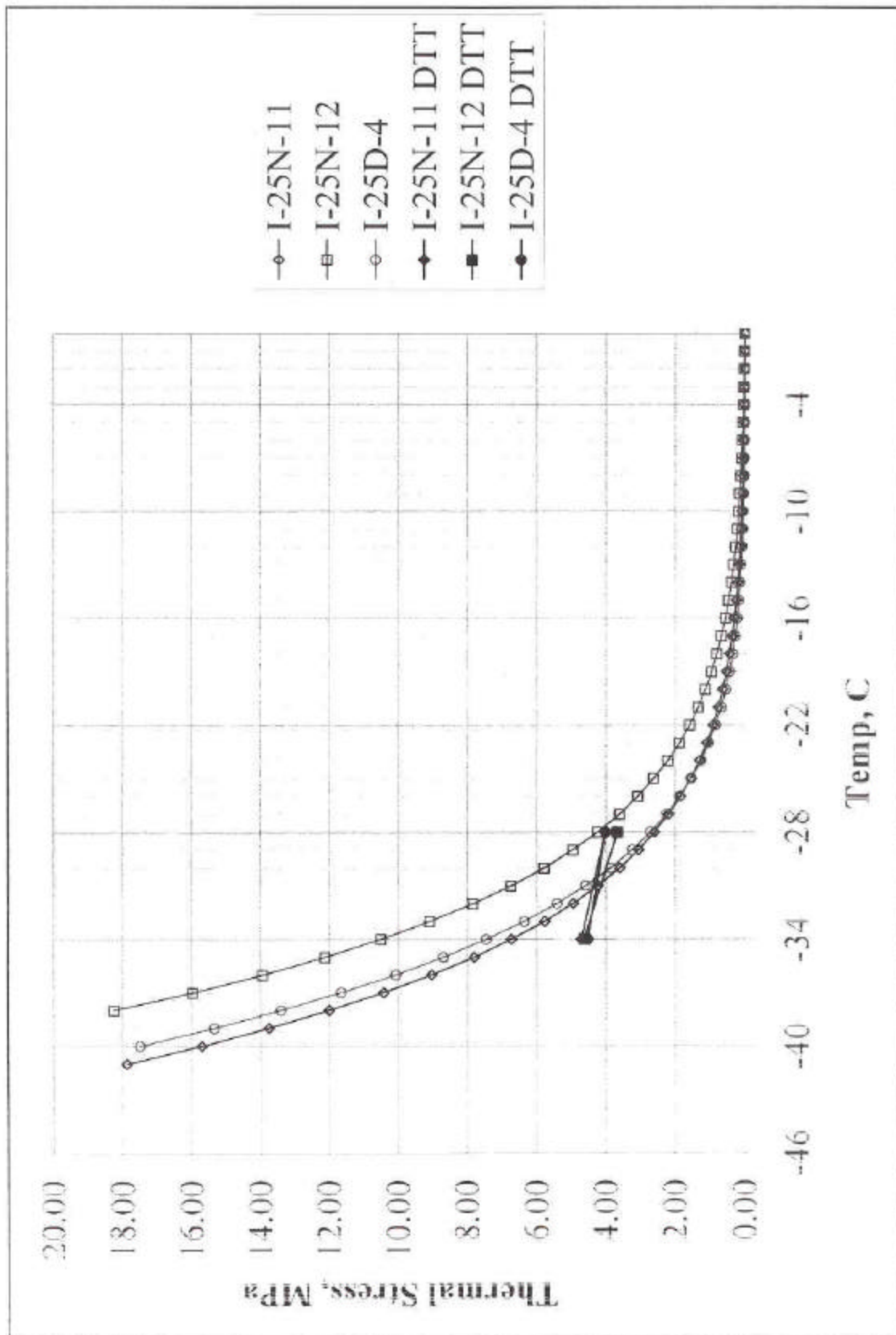


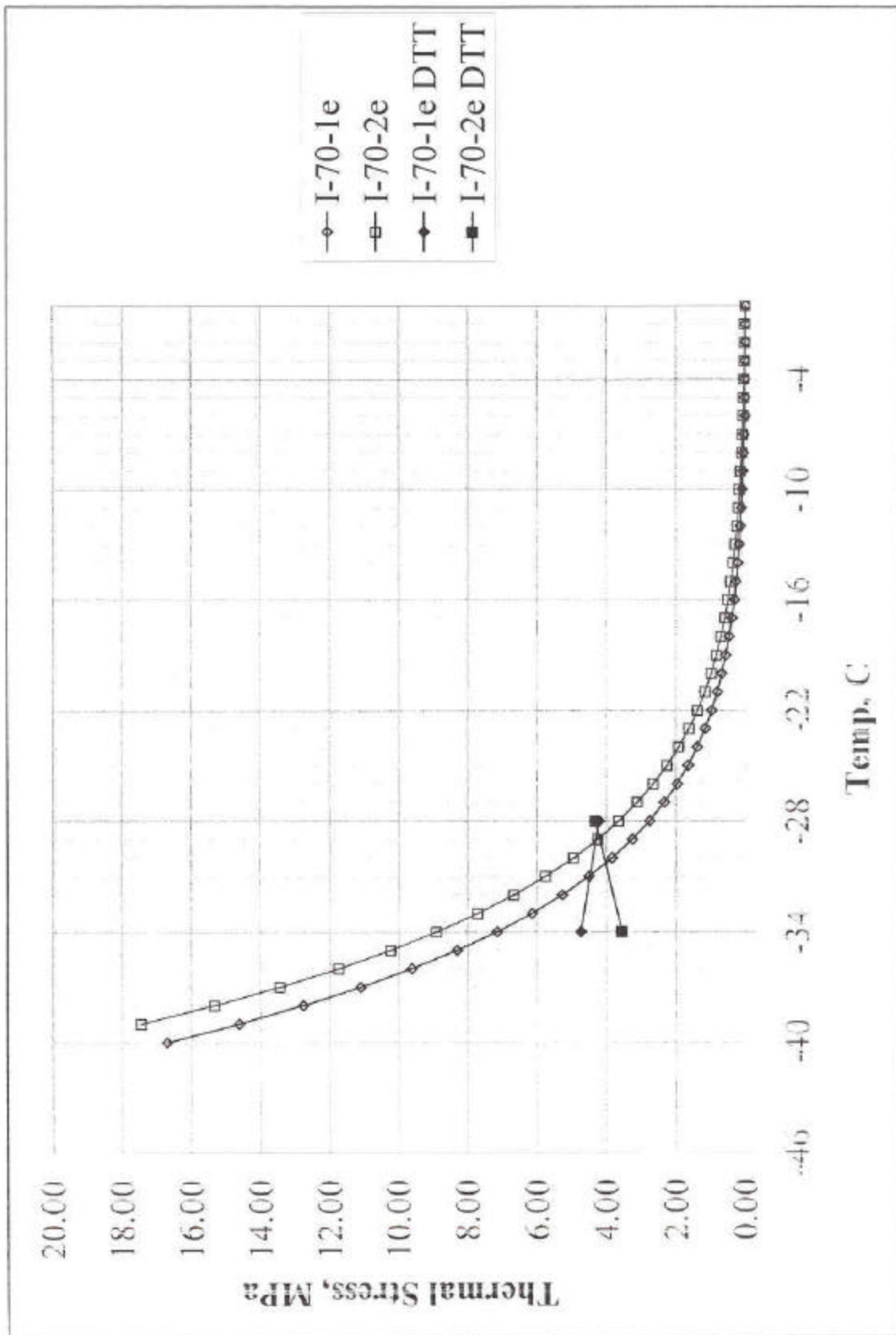
Thermal Stress Analysis (TSARPlus) - Recovered Asphalt Binders

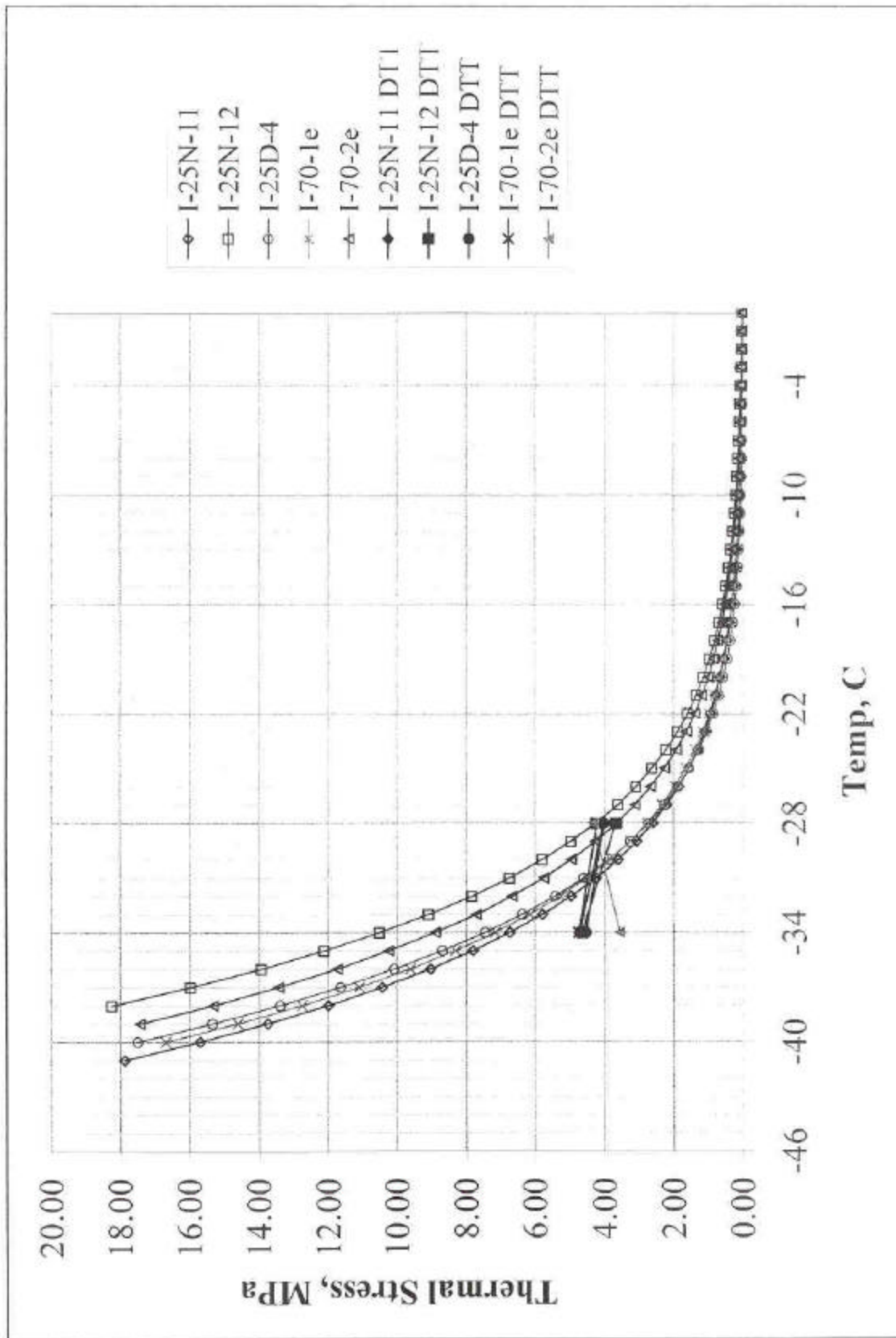
Temp, °C	I-70-1e		I-70-2e		I-25N-11		I-25N-12		I-25D-4	
	Thermal Stress, MPa		Thermal Stress, MPa		Thermal Stress, MPa		Thermal Stress, MPa		Thermal Stress, MPa	
	Pvmt(18)	Binder	Pvmt(18)	Binder	Pvmt(18)	Binder	Pvmt(18)	Binder	Pvmt(18)	Binder
0	0.00	0.00	0.00	0.00	0.00	0.00	0.00	0.00	0.00	0.00
-1	0.01	0.00	0.02	0.00	0.01	0.00	0.02	0.00	0.00	0.00
-2	0.01	0.00	0.02	0.00	0.01	0.00	0.03	0.00	0.01	0.00
-3	0.02	0.00	0.03	0.00	0.02	0.00	0.04	0.00	0.01	0.00
-4	0.03	0.00	0.05	0.00	0.03	0.00	0.05	0.00	0.01	0.00
-5	0.03	0.00	0.06	0.00	0.03	0.00	0.07	0.00	0.02	0.00
-6	0.04	0.00	0.07	0.00	0.04	0.00	0.08	0.00	0.02	0.00
-7	0.05	0.00	0.09	0.01	0.05	0.00	0.10	0.01	0.03	0.00
-8	0.07	0.00	0.11	0.01	0.06	0.00	0.13	0.01	0.03	0.00
-9	0.08	0.00	0.14	0.01	0.08	0.00	0.16	0.01	0.04	0.00
-10	0.10	0.01	0.17	0.01	0.10	0.01	0.19	0.01	0.06	0.00
-11	0.12	0.01	0.20	0.01	0.12	0.01	0.23	0.01	0.07	0.00
-12	0.15	0.01	0.24	0.01	0.14	0.01	0.28	0.02	0.09	0.01
-13	0.18	0.01	0.29	0.02	0.18	0.01	0.34	0.02	0.12	0.01
-14	0.22	0.01	0.35	0.02	0.21	0.01	0.40	0.02	0.15	0.01
-15	0.27	0.02	0.42	0.02	0.26	0.01	0.48	0.03	0.19	0.01
-16	0.32	0.02	0.50	0.03	0.31	0.02	0.57	0.03	0.23	0.01
-17	0.39	0.02	0.59	0.03	0.37	0.02	0.68	0.04	0.29	0.02
-18	0.47	0.03	0.71	0.04	0.45	0.03	0.81	0.05	0.36	0.02
-19	0.57	0.03	0.84	0.05	0.54	0.03	0.96	0.05	0.45	0.03
-20	0.68	0.04	0.99	0.06	0.65	0.04	1.14	0.06	0.56	0.03
-21	0.81	0.05	1.17	0.07	0.77	0.04	1.35	0.08	0.69	0.04
-22	0.97	0.05	1.38	0.08	0.92	0.05	1.59	0.09	0.85	0.05
-23	1.16	0.06	1.63	0.09	1.10	0.06	1.88	0.10	1.04	0.06
-24	1.39	0.08	1.92	0.11	1.31	0.07	2.22	0.12	1.27	0.07
-25	1.65	0.09	2.26	0.13	1.56	0.09	2.62	0.15	1.55	0.09
-26	1.96	0.11	2.65	0.15	1.85	0.10	3.08	0.17	1.88	0.10
-27	2.33	0.13	3.11	0.17	2.20	0.12	3.61	0.20	2.26	0.13
-28	2.75	0.15	3.64	0.20	2.60	0.14	4.24	0.24	2.72	0.15
-29	3.25	0.18	4.25	0.24	3.06	0.17	4.96	0.28	3.25	0.18
-30	3.83	0.21	4.95	0.28	3.60	0.20	5.79	0.32	3.87	0.22
-31	4.50	0.25	5.75	0.32	4.23	0.24	6.74	0.37	4.59	0.26
-32	5.27	0.29	6.67	0.37	4.95	0.28	7.84	0.44	5.42	0.30
-33	6.15	0.34	7.71	0.43	5.78	0.32	9.09	0.51	6.37	0.35
-34	7.16	0.40	8.90	0.49	6.73	0.37	10.51	0.58	7.46	0.41
-35	8.31	0.46	10.24	0.57	7.81	0.43	12.12	0.67	8.69	0.48
-36	9.62	0.53	11.74	0.65	9.04	0.50	13.94	0.77	10.08	0.56
-37	11.10	0.62	13.44	0.75	10.43	0.58	15.97	0.89	11.65	0.65
-38	12.76	0.71	15.33	0.85	12.00	0.67	18.25	1.01	13.40	0.74
-39	14.62	0.81	17.43	0.97	13.75	0.76			15.35	0.85
-40	16.69	0.93			15.70	0.87			17.50	0.97
-41					17.87	0.99				

Direct Tension Fracture Strength, MPa

-28	4.22	4.32	4.03	3.68	4.02
-34	4.74	3.55	4.71	4.64	4.53

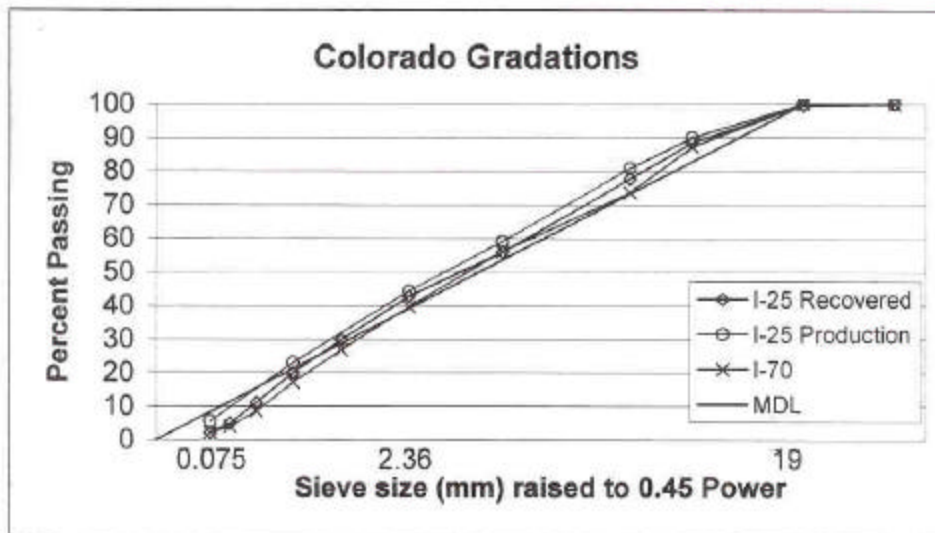






MIX COMPOSITION

Sieve	I-25D-4	I-25D-8	I-25N-11	I-25N-12	Ave Rec.	Ave Prod.	I-70-1e	I-70-2e	Ave Rec.
1"	100	100	100		100.0	100.0	100	100	100.0
3/4"	98.7	100	100		99.6	100.0	100	100	100.0
1/2"	88.6	87.2	89.5		88.4	89.9	87.7	86.8	87.3
3/8"	79.3	76.4	77.3		77.7	80.8	75.1	72.1	73.6
#4	58.2	55.6	53.6		55.8	59.0	57.3	54.8	56.1
#8	44.4	43.1	40.6		42.7	44.3	40.6	38.8	39.7
#16	30.6	30.7	27.8		29.7		27.1	26.4	26.8
#30	20.3	21.2	18.5		20.0	22.9	17.4	16.9	17.2
#50	11.1	12.2	10.1		11.1		8.6	8.5	8.6
#100	4.9	5.5	4.3		4.9		3.9	4.2	4.1
#200	2.2	2.4	1.8		2.1	5.6	2.1	2.4	2.3
AC, %	4.3	4.0	4.0	4.2	4.1	4.6	4.9	4.7	4.8



Gmm

	Rep 1	Rep 2	Average	Design
I-25D-4	2.476	2.473	2.475	2.466
I-25N-11	2.476	2.474	2.475	2.466
I-70-1e	2.551	2.549	2.550	

Specimen	Gmb		Gmm	Air Voids	
	ASTM	CoreLok		ASTM	CoreLok
I-25D-3	2.277	2.278	2.475	8.0%	8.0%
I-25D-4	2.266	2.267	2.475	8.4%	8.4%
I-25D-5 cut	2.279	2.280	2.475	7.9%	7.9%
I-25D-6 cut	2.259	2.264	2.475	8.7%	8.5%
I-25D-7 cut	2.263	2.266	2.475	8.6%	8.4%
I-25D-8					
Average	2.269	2.271	2.475	8.3%	8.2%
I-25N-11	2.294	2.295	2.475	7.3%	7.3%
I-25N-12	2.288	2.288	2.475	7.6%	7.6%
I-25N-13 cut	2.295	2.301	2.475	7.3%	7.0%
I-25N-14 cut					
I-25N-15 cut	2.298	2.305	2.475	7.2%	6.9%
I-25N-16 cut	2.298	2.305	2.475	7.2%	6.9%
Average	2.295	2.299	2.475	7.3%	7.1%
I-70-1e	2.364	2.366	2.550	7.3%	7.2%
I-70-2e	2.360	2.358	2.550	7.8%	7.5%
I-70-3e cut	2.412	2.400	2.550	5.4%	5.9%
I-70-4e cut	2.397	2.391	2.550	6.0%	6.2%
I-70-5e cut	2.405	2.406	2.550	5.7%	5.6%
I-70-6e cut					
I-70-7e cut					
Average	2.386	2.384	2.550	6.4%	6.5%



Project: Colorado Cores
 Date: 18-Jan-01
 Technologist: Gary D. Irvine
 Test: Frequency Sweep @ Constant Height (FSCH)
 Procedure: AASHTO TP-7

I25D Top <<<

G*, kPa	16C					
Freq	I25D-5T	I25D-6T	I25D-7T	average	stdev	CV
2.0 inch Gauge Length						
10	2,007,686	1,671,760	1,723,020	1,800,822	147,765	8%
5	1,841,396	1,508,119	1,560,373	1,636,629	146,355	9%
2	1,625,957	1,291,225	1,363,026	1,426,736	143,888	10%
1	1,450,649	1,124,355	1,199,517	1,258,174	139,517	11%
0.5	1,280,274	971,844	1,055,127	1,102,415	130,280	12%
0.2	1,083,134	795,115	880,806	919,685	120,755	13%
0.1	955,809	675,207	754,260	795,092	118,138	15%
0.05	815,739	574,338	647,470	679,182	101,070	15%
0.02	663,176	460,077	519,584	547,613	85,251	16%
0.01	565,941	386,416	446,074	466,144	74,652	16%
Avg. >						12%

I25D Top <<<

G*, kPa	22C					
Freq	I25D-5T	I25D-6T	I25D-7T	average	stdev	CV
2.0 inch Gauge Length						
10	1,571,986	1,313,622	1,389,046	1,424,885	108,478	8%
5	1,398,485	1,148,533	1,217,933	1,254,984	105,352	8%
2	1,175,408	943,161	1,015,508	1,044,692	97,034	9%
1	1,004,675	796,446	863,287	888,136	86,806	10%
0.5	852,930	668,230	733,636	751,598	76,466	10%
0.2	681,607	520,794	583,727	595,376	66,166	11%
0.1	574,602	440,079	487,339	500,674	55,722	11%
0.05	485,891	364,018	412,454	420,788	50,102	12%
0.02	393,614	282,312	319,022	331,649	46,308	14%
0.01	333,295	239,629	277,819	283,581	38,455	14%
Avg. >						11%

I25D Top <<<

G*, kPa	28C					
Freq	I25D-5T	I25D-6T	I25D-7T	average	stdev	CV
2.0 inch Gauge Length						
10	1,189,670	854,399	1,004,854	1,016,308	137,113	13%
5	1,018,895	713,915	850,584	861,132	124,731	14%
2	815,366	551,944	682,674	683,328	107,543	16%
1	668,067	445,263	562,451	558,593	91,000	16%
0.5	547,775	357,247	465,022	456,681	78,006	17%
0.2	414,992	268,669	360,081	347,914	60,352	17%
0.1	336,078	219,379	300,017	285,158	48,787	17%
0.05	272,429	178,017	250,047	233,498	40,281	17%
0.02	205,968	138,480	202,959	182,469	31,129	17%
0.01	169,470	115,433	171,219	152,041	25,895	17%
Avg. >						16%



Project: Colorado Cores

Date: 18-Jan-01

Technologist: Gary D. Irvine

Test: Frequency Sweep @ Constant Height (FSCH)

Procedure: AASHTO TP-7

I25D Intermediate <<<

G*, kPa	16C					
Freq	I25D-5I	I25D-6I	I25D-7I	average	stdev	CV
1.5 inch Gauge Length						
10	2,351,658	2,362,243	2,390,167	2,368,023	16,244	1%
5	2,089,982	2,109,158	2,180,179	2,126,440	38,798	2%
2	1,752,786	1,790,840	1,893,539	1,812,389	59,448	3%
1	1,501,295	1,563,140	1,667,164	1,577,200	68,442	4%
0.5	1,262,438	1,341,222	1,441,410	1,348,357	73,239	5%
0.2	996,346	1,083,659	1,191,444	1,090,483	79,794	7%
0.1	816,318	898,297	1,006,179	906,931	77,750	9%
0.05	669,982	754,101	842,138	755,407	70,288	9%
0.02	495,791	577,380	660,373	577,848	67,191	12%
0.01	399,659	487,197	554,268	480,375	63,303	13%
Avg. >					7%	

I25D Intermediate <<<

G*, kPa	22C					
Freq	I25D-5I	I25D-6I	I25D-7I	average	stdev	CV
1.5 inch Gauge Length						
10	1,699,649	1,691,880	1,799,872	1,730,467	49,179	3%
5	1,427,369	1,454,292	1,558,379	1,480,013	56,492	4%
2	1,118,518	1,171,806	1,285,836	1,192,053	69,792	6%
1	904,749	967,822	1,068,293	980,288	67,346	7%
0.5	714,026	785,282	875,410	791,573	66,035	8%
0.2	516,292	591,820	667,659	591,924	61,796	10%
0.1	404,076	469,418	538,753	470,749	54,990	12%
0.05	313,300	379,486	435,467	376,084	49,932	13%
0.02	225,606	280,478	326,078	277,387	41,076	15%
0.01	183,159	228,634	268,377	226,723	34,816	15%
Avg. >					9%	

I25D Intermediate <<<

G*, kPa	28C					
Freq	I25D-5I	I25D-6I	I25D-7I	average	stdev	CV
1.5 inch Gauge Length						
10	1,166,480	1,212,130	1,305,922	1,228,177	58,047	5%
5	923,924	990,060	1,075,979	996,654	62,251	6%
2	671,573	748,250	818,195	746,006	59,879	8%
1	512,987	592,994	654,030	586,670	57,754	10%
0.5	387,959	461,374	512,016	453,783	50,929	11%
0.2	263,445	332,034	369,033	321,504	43,744	14%
0.1	198,211	258,019	291,201	249,144	38,479	15%
0.05	152,432	200,153	226,248	192,944	30,563	16%
0.02	107,479	151,979	164,359	141,273	24,424	17%
0.01	86,271	124,309	138,524	116,368	22,059	19%
Avg. >					12%	



Project: Colorado Cores
 Date: 18 Jan-01
 Technologist: Gary D. Irvine
 Test: Frequency Sweep @ Constant Height (FSCH)
 Procedure: AASHTO TP-7

I25N Top <<<

G*, kPa	16C					
Freq	I25N-13T	I25N-14T	I25N-15T	average	stdev	CV
2.0 inch Gauge Length						
10	2,103,320	2,052,322	1,968,846	2,041,496	55,430	3%
5	1,932,662	1,886,515	1,798,147	1,872,442	55,810	3%
2	1,709,199	1,649,859	1,574,746	1,644,601	55,016	3%
1	1,519,891	1,465,636	1,395,546	1,460,357	50,901	3%
0.5	1,356,671	1,293,709	1,225,026	1,291,802	53,761	4%
0.2	1,143,544	1,083,555	1,023,408	1,083,502	49,045	5%
0.1	1,001,383	936,882	878,770	939,012	50,079	5%
0.05	865,377	804,554	747,643	805,858	48,074	6%
0.02	712,439	663,746	609,122	661,769	42,202	6%
0.01	616,383	571,773	522,581	570,246	38,309	7%
Avg. >						5%

I25N Top <<<

G*, kPa	22C					
Freq	I25N-13T	I25N-14T	I25N-15T	average	stdev	CV
2.0 inch Gauge Length						
10	1,683,490	1,649,328	1,588,884	1,640,567	39,116	2%
5	1,495,396	1,458,895	1,416,046	1,456,779	32,429	2%
2	1,266,226	1,231,671	1,186,490	1,228,129	32,648	3%
1	1,085,977	1,056,445	1,014,638	1,052,354	29,267	3%
0.5	923,475	892,004	862,093	892,524	25,062	3%
0.2	743,123	716,475	678,974	712,858	26,313	4%
0.1	622,349	600,003	574,660	599,004	19,482	3%
0.05	526,577	505,566	480,907	504,350	18,664	4%
0.02	417,938	398,639	377,702	398,093	16,431	4%
0.01	353,514	337,189	313,044	334,582	16,624	5%
Avg. >						3%

I25N Top <<<

G*, kPa	28C					
Freq	I25N-13T	I25N-14T	I25N-15T	average	stdev	CV
2.0 inch Gauge Length						
10	1,244,118	1,212,572	1,154,232	1,203,641	37,235	3%
5	1,072,419	1,035,207	979,490	1,029,038	38,188	4%
2	858,498	815,090	768,853	814,147	36,603	4%
1	707,561	668,912	626,362	667,612	33,162	5%
0.5	584,569	541,224	507,060	544,284	31,717	6%
0.2	450,264	409,694	379,761	413,239	28,892	7%
0.1	369,517	336,044	308,466	338,009	24,963	7%
0.05	312,679	269,069	245,298	275,682	27,903	10%
0.02	246,807	208,793	187,748	214,449	24,440	11%
0.01	207,439	173,766	155,072	178,759	21,668	12%
Avg. >						7%



Project: Colorado Cores
Date: 18-Jan-01
Technologist: Gary D. Irvine
Test: Frequency Sweep @ Constant Height (FSCH)
Procedure: AASHTO TP-7

I25N Intermediate <<<

G*, kPa	16C					
Freq	I25N-13I	I25N-15I	I25N-16I	average	stdev	CV
1.5 inch Gauge Length						
10	2,314,640	2,422,418	2,525,303	2,420,787	86,011	4%
5	2,120,053	2,243,494	2,343,247	2,235,598	91,290	4%
2	1,878,139	1,992,071	2,090,817	1,987,009	86,899	4%
1	1,677,197	1,812,340	1,909,706	1,799,748	95,338	5%
0.5	1,491,635	1,623,936	1,716,906	1,610,826	92,433	6%
0.2	1,282,510	1,381,235	1,482,900	1,382,215	81,812	6%
0.1	1,127,722	1,225,688	1,303,686	1,219,032	71,991	6%
0.05	991,585	1,065,995	1,148,043	1,068,541	63,899	6%
0.02	823,646	877,859	942,782	881,429	48,702	6%
0.01	709,016	750,906	815,656	758,526	43,868	6%
Avg. >						5%

I25N Intermediate <<<

G*, kPa	22C					
Freq	I25N-13I	I25N-15I	I25N-16I	average	stdev	CV
1.5 inch Gauge Length						
10	1,746,528	1,916,924	2,029,469	1,897,640	116,312	6%
5	1,564,085	1,711,200	1,824,574	1,699,953	106,641	6%
2	1,329,437	1,452,747	1,566,804	1,449,662	96,929	7%
1	1,144,199	1,258,595	1,364,130	1,255,641	89,811	7%
0.5	978,130	1,070,404	1,174,187	1,074,240	80,086	7%
0.2	788,884	864,577	948,046	867,169	65,004	7%
0.1	675,861	720,671	794,935	730,489	49,105	7%
0.05	568,461	601,210	672,797	614,156	43,568	7%
0.02	448,658	480,421	524,845	484,641	31,246	6%
0.01	378,186	392,328	444,640	405,051	28,583	7%
Avg. >						7%

I25N Intermediate <<<

G*, kPa	28C					
Freq	I25N-13I	I25N-15I	I25N-16I	average	stdev	CV
1.5 inch Gauge Length						
10	1,297,028	1,386,127	1,496,120	1,393,092	81,428	6%
5	1,123,927	1,190,050	1,294,357	1,202,778	70,157	6%
2	902,279	961,681	1,045,129	969,696	58,593	6%
1	749,795	795,046	871,787	805,543	50,353	6%
0.5	618,878	649,598	715,558	661,345	40,334	6%
0.2	482,703	491,591	544,569	506,288	27,311	5%
0.1	399,580	396,437	440,828	412,282	20,226	5%
0.05	326,022	319,658	357,374	334,351	16,486	5%
0.02	253,285	239,600	266,029	252,971	10,792	4%
0.01	203,763	192,456	216,677	204,299	9,895	5%
Avg. >						5%



Project: Colorado Cores

Date: 18-Jan-01

Technologist: Gary D. Irvine

Test: Frequency Sweep @ Constant Height (FSCH)

Procedure: AASHTO TP-7

I-70-3e Specimen surface was not totally glued - gap

I70 Top <<<

G*, kPa	16C					
Freq	I70-3ET	I70-4ET	I70-5ET	average	stdev	CV
1.5 inch Gauge Length						
10	1,829,618	2,633,199	2,500,857	2,567,028	66,171	3%
5	1,641,890	2,379,631	2,271,059	2,325,345	54,286	2%
2	1,398,747	2,104,976	1,975,932	2,040,454	64,522	3%
1	1,219,403	1,847,392	1,745,086	1,796,239	51,153	3%
0.5	1,044,350	1,610,405	1,524,038	1,567,221	43,184	3%
0.2	853,730	1,346,852	1,252,322	1,299,587	47,265	4%
0.1	721,416	1,152,397	1,078,353	1,115,375	37,022	3%
0.05	624,389	993,152	918,383	955,767	37,384	4%
0.02	505,362	804,105	738,314	771,210	32,896	4%
0.01	431,329	692,705	640,806	666,755	25,950	4%
Avg. >						3%

I70 Top <<<

G*, kPa	22C					
Freq	I70-3ET	I70-4ET	I70-5ET	average	stdev	CV
1.5 inch Gauge Length						
10	2,009,660	2,462,548	2,176,853	2,319,701	142,847	6%
5	1,817,888	2,237,829	1,926,059	2,081,944	155,885	7%
2	1,547,953	1,924,307	1,620,651	1,772,479	151,828	9%
1	1,354,311	1,691,197	1,389,384	1,540,290	150,906	10%
0.5	1,169,757	1,472,674	1,184,316	1,328,495	144,179	11%
0.2	962,757	1,209,598	940,449	1,075,023	134,574	13%
0.1	829,539	1,044,218	793,376	918,797	125,421	14%
0.05	701,537	890,969	676,590	783,780	107,190	14%
0.02	577,009	709,596	553,436	631,516	78,080	12%
0.01	473,900	587,099	476,855	531,977	55,122	10%
Avg. >						11%

I70 Top <<<

G*, kPa	28C					
Freq	I70-3ET	I70-4ET	I70-5ET	average	stdev	CV
1.5 inch Gauge Length						
10	1,030,142	1,427,286	1,391,723	1,409,504	17,781	1%
5	859,216	1,209,839	1,163,188	1,186,514	23,325	2%
2	670,570	939,649	902,637	921,143	18,506	2%
1	546,332	758,172	720,043	739,107	19,065	3%
0.5	445,158	614,508	575,033	594,770	19,737	3%
0.2	343,237	465,131	427,027	446,079	19,052	4%
0.1	283,716	379,197	340,877	360,037	19,160	5%
0.05	233,949	306,822	277,285	292,054	14,768	5%
0.02	193,775	238,253	215,878	227,066	11,187	5%
0.01	169,647	202,935	177,370	190,153	12,783	7%
Avg. >						4%



Project: Colorado Cores
Date: 18-Jan-01
Technologist: Gary D. Irvine
Test: Frequency Sweep @ Constant Height (FSCH)
Procedure: AASHTO TP-7

I70 Intermediate <<<

G*, kPa	16C					
Freq	I70-3EI	I70-4EI	I70-5EI	average	stdev	CV
2.0 inch Gauge Length						
10	1,091,518	1,303,983	1,498,666	1,298,056	166,270	13%
5	928,933	1,147,118	1,324,779	1,133,610	161,886	14%
2	744,965	938,586	1,101,937	928,496	145,908	16%
1	617,135	797,523	942,692	785,783	133,167	17%
0.5	508,971	680,189	797,909	662,356	118,631	18%
0.2	395,383	542,990	641,895	526,756	101,290	19%
0.1	328,223	450,746	540,693	439,887	87,080	20%
0.05	271,667	385,414	453,580	370,220	75,039	20%
0.02	211,009	301,157	358,971	290,379	60,884	21%
0.01	180,169	260,160	304,469	248,266	51,437	21%
Avg. >						18%

I70 Top <<<

G*, kPa	22C					
Freq	I70-3EI	I70-4EI	I70-5EI	average	stdev	CV
2.0 inch Gauge Length						
10	681,017	851,564	1,026,327	852,969	140,976	17%
5	562,202	707,015	864,542	711,253	123,466	17%
2	432,342	553,664	689,128	558,378	104,885	19%
1	350,030	451,640	565,564	455,745	88,039	19%
0.5	285,259	365,104	464,030	371,464	73,121	20%
0.2	219,808	276,892	357,324	284,675	56,410	20%
0.1	182,271	228,621	294,475	235,123	46,037	20%
0.05	152,193	186,591	237,989	192,258	35,255	18%
0.02	119,853	147,717	186,434	151,335	27,302	18%
0.01	106,354	123,580	159,047	129,660	21,937	17%
Avg. >						18%

I70 Top <<<

G*, kPa	28C					
Freq	I70-3EI	I70-4EI	I70-5EI	average	stdev	CV
2.0 inch Gauge Length						
10	456,784	556,782	676,890	563,485	89,983	16%
5	369,309	450,041	550,073	456,474	73,936	16%
2	275,778	335,336	415,160	342,091	57,103	17%
1	220,194	266,328	331,310	272,611	45,580	17%
0.5	177,674	211,604	264,496	217,925	35,725	16%
0.2	136,313	159,863	197,508	164,561	25,203	15%
0.1	113,861	131,413	159,793	135,022	18,925	14%
0.05	102,446	108,466	127,851	112,921	10,839	10%
0.02	76,918	85,215	105,531	89,221	12,020	13%
0.01	66,053	74,557	86,561	75,724	8,413	11%
Avg. >						15%



Project: Colorado Corés

Date: 18-Jan-01

Technologist: Gary D. Irvine

Test: Frequency Sweep @ Constant Height (FSCH)

Procedure: AASHTO TP-7

Note: I70 Top - 2 Replicates

I70 Top

GL=1.5

G*, kPa, avg. 16C 22C 28C
Avg. CV > 3.3% 10.5% 3.7%

10	2,567,026	2,319,701	1,409,504
5	2,325,345	2,091,944	1,185,514
2	2,040,454	1,772,479	921,143
1	1,796,239	1,540,290	739,107
0.5	1,567,221	1,328,495	594,770
0.2	1,299,587	1,075,023	446,079
0.1	1,115,375	918,797	360,037
0.05	955,767	783,780	292,054
0.02	771,210	631,518	227,066
0.01	686,755	531,977	190,153
b	0.1988	0.2159	0.2673

I70 Intermediate

GL=2.0

G*, kPa, avg. 16C 22C 28C
Avg. CV > 17.9% 18.4% 14.5%

10	1,288,056	852,969	583,485
5	1,133,810	711,253	456,474
2	928,496	558,378	342,091
1	785,783	455,745	272,811
0.5	682,356	371,484	217,925
0.2	526,755	284,875	184,561
0.1	439,867	235,123	135,022
0.05	370,220	192,258	112,921
0.02	290,379	151,335	89,221
0.01	248,266	129,860	75,724
b	0.2438	0.2783	0.2944

I25N Top

GL=2.0

G*, kPa, avg. 16C 22C 28C
Avg. CV > 4.6% 3.3% 7.0%

10	2,041,406	1,640,567	1,203,641
5	1,872,442	1,456,779	1,023,938
2	1,644,601	1,228,129	814,147
1	1,460,357	1,052,354	667,612
0.5	1,291,802	892,524	544,284
0.2	1,063,502	712,858	413,239
0.1	939,012	599,004	336,009
0.05	805,858	504,350	275,682
0.02	661,769	388,003	214,449
0.01	570,246	334,582	178,759
b	0.1875	0.2341	0.2822

I25N Intermediate

GL=1.5

G*, kPa, avg. 16C 22C 28C
Avg. CV > 5.2% 6.9% 5.4%

10	2,420,787	1,897,640	1,383,082
5	2,235,598	1,669,953	1,202,778
2	1,987,009	1,449,562	969,896
1	1,799,748	1,255,641	805,543
0.5	1,610,826	1,074,240	661,346
0.2	1,382,215	967,169	506,288
0.1	1,219,032	790,489	412,282
0.05	1,068,541	614,156	334,351
0.02	861,429	484,841	252,971
0.01	758,526	405,051	204,299
b	0.1693	0.2267	0.2816

I25D Top

GL=2.0

G*, kPa, avg. 16C 22C 28C
Avg. CV > 12.5% 10.7% 16.3%

10	1,800,822	1,424,885	1,016,308
5	1,636,629	1,254,964	861,132
2	1,426,736	1,044,692	683,328
1	1,258,174	886,136	558,593
0.5	1,102,415	751,598	456,681
0.2	919,885	595,376	347,914
0.1	795,092	500,674	285,158
0.05	679,182	420,788	233,496
0.02	547,613	331,649	182,469
0.01	468,144	283,581	152,041
b	0.1375	0.2388	0.2802

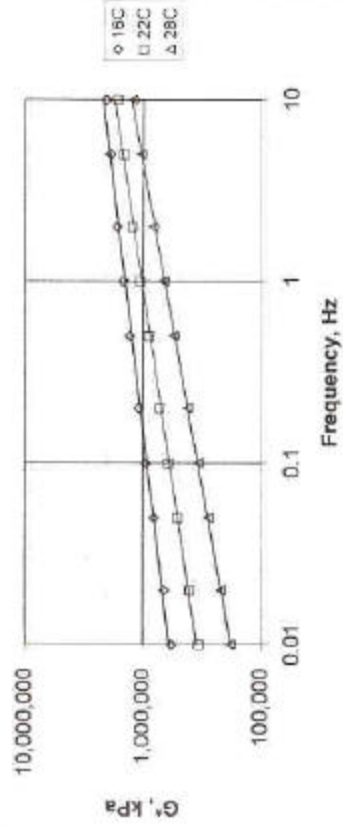
I25D Intermediate

GL=1.5

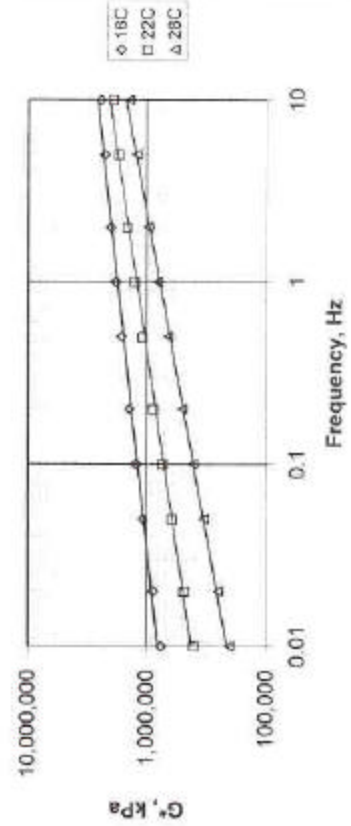
G*, kPa, avg. 16C 22C 28C
Avg. CV > 6.6% 9.3% 12.1%

10	2,368,023	1,730,457	1,228,177
5	2,126,440	1,480,013	996,654
2	1,812,389	1,192,053	746,006
1	1,577,200	980,288	586,670
0.5	1,348,357	781,573	453,783
0.2	1,090,483	591,924	321,504
0.1	906,931	470,749	249,144
0.05	755,407	376,084	192,944
0.02	577,848	277,387	141,273
0.01	480,375	226,723	116,368
b	0.2339	0.3011	0.3506

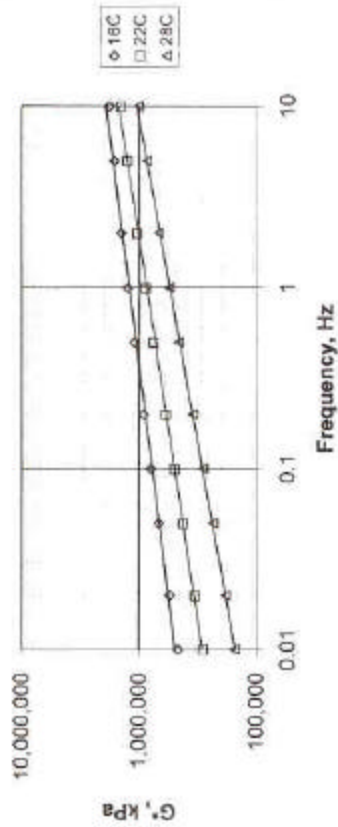
Colorado IH-25 Non-Distressed: Top Layer



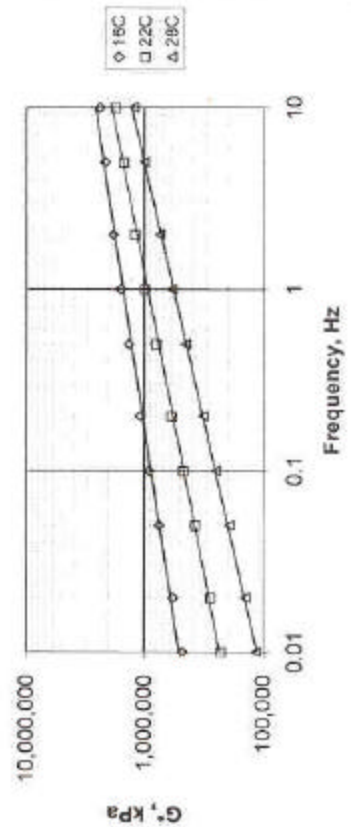
Colorado I-25 Non-Distressed: Intermediate Layer

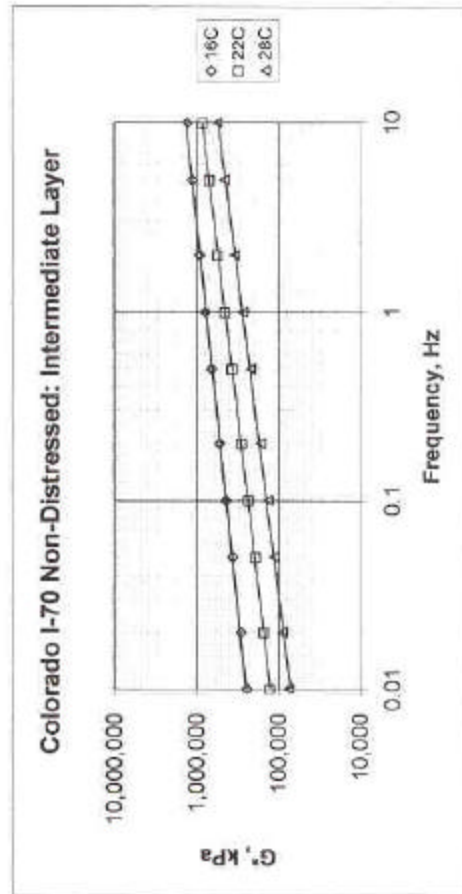
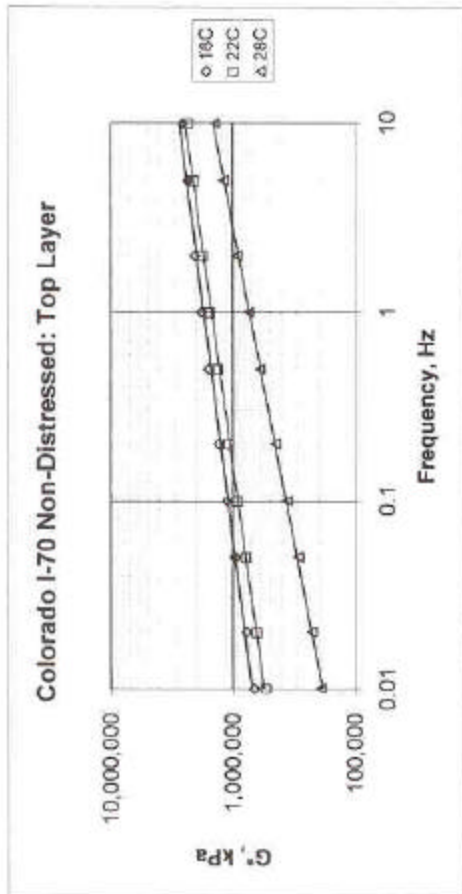


Colorado I-25 Distressed: Top Layer

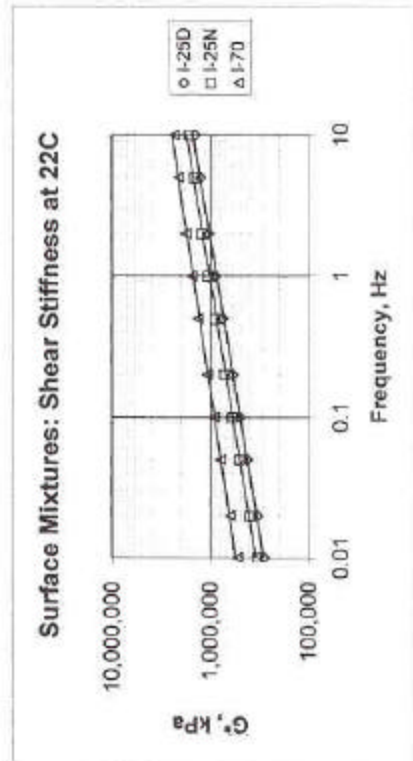
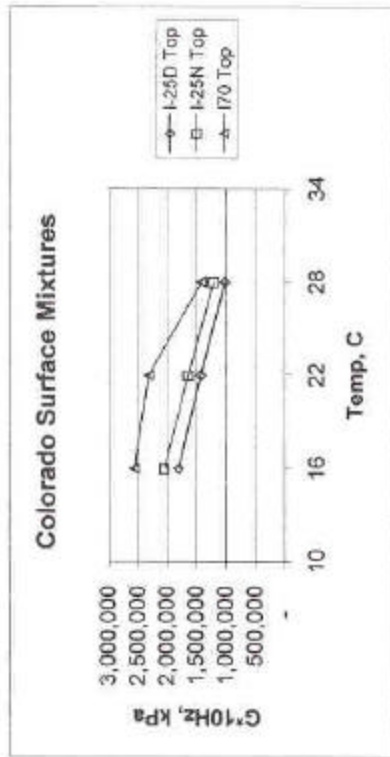
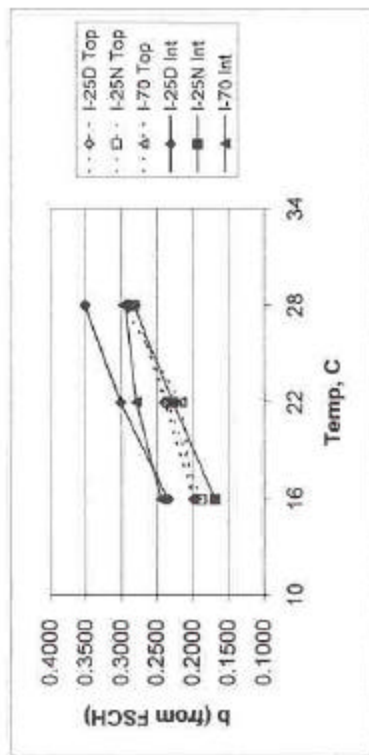


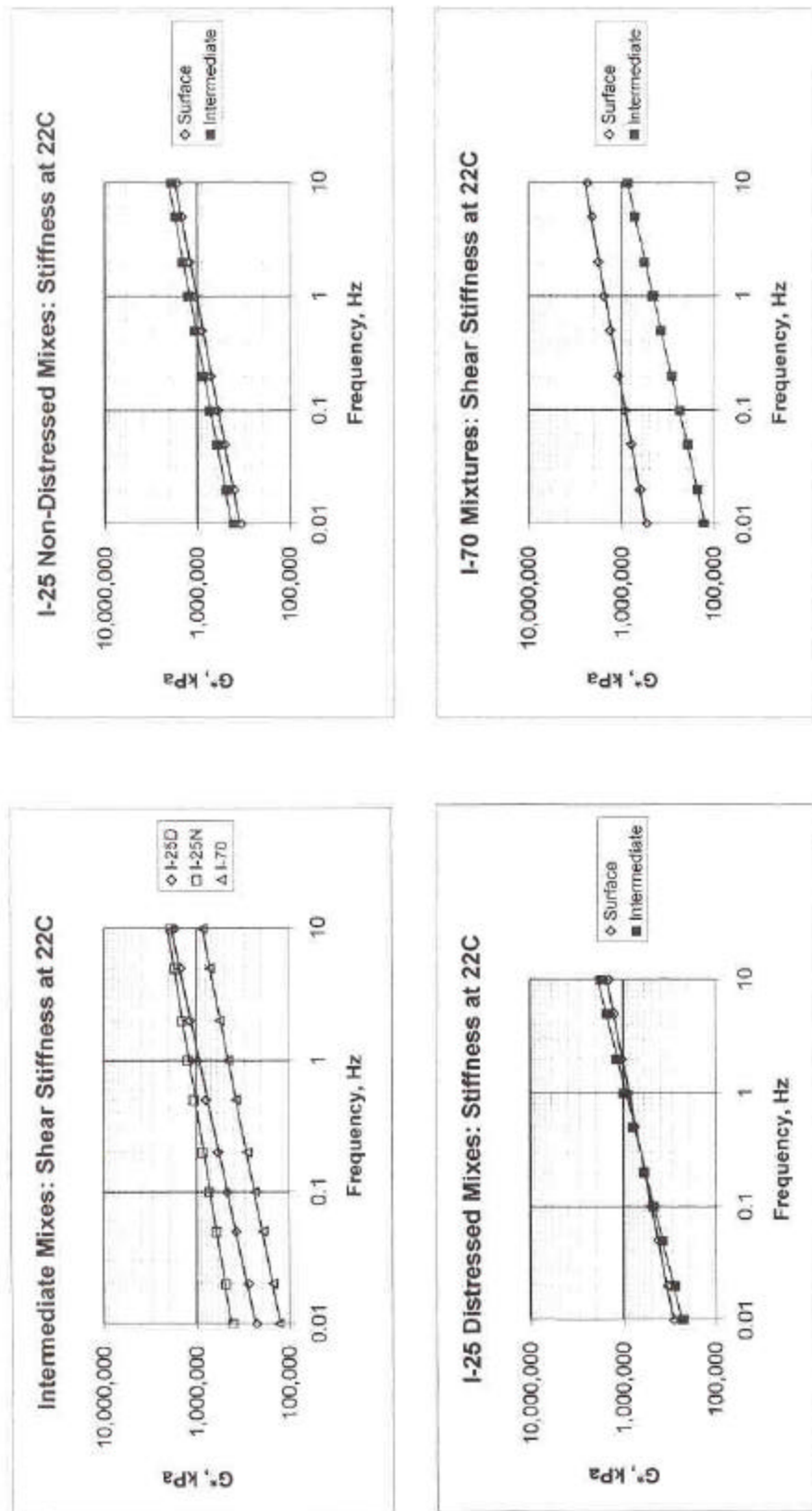
Colorado I-25 Distressed: Intermediate Layer

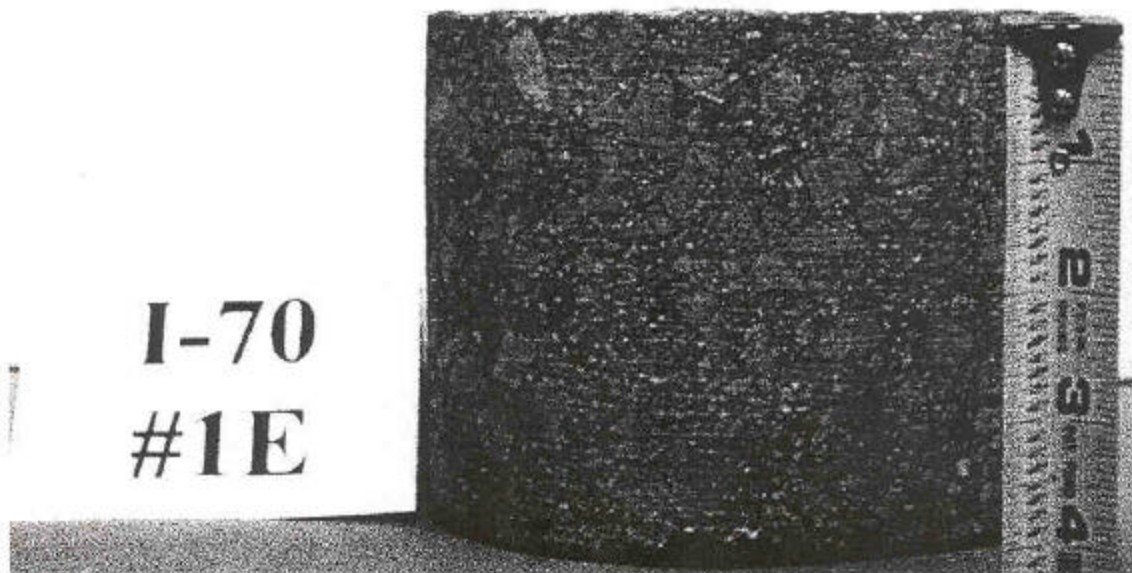
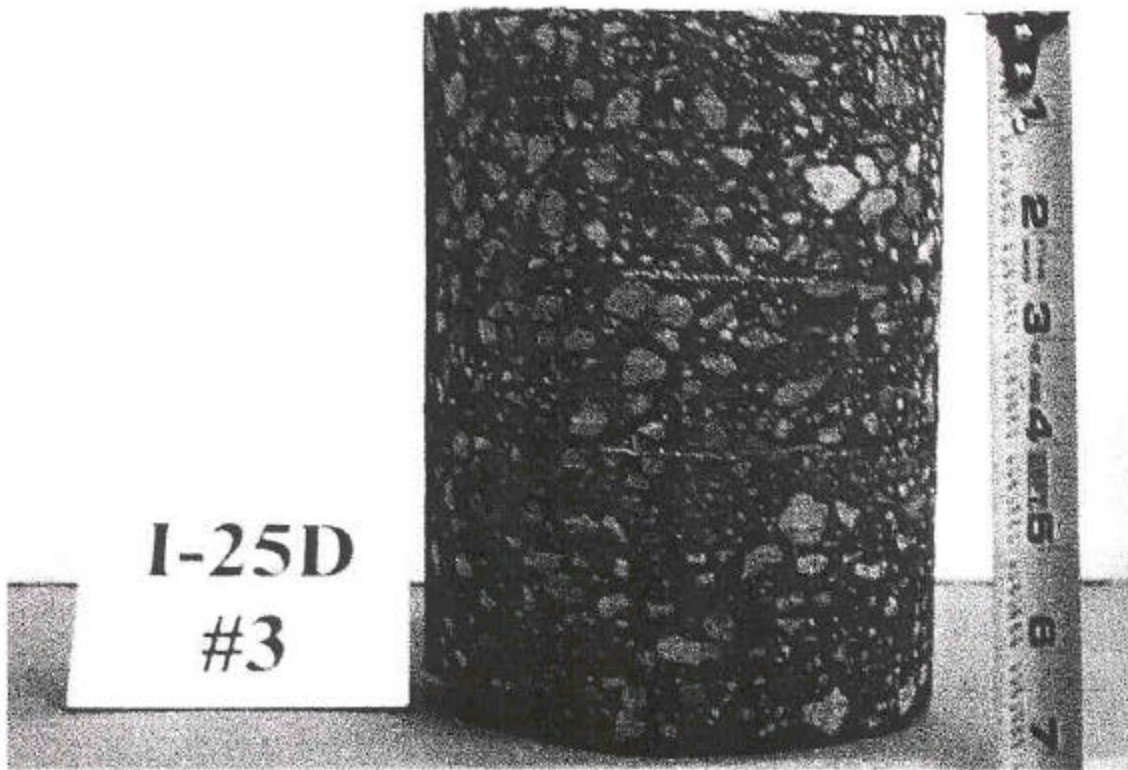




	I-25D Top	I-25D Int	I-25N Top	I-25N Int	I-70 Top	I-70 Int
16	0.1975	0.2338	0.1875	0.1683	0.1989	0.2438
22	0.2388	0.3011	0.2341	0.2267	0.2159	0.2783
28	0.2802	0.3506	0.2822	0.2816	0.2973	0.2944







[This page left blank]

Appendix D

**Colorado Department
of Transportation Cores**

[This page left blank]

The following test data was performed by the Colorado Department of Transportation.

Cores Taken at 20 Inches

		Core Number								Average	
		7	8	9	19	20	21	31	32		33
Passing											
3/4"	100	100	100	100	100	100	100	100	99	100	99.9
1/2"	92	92	95	91	94	92	92	92	92	95	92.8
3/8"	85	83	87	83	85	84	85	85	85	87	84.9
#4	63	64	64	64	64	65	64	64	64	66	64.2
#8	49	50	50	50	50	50	51	50	50	52	50.2
#16	37	37	37	37	38	37	38	38	38	39	37.6
#30	26	27	27	27	27	27	27	27	27	28	27.0
#100	10	11	11	11	11	11	11	10	11	11	10.8
#200	6.9	7.1	6.9	6.7	6.9	6.6	6.6	6.6	6.8	7	6.8
%AC (uncorrected)	5.07	5.12	5.24	5.16	5.21	5.08	5.24	5.19	5.23	5.17	

Cores Taken On Crack at 44 Inches

		Core Number								Average	
		1	2	3	13	14	15	25	26		27
Passing											
3/4"	100	100	100	100	100	100	100	100	100	100	100.0
1/2"	87	89	90	85	87	86	82	84	83	83	85.9
3/8"	77	76	79	73	71	73	67	69	67	67	72.4
#4	53	53	54	46	43	48	41	44	42	42	47.1
#8	41	40	42	36	33	37	32	34	32	32	36.3
#16	31	31	32	27	26	29	25	27	25	25	28.1
#30	23	23	24	20	20	22	20	20	20	20	21.3
#100	9	9	10	9	9	9	9	9	9	9	9.1
#200	6.2	5.9	6.4	5.5	5.7	6.1	5.6	5.8	5.6	5.6	5.9
%AC (uncorrected)	4.55	4.54	4.72	4.16	4.06	4.21	3.83	3.94	3.81	3.81	4.20